AD-A064 079 PURDUE UNIV LAFAYETTE IND GREAT LAKES COASTAL RESEAR--ETC F/G 8/3
A FIELD INVESTIGATION OF THE SPATIAL AND TEMPORAL STRUCTURE OF --ETC(U)
DEC 78 G A MEADOWS N00014-75-C-0716
UNCLASSIFIED TR-6 NL

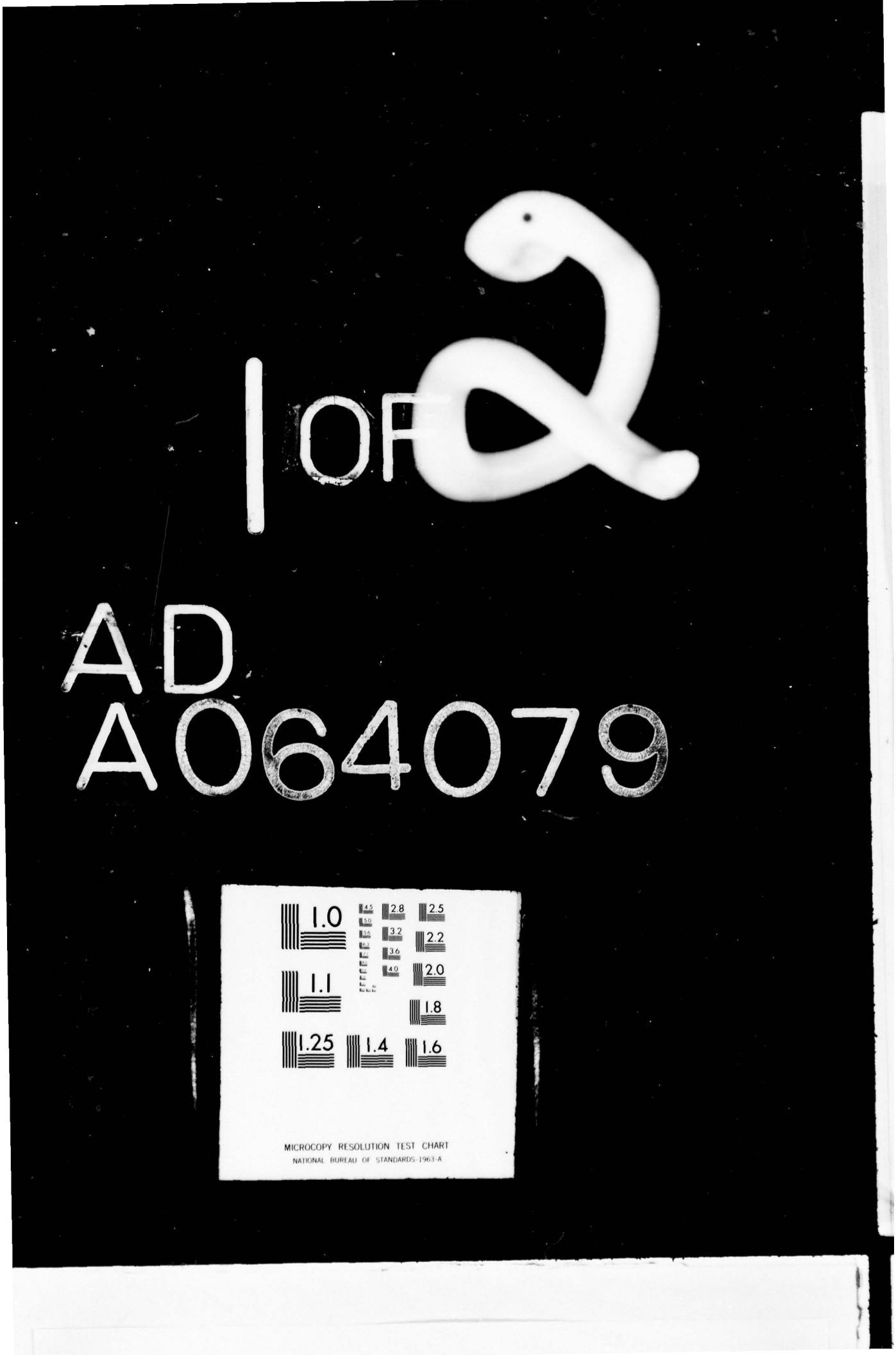
1 OF 2
AD
A064079
1.0
1.1
1.25
1.4
1.6
2.8
2.5
3.2
2.2
3.6
2.0
4.0
1.8
MICROCOPY RESOLUTION TEST CHART
NATIONAL BUREAU OF STANDARDS-1963-A

GREAT LAKES COASTAL RESEARCH LABORATORY
Department of Geosciences
Purdue University
West Lafayette, Indiana 47907

LEVEL II

AD A064079

DDC FILE COPY

A FIELD INVESTIGATION OF THE SPATIAL AND TEMPORAL STRUCTURE OF LONGSHORE CURRENTS

Guy A. Meadows

Technical Report No. 6

December 1978

192 p.

Office of Naval Research
Contract Number N00014-75-C-0716
Project NR 388-089

DDC RECEIVED FEB 1 1979 B

79 01 25 007

Great Lakes Coastal Research Laboratory
Department of Geosciences
Purdue University
West Lafayette, Indiana 47907

Technical Report No. 6

A FIELD INVESTIGATION OF THE SPATIAL AND TEMPORAL STRUCTURE OF LONGSHORE CURRENTS

Guy A. Meadows

December 1978

In memory of: William H. Meadows

July 31, 1915 - June 5, 1977

ACKNOWLEDGMENTS

I wish to express my sincere appreciation to Dr. William L. Wood, Department of Geosciences, Purdue University, for his guidance, assistance and friendship throughout this investigation.

I also wish to extend my appreciation to the staff of the Great Lakes Coastal Research Laboratory for their assistance in the field portion of this study. Special gratitude is due Steven R. Davis for his untiring assistance in the design and construction of the light emitting diode current meter circuitry.

I would also like to thank Dr. Evans Waddell for his comments and discussion on the time series analysis used in this investigation as well as for his assistance in the field.

Special appreciation is due the late Dr. Robert L. Miller for his support and inspiration throughout this investigation.

I would also like to acknowledge the many helpful comments and suggestions put forth by Drs. E. M. Agee, D.G. Vincent and T.V. Jennings.

Lastly, special thanks are due Ms. Tanda Waugh Meadows for tolerating and financially supporting me throughout this endeavor.

This study was supported by the Office of Naval Research, Geography Branch.

TABLE OF CONTENTS

LIST OF TABLES

LIST OF FIGURES

Figure Page

LIST OF SYMBOLS

Symbols from the Roman Alphabet

a	wave amplitude
B	bottom friction
c	wave phase velocity
c_g	wave group velocity
C_f	coefficient of bottom friction
D	rate of energy dissipation
E	wave energy density
F	energy flux
f( )	function of ( )
g	acceleration due to gravity
H	wave height
h	depth below still water level
k	wave number
N	coefficient of lateral mixing
M	mass transport velocity
P	lateral mixing parameter
p	pressure
P( )	probability of ( )
S	radiation stress tensor
s	bottom slope
t	time
u	velocity component in x-direction

v	velocity component in y-direction
V_o	velocity at the breaker line with no lateral mixing
X	non-dimensional surf zone width
x	horizontal coordinate, zero at still water on beach
y	horizontal coordinate, parallel to shore
z	vertical coordinate, positive upwards

Symbols from the Greek Alphabet

α	ratio of wave amplitude to water depth
η	elevation of the water surface
π	pi $\simeq 3.141593$
ρ	density
γ	confidence interval
σ	wave frequency
θ	incident wave angle, measured from y-axis
τ	momentum flux
μ_e	horizontal eddy viscosity

Subscripts

B	at wave break point
i	component in the i=1,2 or 3 direction
L	long wave period
o	in deep water
W	incident breaking wave period
x	x-direction
y	y-direction

Superscripts

$\bar{}$	mean value with respect to time
$'$	time dependent fluctuating component

ABSTRACT

Meadows, Guy Allen, Ph.D., Purdue University, December 1977. A Field Investigation of the Spatial and Temporal Structure of Longshore Currents. Major Professor: William L. Wood.

Longshore currents are generated by wind waves approaching a coastline at an angle and are strong narrow currents flowing parallel to the beach through the surf zone. Knowledge of the spatial and temporal character of this flow field has been markedly lacking. The horizontal and vertical distribution of the longshore current flow field has not previously been measured on a natural beach.

This field investigation was conducted to obtain simultaneous and continuous measurements of the horizontal, vertical and temporal variability of the longshore current flow field. The present study has resulted in a two-dimensional mapping, across the surf zone and with depth, of the longshore current flow field. The vertical structure of the mean longshore current flow field is nearly uniform with depth, with a narrow bottom boundary layer and sharp velocity gradients at the water-sediment interface. This investigation has also shown that the total longshore current velocity vector, at any point across the surf zone, is composed of three distinct velocity components. These components are: i) a steady longshore current velocity component; ii) a long-period fluctuating velocity component which tends to be out-of-phase with the incident wave field and; iii) a short-period fluctuating longshore cur-

rent velocity component which tends to be in-phase with the incident wave field.

The results of this study have further indicated that neither the deterministic radiation stress approach to the prediction of longshore currents, nor a probabilistic formulation, provide adequate prediction of the magnitude or distribution of the longshore current velocity across the surf zone. In addition, the existence of a low velocity zone in the longshore current flow field has been isolated over the submarine bar. It appears that existing analytical formulations for longshore current flow prediction must be re-evaluated in light of the findings of this study.

CHAPTER I

INTRODUCTION

Longshore currents are generated by wind waves approaching a coastline at an angle. These obliquely incident surface water waves, provide energy and impart momentum to the fluid of the surf zone producing a net flow in the longshore direction. Longshore currents are strong, narrow currents flowing parallel to the beach and are bounded by the water surface, the sub-aqueous beach and the somewhat arbitrary limit of the breaker zone on the seaward side. Knowledge of the spatial and temporal character of this flow field is markedly lacking. The horizontal distribution of the mean longshore current velocity across the surf zone has not previously been measured on a natural beach. In addition, the vertical structure of the longshore current flow field, as well as its temporal dependency, have received no previous experimental or theoretical attention. Yet, it is this fluid flow which is responsible for the transport of beach sediment, resulting in areas of severe coastal erosion.

The first documented observations of longshore currents were made by Shepard, Emery and LaFord (1941) who noted floats released in the surf zone exhibited a net

drift parallel to the beach. They also noted that the magnitude of this current correlated with the heights of the incomming waves. Since these initial observations, both theoretical development on and experimental observation of longshore currents have improved greatly. However, to date neither theories, nor experimental observations provide an adequate understanding of the generation and maintenance of longshore currents.

Steady state longshore current theory has been developed in an Eulerian reference frame; however, most existing field data are the result of Lagrangian measurements. Hence, little basis exists for comparison of theory with existing experimental data. It is, therefore, apparent that existing field are lacking in several respects. Specifically, no complete one-dimensional mapping exists of the mean longshore current flow field across the surf zone. Likewise, the vertical structure of the longshore flow field has not been experimentally measured, nor theoretically analyzed. Furthermore, insight into the time dependent vertical structure of the longshore current velocity field is perhapse the most important aspect necessary to provide a better understanding of nearshore physical processes.

A comprehensive field investigation of longshore currents is clearly needed. Such a study should be conducted in an Eulerian frame-of-reference to provide for the best comparisons with existing steady state longshore current theory. Since longshore currents are wind wave induced, measurements of surface gravity wave transformations through the surf zone must be made simultaneously

with longshore current measurements. This investigation must provide physically sound expectations of the driving forces of longshore currents. Likewise, interactions between waves and wave groups should be considered, to more fully understand the complex nature of the total, time-dependent, longshore current flow vector at a given location in the surf zone.

To analytically predict the total two-dimensional longshore current velocity field from the non-linear, time dependent, Navier-Stokes equations is untenable. Solutions to this system of equations using the prescribed boundary conditions for shallow-water wave-induced motions only exist under very restrictive, linearizing assumptions. These solutions were first set forth by Longuet-Higgins and Stewart (1960, 1962, 1963, 1964), Whitham (1962) and Longuet-Higgins (1970 a and b), subject to the following boundary conditions. The incident wave field is required to be two-dimensional and statistically steady in its mean. This restriction eliminates the existence of significant long period fluctuations in the longshore current velocity field which are induced by either growth or decay of the wave field incident at the outer surf zone. This restriction, however, does not necessarily preclude either wave transformations within the surf zone or periodic variation of wave characteristics due to the presence of wave groups. The total longshore current velocity vector is constrained to vanish at both the maximum wetted extent of the swash on the beach and at a sufficient distance beyond the region of wave breaking in the surf zone. The bottom boundary is assumed rigid and impermeable, and its offshore variation

is represented by a smoothly varying continuous function of x, the offshore variable. Subject to these conditions, a total analytical solution for two-dimensional, time-dependent, longshore current flow is still untenable. Therefore, a field study was undertaken, in order to evaluate longshore currents and their driving forces.

The purpose of this study was to provide a comprehensive and well-documented set of observations of longshore current velocities in a natural but selected situation and to develop a physical understanding of the behavior of longshore currents. The first objective of this study was to obtain a comprehensive, integrated, time synchronous, base of wave and current data which could be used to produce a two-dimensional mapping of the longshore current flow field. The second objective of this investigation was to identify and isolate driving forces of longshore currents within the surf zone. The third objective was to obtain field observations of the vertical structure of the longshore current flow field.

Field investigations were conducted along a relatively straight section of Lake Michigan shoreline characterized by a multiple barred configuration (Figure 1.1). The field site was centrally located along an unrestricted thirteen kilometer section of beach between the cities of Ludington and Pentwater, Michigan. Synoptic scale atmospheric disturbances pass through this site on three- to five-day intervals during the spring and fall seasons. Generally, these disturbances generate surf of approximately one meter in height arriving at the shoreline at low incidence angles.

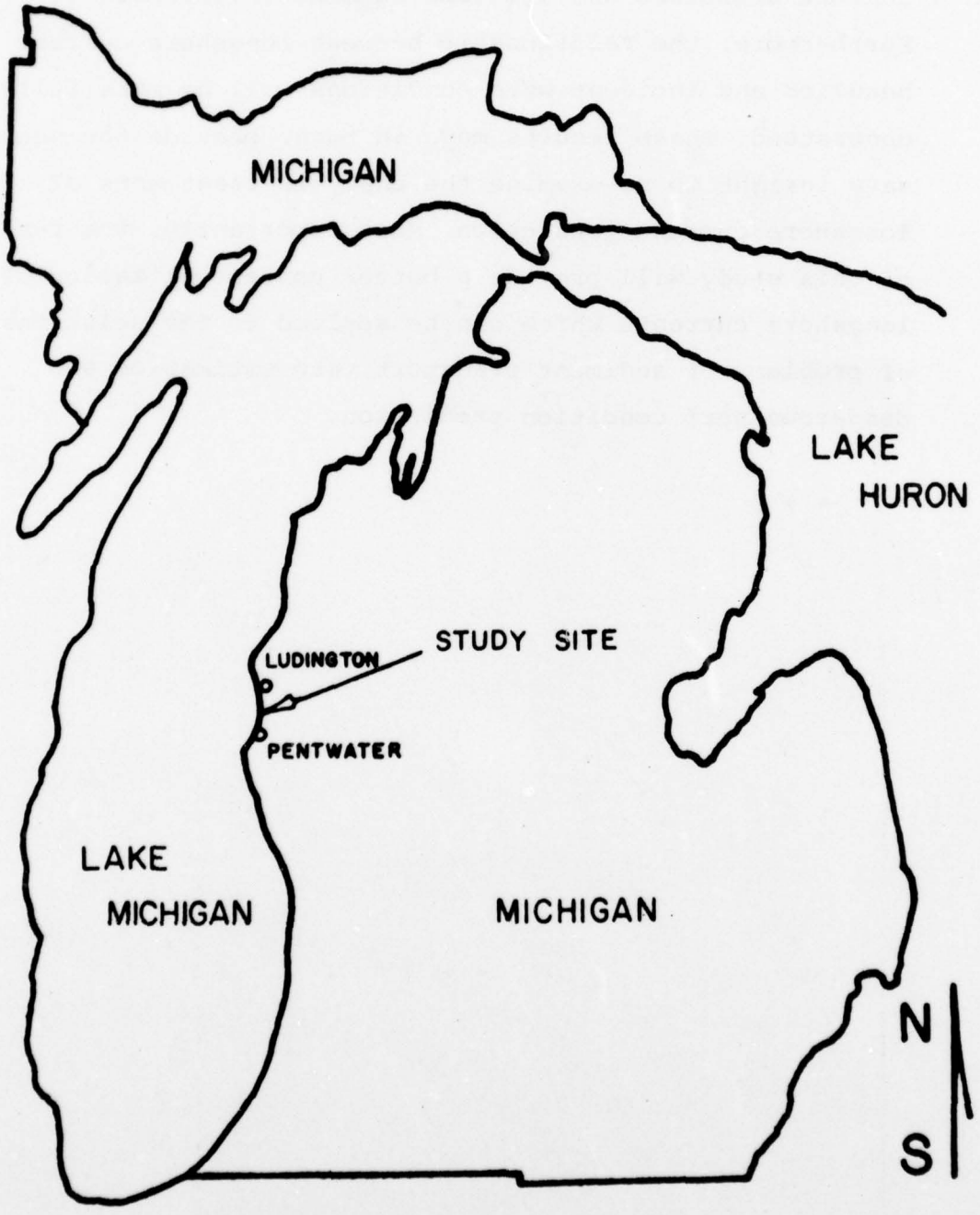

Figure 1.1 Location map showing site of field investigations.

It is anticipated that results from this investigation will provide a better physical understanding of longshore current structure and its time-dependent variability. Furthermore, the relationship between longshore current behavior and incident wave conditions will be more fully understood. These results may, in turn, provide the necessary insight to re-examine the analytic treatments of longshore current prediction. Most importantly, the results of this study will provide a better conceptualization of longshore currents which can be applied to the solutions of problems of sediment transport rate estimation and dangerous surf condition prediction.

CHAPTER II

REVIEW OF PERTINENT LITERATURE

Classically, longshore current velocity has been modeled as a function of wave height, period, celerity and angle of approach at breaking as well as the local water depth (Galvin, 1967). Theoretical approaches to the prediction of longshore current velocity can generally be grouped into one of four categories: i) conservation of energy (or momentum) (Putnam, Munk and Traylor, 1949; Galvin and Eagleson, 1965; Eagleson, 1965); ii) conservation of mass (Bruun, 1963; Inman and Bagnold, 1963; Galvin and Eagleson, 1965); iii) empirical correlation (Inman and Quinn, 1951; Brebner and Kamphuis, 1963; Harrison and Krumbein, 1964; Harrison, 1968) and iv) radiation stress forcing (Longuet-Higgins and Stewart, 1963; Bowen, 1969; Longuet-Higgins, 1970a ; James, 1974 a and b). The latter of these four approaches is perhaps most successful. The approaches themselves are exact with respect to physical arguments, however, weaknesses in the solutions are introduced in the form of simplifying assumptions which

allow exact solutions to an approximation of the actual physical problem, rather than an approximate solution to the exact problem.

Conservation of momentum and energy approaches to the analytical solution of the longshore current flow field were first set forth by Putnam, Munk and Traylor (1949). The basic approach encompassed by these methods was to consider momentum and energy fluxes into and out of a unit control volume of surf zone. The use of solitary wave theory in conjunction with the assumption of constant partitioning of the energy flux in the surf zone formed the basis for the development of an energy equation for the mean longshore current velocity. A second equation for the mean longshore current velocity was also obtained from a conservation of momentum approach within the surf zone. These two expressions, containing three unknowns; the longshore current velocity, the fraction of incoming energy flux available to drive the longshore current and the Darcy-Weisbach friction factor, provide no means for an independent solution. Hence, an implicit solution for one of the independent variables is necessary. Furthermore, bathymetry is restricted to straight and parallel contours with constant slope and the angle of wave approach is held constant with no provisions for shoaling induced refraction of wave crests through the surf zone. Therefore, the derived expressions are independent of local water depth and distance from the shoreline.

This formulation predicts no variation of the longshore current velocity either across the surf zone or with depth and hence, does not require the velocity to vanish at the boundaries. The breaking wave height is assumed to be a manifestation of the magnitude of the longshore component of the breaking wave horizontal particle velocity resolved in the longshore direction, $c_B \sin \theta_B$. It is further assumed that this truly oscillatory component, when time averaged, was the primary driving force in the surf zone responsible for producing a mean longshore current. It is assumed that in shallow water the wave celerity at breaking can be adequately represented by

$$c_B = \sqrt{g(H_B + z)}$$

which leads to an ambiguous conclusion. Accepting the premise that energy losses, not accounted for by this approximation exist, the driving component associated with the horizontal component of the wave particle velocity must be of greater magnitude than the resulting longshore current velocity,

$$V^2 = f(c_B \sin \theta_B - V)$$

or

$$c_B \sin \theta_B > V$$

This result is not usually observed in nature, implying other mechanisms, not accounted for by a simple time averaged momentum balance, must be associated with the generation of longshore currents.

Longshore current prediction formula set forth by Galvin

and Eagleson (1965) and Eagelson (1965) represent additional attempts to incorporate the contribution of the longshore component of the breaking wave horizontal particle velocity into theory. However, both of these formulations only agree with early Lagrangian velocity observations of longshore currents and do not agree with data now available.

Early conservation of momentum and energy approaches have led to the investigation of longshore currents based on continuity considerations (Bruun, 1963). The conservation of mass formulation attempts to recognize the existence of driving forces, within the surf zone, other than the longshore horizontal momentum component of breaking waves. An attempt to establish a more realistic representation of the nearshore sea surface is exemplified by the use of the significant wave height. This approach discriminates those waves most likely to make significant contributions to the longshore current dynamics from the total spectrum of waves that enter the surf zone. This approximation, however, only represents about one-sixth of the total waves passing the break point. The basic assumption in the conservation of mass approach is that a wave breaking at an angle to the beach contributes mass to the surf zone and raises the local mean water level. This creates a slope in the water surface which generates a longshore current. Variation of still water level at different locations along the beach imparts a longshore slope to the free water surface. The differential pressure head associated with this slope

initiates flow from areas of high to low pressure. Hence, the velocity of the longshore current is controlled by the frictional pressure head loss within the current itself. The non-uniformity of these conditions implies variation of the longshore current flow field in the longshore direction and forms the basis for theoretical treatments of rip-cell generation (Bruun, 1963; Bowen, 1967). Rip-channels are formed at low areas of wave and slope water set-up and flow perpendicular to the beach. This is a necessary and sufficient condition to satisfy conservation of mass in the surf zone since the continuity constraint can not justifiably be met by imposing return flow, with depth throughout the surf zone.

Modifications of the conservation of mass formulation, set forth by Bruun (1963), have been suggested by Inman and Bagnold (1963), and Galvin (1967). These alterations, however, vary only slightly from the expressions developed by Bruun. Although accounting for return flow of nearshore water through rip cell circulations, they also predict no variation of the longshore current profile with distance offshore or with depth.

The empirical correlations of Inman and Quinn (1951), Brebner and Kamphuis (1963) and Harrison and Krumbein (1964) are perhaps the best predictors of longshore current velocity. "Because of the inadequacies of physical theory, empirical correlation offers the most promise (Brebner and Kamphuis, 1963), but as yet such correlations have not been developed

from useful data" (Galvin 1967). In general, the dependence of these correlations on deep water wave parameters has made them difficult to evaluate with existing nearshore measurements. Harrison and Krumbein (1964) performed multiple linear regression on eleven field variables and found that the greatest variance was accounted for by the wave period, deep water wave height, beach slope, onshore wind speed, offshore wind speed and deep water wave direction.

All the above mentioned theories, as well as empirical correlations, are greatly compromised by over simplifications and the lack of reliable field data (Galvin, 1967). These theories employ only theoretical relations for wave characteristics, energy dissipation within the surf zone and current flow regimes and also fail to distinguish between breaker type and the method of energy dissipation within the wave itself.

Perhaps the most sophisticated and least restrictive approach to the study of longshore currents has been set forth in terms of the radiation stress associated with water waves (Longuet-Higgins and Steward 1960, 1962, 1963, 1964; Whitham 1962; Bowen 1969; Longuet-Higgins, 1970 a & b, and James, 1974b). The methodology of this approach implies that the magnitude of the longshore current velocity is proportional to the incoming wave energy and that the momentum of the imcoming waves is proportional to the radiation stress. This local stress due to momentum fluxes in the longshore

direction can also be shown to be proportional to the rate of dissipation of wave energy, where dissipation is distributed between bottom friction and internal losses within the breaking waves themselves. The applicability of this approach is limited by the lack of an adequate understanding of the complex interactions within the surf zone. Also, no satisfactory theory of breaking waves, under natural conditions, exists. The extensive use of small amplitude wave theory in the shallow water regions where the neglected non-linear effects are of critical importance, must be questioned. "The remarkable fact that these theories often give results in reasonable agreement with observation may be due partly to good luck, and partly to the fact that they may be dimensionally correct", Lonquet-Higgins (1972).

Utilization of the radiation stress concept allows the local energy density, associated with surface water waves, to be expressed as a function of the wave height squared (per unit horizontal area of the surf zone). This expression, although correct to second order in small amplitude wave theory, is not broad enough to fully represent both the laminar and turbulent regimes of surf zone dynamics. The energy flux toward the shoreline is represented as a function of the wave energy density incident at the outer surf zone and the rate of energy propagation of the wave train, the group velocity. The existence of energy dissipation mechanisms within the surf zone such as bottom friction,

wave breaking and the generation of turbulence insure that the energy flux through the surf zone is not constant. Hence, the longshore current velocity which is directly related to the rate of energy dissipation, becomes a function of the distance offshore and surf zone width.

Outside the breaker line the flux of energy is approximately constant. Dissipative stresses are assumed small, therefore, to an order of approximation, no driving forces for the longshore current are operative. However, the mean velocity of the longshore current is directly proportional to the local water depth, hence, the maximum flow can be anticipated to exist at the break point. Conversely, longshore current velocity, under the assumption of no lateral mixing, should theoretically vanish at the break point. However, under either condition no flow is expected to be generated beyond the breaking depth of the incident waves. Therefore, a discontinuity in the velocity profile exists at the breaker line.

The addition of horizontal mixing to the formulation of longshore current theory has marked affects on the applicability of the method (Lonquet-Higgins 1970b). This addition causes a shoreward shift in the maximum of the longshore current velocity profile. The profile also loses its linearity and expands offshore, outside the break point. Estimates of horizontal eddy viscosity based on mixing length theory, eliminate the momentum discontinuity and the

associated velocity discontinuity across the breaker line. This "averaging" across the breaker line results in a smooth velocity profile and a more conservative longshore current velocity estimate. These modifications bring the radiation stress predictions of longshore current velocity closer to observed current velocities.

Variations, on the radiation stress approach to the study of longshore currents, have been suggested by several authors (Bowen, 1969; Komar, 1971; Thornton, 1971; Earl, 1974; James, 1974b). These modifications incorporate the effects of wave induced set-up and set-down within the surf zone and wave shoaling transformations to generate longshore current flow. However, longshore current velocities predicted from these radiation stress formulations agree only with experimental results under idealized conditions.

Komar and Inman (1970) formulated a relationship between the average longshore current velocity and the maximum horizontal particle velocity under waves in the surf zone. From the simultaneous solution of two independent estimates of longshore sediment transport, a direct comparison was made between the average longshore current velocity and the longshore component of the breaking wave particle velocity. However, it was assumed that the stress exerted on the beach by the incident wave field was a constant fraction of the radiation stress in the onshore direction. As stated by Longuet-Higgins (1972), "experimental evidence

shows that the onshore component of the radiation stress is largely balanced by the wave set-up (Longuet-Higgins and Stewart, 1963; Bowen, Inman and Simmons 1968)".

The assumptions employed in all of these solutions, especially the use of linear wave theory in shallow water, still remain far too restrictive to produce physically realistic predictions under natural conditons. In an effort to provide a more realistic representation of the surf zone driving forces, a treatment of surface wave climates by statistical means has been employed, (Longuet-Higgins, 1957). Application of this approach to nearshore wave induced circulation has been the subject of recent work by Collins (1972). Utilizing probability distributions of wave characteristics across the surf zone, in contrast to a monochromatic wave assumption, provides a much better approximation of observed shallow water wave conditions. The modification on the dynamics of nearshore processes results from waves no longer being forced, by wave height to depth limitations, to break at one fixed point. Instead, the breaker line becomes a breaker zone and the region of the surf zone over which energy dissipation due to wave breaking is the primary dissipative force, becomes broad. Hence, the unresolved question of the validity of the assignment of a wide range of values of horizontal eddy viscosity across the breaker line (Thornton, 1971) is eliminated. This relaxation in the rigidity of the basic formulation greatly

increases the intuitive validity of the physical arguments for the generation of longshore current flow, from the fluid dynamics standpoint.

Employing this computational approach suggested by Collins (1972), both barred and unbarred subaqueous bench topography can be easily evaluated. Variation of bottom configuration produces marked alterations in the prediction of both longshore current velocities and the surface current profile across the surf zone. Addition of a subaqueous sand bar in the nearshore bathymetry results in the prediction of a double maximum in the longshore current velocity profile across the surf zone (Collins, 1972). Maxima are located on the offshore side of the subaqueous bar and between the bar and the shoreline. Under variable sea state conditions the flow field becomes more sensitive to beach steepness. As beach slope increases, strong and more concentrated longshore currents are expected. However, under these conditions wave set-up tends to decrease in magnitude. In general, the non-monochromatic sea tends to generate less variation in both set-up and set-down across the surf zone.

The initiation of probability distributions to characterize shoaling surface gravity waves is perhaps a step forward from the monochrmoatic assumption. However, caution must be exercised in their use. Although the probability distribution may adequately represent the ensemble of waves present over a given time period, those waves did not

necessarily arrive in a random manner. In addition, the subsequent use of linear wave theory through the surf zone in the computational procedure detracts from this approach. The recognition of complex interactions between waves and currents and their associated non-linearities cannot be adequately expressed within the context of linear wave theory or with probability distributions derived from this approach.

The results of this approach may be summarized as follows: The maximum of the mean longshore current velocity profile is shifted shoreward from its position under monochromatic wave incidence. The mean longshore current velocity profile across the surf zone becomes somewhat flattened, suggesting a more gradual dissipation of wave energy through the surf zone, thereby decreasing the maximum expected velocity. The tail of the longshore current velocity profile extending beyond the breaker zone in the offshore region is more pronounced than in the monochromatic case, suggesting a greater contribution to the net horizontal mixing across the surf zone. Variations in wave induced set-up and set-down through the surf zone tend to be more subtle thus, suggesting that the slope water contribution to the longshore current flow field may be of less significance than originally anticipated. Dependence of the longshore current on incident wave angle is also modified from previous theoretical developments, suggesting the current

should achieve its maximum velocity at incident wave angles of sixty degrees.

Other variations of longshore current theories have been suggested which employ specific forms of probability distributions of the incident wave field. The use of a Rayleigh distributed sea surface, a good approximation for fully developed sea, provides a reasonable prediction of wave conditions outside the surf zone. However, the extension of this assumption through the surf zone is of marginal value. Non-linearities associated with shoaling waves produce skewness in the distribution of wave characteristics through the surf zone (Wood, 1977).

Power spectra derived from a Rayleigh distribution of wave heights has been applied to the theoretical development of the longshore current flow field (Earl, 1974). The inclusion of a horizontal eddy viscosity that is dependent on position within the surf zone, under the assumption that surf conditions are restricted to only spilling breakers, has been set forth in a theoretical development by Thornton (1971). Results obtained from these approaches are similar to those discussed earlier. The maximum longshore current velocity is decreased and shifted shoreward from the monochromatic case. The addition of lateral diffusion of momentum across the surf zone results in the longshore current velocity profile extending beyond the zone of active wave breaking.

Under conditions of obliquely incident sea waves, topographically controlled meanders of the longshore current flow field have been predicted by numerical solutions (Noda, 1974). By forcing a zero velocity streamline into the flow field perpendicular to the beach, these meanders can be transformed into longshore current flow and rip cell circulation. A similar flow condition has been observed by Sonu (1972) under field conditions.

One observation appears to stand out before all others, modeling of longshore current flow is lacking both experimental observations and reasonable modeling criteria. In a thorough evaluation of published longshore current studies, Galvin (1967), also states that "the two principal unkowns responsible for uncertainty in field data are: the effect of variations in nearshore hydrography (Sonu, et al., 1967) and the effect of substituting a mean value for the distribution of values of each measured variable."

The effect of variations in nearshore hydrography has since been investigated in some detail (Harrison, 1968; Sonu, 1973; Noda, 1974). However, the practice of using mean values for the distribution of variables has continued and as a consequence has reinforced the development of steady and quasi-steady longshore current theory (Bowen, 1969; Thornton, 1971, Longuet-Higgins, 1970a and b, 1972). Significant temporal variations have been observed in longshore current velocity measurements. Putnam, Munk, and

Traylor (1949) observed velocity variations as large as ± 25 percent of the mean during their Lagrangian field measurements of longshore currents. These observed variations were determined to be time dependent with a period from three to five minutes. Inman and Quinn (1951) noted a large variability, 300 to 500 percent, in successive thirty second time averaged Lagrangian measurements of longshore currents. They attributed these large variations to variability of wave height with time and to the "cell-like" circulation along the shore. It was their conclusion that at least 5 successive thirty second observations must be made in order to obtain a mean longshore current with an average coefficient of variation comparable to the standard error obtained from their prediction formula. Harrison (1968) observed variations in longshore current velocities measured along successive adjacent segments of the beach using Lagrangian techniques. Deviations in longshore current velocity between two adjacent 30.5 meter lengths was determined to be within ± 10 percent of the "true" velocity under similar conditions. The general conclusion of these and other field and laboratory studies is that temporal variations in longshore currents are relatively unimportant to the determination of longshore current velocity.

Recently, an investigation by Dette (1974), using a two component electromagnetic current meter, showed temporal variations in longshore current velocities of ± 100 percent

with as many as nine fluctuations per wave period. Dette (1974) observed changes in the instantaneous longshore speed from 0 m/sec to 2.0 m/sec within a fraction of a wave period. These field measurements by Dette as well as similar observations by Huntley and Bowen (1974) and field measurements of the vertical, time dependent, longshore current structure made by Wood and Meadows (1975) strongly support the concept that significant unsteady motion does occur in longshore currents over relatively short periods of time and that time averaging is a physically inappropriate procedure.

CHAPTER III

SPATIAL AND TEMPORAL CHARACTERISTICS OF LONGSHORE CURRENTS

Introduction

Classically, the generation of wave-induced longshore currents has been analytically treated as a steady flow parallel to the shoreline. Longshore current theory has subsequently been developed in an attempt to predict the one-dimensional, steady-state surface distribution of longshore current velocity, across the surf zone.

It has long been recognized that the general flow distribution of the longshore current velocity field is non-uniform across the surf zone. Assumptions in the theoretical formulation, that the flow velocities must vanish at both the onshore and offshore limits of the longshore current, give rise to the expectation of a velocity distribution across the surf zone which contains a single maximum. The location of this velocity maximum is dependent upon several factors, yet, its location is generally hypothesized to be near the incident wave break point. It is at this point in the surf zone that both the wave height and wave horizontal particle velocity reach their maximum values. Hence, it is in this region that surf zone forcing

functions of longshore currents are also theorized to attain their greatest values. This expectation is supported by longshore current velocity profiles observed during the model studies of Galvin and Eagleson (1965). However, prior to this present investigation no field verification of this hypothesis existed.

Longshore current theory has been derived under the assumption that vertical uniformity exists in the flow field. This assumption is applied by vertically integrating the continuity equation from the bottom to the free surface. Hence, any vertical variation in the flow field has been eliminated and the longshore current can be treated analytically as a vertically uniform one-dimensional flow.

Existing semi-theoretical longshore current formulations restrict the longshore dependence of the flow field to one of two general cases. First, the longshore flow field is presumed to be uniform and invariant in the longshore direction. Second, it is considered to be an integral component of a closed nearshore cellular circulation. Both cases have received little theoretical attention, hence, few theoretical formulations are available to predict the two-dimensional, surface circulation of the surf zone.

Perhaps the most restrictive assumption employed in the development of classical longshore current theory results from time averaging of the equations of motion. This steady state approach is employed in all existing longshore

current theories. Hence, the mean velocity of the flow field is assumed to be an adequate representation of the flow at any instant of time. This approach has been employed in an attempt to create an analytically tractable formulation. However, inclusion of the temporal variability of longshore currents may be necessary to the understanding of surf zone dynamics and sediment transport.

It is, therefore, apparent that present theory related to the structure of the longshore current flow field has resulted in an expectation for a steady one-dimensional surface flow. However, field observations and basic physical principles concerning shallow water wave induced motions indicate that this flow field should be three-dimensional and time-dependent. Therefore, one of the purposes of this investigation is to extend the understanding of longshore current flow fields into two-dimensional space and time.

Initial Conditions

In order to evaluate the wave-induced longshore current flow field, it is necessary to specify the initial conditions of the wave field, incident at the outer surf zone. It is advantageous to remove from the analysis all long period transient variations of the velocity field not directly related to the incident breaking waves. Thus, the wave field must be required to be statistically steady in its mean, with respect to these

variations ($\partial\bar{\eta}/\partial t = 0$, where η is the free surface evaluation). This restriction precludes fluctuations in the longshore current velocity field induced by either growth or decay of the wave field. This restriction does not preclude individual wave transformations within the surf zone, hence, $\partial\eta/\partial x \neq 0$. The approximation $\partial\eta/\partial y = 0$, requires that the incident waves remain long crested and two-dimensional as they move through the surf zone.

An alternative assumption on the nearshore wave field is that a non-uniform sea surface exists in the longshore direction, $\partial\eta/\partial y \neq 0$. Under this initial condition, additional driving forces may be expected in the longshore current velocity field. This condition may arise due to either an interactive short-crested sea surface or long period edge waves. These types of alongshore wave motions may result in an additional release of energy to the longshore current. With a two-dimensional analysis, these secondary alongshore velocity components would not be anticipated, although when analyzing field data, their magnitudes may appear as a residual after all other two-dimensional components are accounted for.

Once the initial conditions describing the incident wave field have been established, the nature of the longshore current flow may be specified. As with the case of the incident wave field, the resulting longshore current flow field may be either uniform or non-uniform in the

longshore direction. The restriction of the incident wave field to a two-dimensional, long-crested sea surface requires that the longshore current be treated as uniform in the y-direction. In summary, Table 3.1 shows the various analytic assumptions which can be applied to the incident wave field and related longshore current. Existing longshore current theory is formulated on the assumption that only one of the eight possible combinations shown is observed in the surf zone (wave field steady and uniform, longshore current steady and uniform).

Bowen (1969) and Longuet-Higgins (1970 a and b) have suggested a uniform monochromatic wave approach to the analytic description of the longshore current flow field. Under this assumption, each wave of a given amplitude is constrained to break at the same, depth controlled, location in the surf zone. As a result, a sharp discontinuity exists in the longshore current profile across the surf zone, at the break point (Figure 3.1).

Since the absence of variations in wave height generally precludes differential wave breaking, a mechanism by which observed longshore current velocities outside the breaker line can be matched to those inside is necessary. Lateral mixing across the surf zone has been explained by two methods. Bowen (1969) and Longuet-Higgins (1970 a and b) have incorporated a horizontal eddy viscosity into longshore current formulation to eliminate the abrupt truncation

Table 3.1

INITIAL CONDITIONS DEFINING POSSIBLE ANALYTICAL CONSIDERATIONS FOR THE DEVELOPMENT OF LONGSHORE CURRENT THEORIES BASED ON THE INCIDENT WAVE FIELD

Incident Wave Field Conditions

Wave Field Steady in Mean Wave Field Uniform in Y-Direction (Alongshore)	Wave Field Steady in Mean Wave Field Non-Uniform in Y-Direction (Alongshore)
$\overline{\frac{\partial \eta}{\partial t}} = 0$	$\overline{\frac{\partial \eta}{\partial t}} = 0$
$\frac{\partial \eta}{\partial x} \neq 0$	$\frac{\partial \eta}{\partial x} \neq 0$
$\frac{\partial \eta}{\partial y} = 0$	$\frac{\partial \eta}{\partial y} \neq 0$

Longshore Current Uniform in Y-Direction (Alongshore)		Longshore Current Non-Uniform in Y-Direction (Alongshore)	
Steady	Unsteady	Steady	Unsteady
$\frac{\partial u_i}{\partial t} = 0$	$\frac{\partial u_i}{\partial t} \neq 0$	$\frac{\partial u_i}{\partial t} = 0$	$\frac{\partial u_i}{\partial t} \neq 0$
$\frac{\partial u_i}{\partial x} \neq 0$	$\frac{\partial u_i}{\partial x} \neq 0$	$\frac{\partial u_i}{\partial x} \neq 0$	$\frac{\partial u_i}{\partial x} \neq 0$
$\frac{\partial u_i}{\partial y} = 0$	$\frac{\partial u_i}{\partial y} = 0$	$\frac{\partial u_i}{\partial y} \neq 0$	$\frac{\partial u_i}{\partial y} \neq 0$

in the longshore current velocity distribution, across the surf zone. However, Collins (1972) has shown that mixing resulting from differential wave breaking due to a non-monochromatic sea surface incident at the outer surf zone is a more frequently observed condition in the field (Figure 3.2).

Boundary Conditions

Longshore currents result in a net translation of fluid particles parallel to the shoreline, which are bounded by the beach, surf zone, bottom and free surface. With the exception of the free surface, flow velocities are constrained to vanish at or near each of these boundaries. There can be no wave-generated longshore current flow beyond the maximum wetted portion of the swash zone on the beach. The longshore current flow field must vanish at some point outside the surf zone as well as at the lower boundary of the longshore current flow field. The last remaining boundary is that of the free surface. It is at this boundary that the flow velocity is anticipated to be a maximum. Hence, theoretically the maximum velocity of the longshore current is expected to lie between the breaker zone and the shoreline and at the surface of the fluid column.

As a result of these imposed conditions at the surface and bottom boundaries, the longshore current velocity is constrained to vanish as: $x \to \infty$, far offshore; as $x \to 0$,

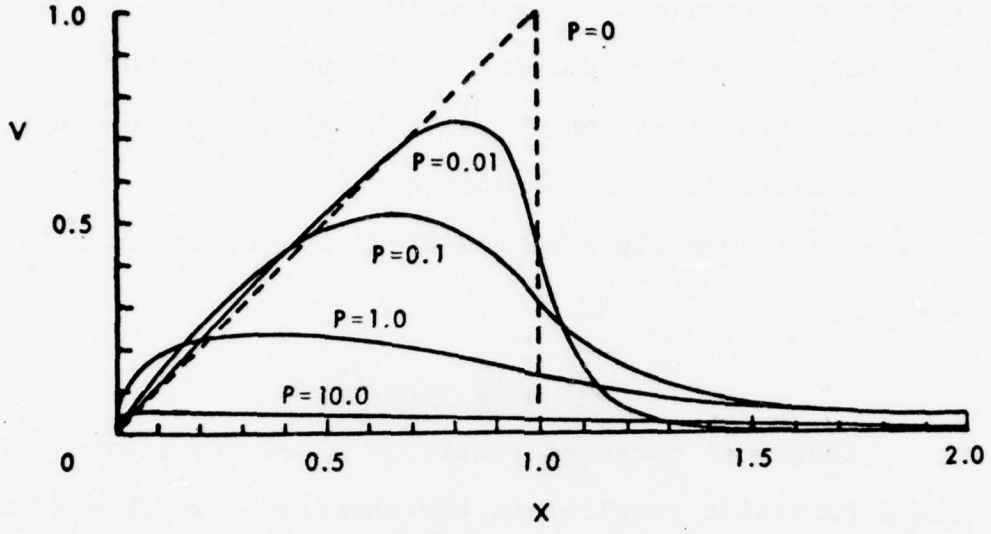

Figure 3.1 Longshore current profiles across the surf zone for values of mixing parameter P.

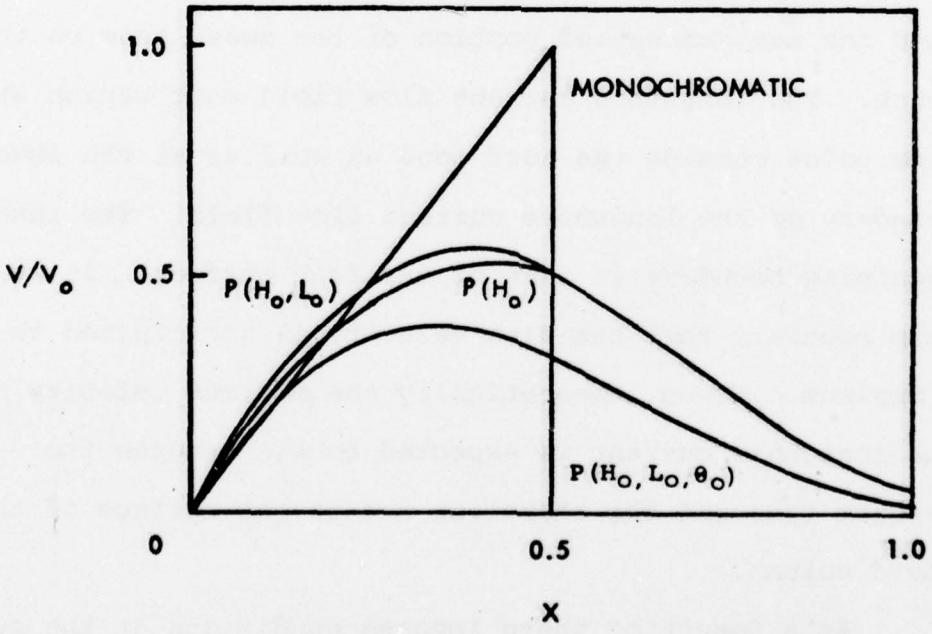

Figure 3.2 A comparison of longshore current predictions for monochromatic, one-, two-, and three-dimensional probability distributions.

at the shoreline and as $z \to -h$ at the bottom boundary. Therefore, $\bar{V}$ must approach $\bar{V}_{max}$ at $0 < x < x_\infty$ and as $z \to z|_o$, at the surface.

The configuration of the offshore bottom must be specified in order to completely formulate the longshore current flow field. In general, the sea bed may be treated as one of three cases: horizontal, sloping or barred. Wave motion over a horizontal shallow bottom has been described by several authors, among them, Phillips (1960), Longuet-Higgins and Stewart (1962) and Whitham (1962). However, these developments have not been extended to include the generation of longshore currents. The case of waves encroaching on a planar sloping beach forms the context within which all existing longshore current theory has been developed. The case of an offshore bar present in the nearshore bathymetry is the most frequently observed condition on natural beaches. This condition, however, has not been theoretically treated in relation to the generation of longshore currents. Collins (1972) suggests that wave height statistics in the surf zone do not appear to be greatly altered by the presence of an offshore bar. However, the response of the longshore current flow field to a submarine bar has not been observed prior to this investigation.

Existing Theoretical Approaches

Velocities associated with the longshore current flow field are generally small compared to wave particle velocities in the surf zone. Longshore current circulation, however, has long been recognized as the result of a dynamic balance within the nearshore region. But, the generation, maintenance and structure of the longshore current flow field is poorly understood.

Analytic formulations of longshore current theory have been derived using one of three basic approaches: conservation of mass, energy or momentum. Investigations of the longshore current flow field based on continuity considerations employ the assumption that waves breaking at an angle to the beach contribute mass to the surf zone (Bruun, 1963). However, an accurate determination of the mass contributed to the surf zone by each breaking wave is extremely difficult on natural beaches. This approach has met with limited success. The recognition that the driving forces necessary to create and sustain the longshore current are most directly related to the breaking wave height has led to the development of the conservation of energy approach to the treatment of the longshore current flow field (Putnam, Munk and Traylor, 1949). Inherent in this formulation is the concept that water surface waves contain energy proportional to their wave height squared. As the wave breaks and moves through

the surf zone incident wave energy is strongly dissipated and converted to heat. However, a small portion of this incident wave energy is available to drive nearshore physical processes. Hence, the total energy content of the longshore current flow field is small compared to that of the incident wave field. Perhaps the most satisfactory and least restrictive approach to the prediction of longshore current velocity has been set forth in terms of conservation of momentum (Longuet-Higgins, 1970 a and b). This approach utilizes the concept of radiation stress (excess flow of momentum due to the presence of wave motion), as developed by Longuet-Higgins and Stewart (1960, 1962, 1963 and 1964) and Whitham (1962), to relate the magnitude of the longshore current velocity to the incoming wave energy flux. From this approach, a theoretical, one-dimensional profile of longshore current velocity across the surf zone may be calculated.

In general, as suggested by Longuet-Higgins and Stewart (1960), for a non-viscous,irrotational fluid, the mean energy density per unit wave length of the incident waves, correct to second order, is given by

$$E = \tfrac{1}{2}\rho g a^2 \qquad (3.1)$$

where a is the wave amplitude. This wave energy is propagated at the group velocity, c_g. The product $E c_g$ is the energy transferred into the nearshore region by the incident wave field and is directed in the direction of wave

propagation. When the wave height, length and speed of propagation are altered as the wave shoals, a net force is exerted on the fluid medium. This force is equal to the rate of change of wave momentum and is given by the radiation stress.

As suggested by Longuet-Higgins and Stewart (1964), the expression for the principal radiation stess may be separated into three components.

$$S_{x'x'} = S_{x'x'}^{(1)} + S_{x'x'}^{(2)} + S_{x'x'}^{(3)} \tag{3.2}$$

where

$$\left.\begin{aligned} S_{x'x'}^{(1)} &= \overline{\int_{-h}^{\eta} \rho u^2 dz} \\ S_{x'x'}^{(2)} &= \overline{\int_{-h}^{0} (p - p_0) dz} \\ S_{x'x'}^{(3)} &= \overline{\int_{0}^{\eta} p dz} \end{aligned}\right\} \tag{3.3}$$

where x' is normal to and y' parallel to the wave front. The first term, $S_{x'x'}^{(1)}$, represents the vertically integrated, time averaged contribution to the momentum flux of the wave particle velocity in the direction of wave propagation. This term is analogous to the Reynolds stress integrated from the bottom to the free surface. $S_{x'x'}^{(2)}$ represents the momentum flux contribution arising from the change in mean pressure within the fluid. The final

term, $S_{x'x'}^{(3)}$, is the potential energy density of the wave, or half the total energy density:

$$S_{x'x'}^{(3)} = \tfrac{1}{2}E. \tag{3.4}$$

The total principal stress, correct to second order, in deep water is

$$S_{x'x'} = E\left(\frac{2kh}{\text{Sinh } 2kh} + \tfrac{1}{2}\right). \tag{3.5}$$

However, for shallow water it reduces to

$$S_{x'x'} = 3/2(E) \tag{3.6}$$

In an analogous manner, Longuet-Higgins and Stewart (1964) show the transverse component of the radiation stress to be

$$S_{y'y'} = \tfrac{1}{2}E,$$

in shallow water. The radiation stress can produce both variations in the water surface elevation and give rise to wave-induced currents (Longuet-Higgins and Stewart, 1963, 1964; Bowen, 1967).

The radiation stress for an incident wave field which is monochromatic results in an identical contribution to the longshore current from each successive wave. Hence, the calculated magnitude of the radiation stress, which is time averaged over the wave period, becomes a constant, static stress acting on the nearshore fluid at any point in the surf zone.

The radiation stress approach to specifying the longshore current flow field, suggested by Longuet-Higgins (1970 a and b) utilizes a modified radiation stress treatment to relate the magnitude of the longshore current velocity to the incoming wave energy flux, given by

$$F_x = E\, c_g \sin\theta \tag{3.8}$$

outside the surf zone and

$$\frac{\partial F_x}{\partial x} = - D \tag{3.9}$$

inside the surf zone, where D is the rate of energy dissipation per unit time and horizontal area, and where x is perpendicular and y parallel to shore. The flux of y-momentum across a line x = constant, parallel to the shoreline is given by the radiation stress component

$$S_{xy} = F_x\left(\frac{\sin\theta}{c}\right) \tag{3.10}$$

where θ is the angle the incoming wave makes with the shoreline and c is the wave phase speed. From balance of momentum flux considerations it can be shown that the waves exert a local stress

$$T_y = - \frac{\partial S_{xy}}{\partial x} \tag{3.11}$$

parallel to the shoreline. Substituting (3.10), where $\sin\theta/c$ is independent of x, gives

$$T_y = - \frac{\partial F_x}{\partial x}\left(\frac{\sin \theta}{c}\right) \tag{3.12}$$

or from (3.9)

$$T_y = D\left(\frac{\sin \theta}{c}\right). \tag{3.13}$$

A simple momentum balance for steady state conditions on a straight coastline can be expressed as

$$T_y - B = 0 \tag{3.14}$$

where B is bottom friction and lateral friction is neglected. Applying linear theory of waves in shallow water to (3.8) under the assumption that θ in the breaker zone is small enough so that cos θ can be approximated by unity gives

$$F_x = \tfrac{1}{2} \rho g \, a^2 \sqrt{gz} = \tfrac{1}{2} \alpha^2 \rho g^{3/2} z^{5/2} \tag{3.15}$$

where ρ is density, g acceleration of gravity, a wave amplitude, z water depth, and $\alpha = a/z$. Longuet-Higgins (1970 a, b) assumed the Chezy Law

$$B = C_f \rho |\bar{u}| \bar{u} \tag{3.16}$$

where $\bar{u}$ is the horizontal velocity, having both a steady and oscillatory component, and C_f is the drag coefficient on the bottom. Combining equations (3.12), (3.15), and the time-averaged expression of (3.16) and substituting into (3.14) gives a longshore velocity

$$\bar{V} = \frac{5\pi}{8} \frac{\alpha s}{C_f} gz \frac{\sin \theta}{c}. \qquad (3.17)$$

The extension of shallow-water theory out to the breaker line and the inclusion of lateral mixing across the breaker line result in

$$V_o = \frac{5\pi}{8} \frac{\alpha}{C_f} \sqrt{g z_B} \, (s \sin \theta_B) \qquad (3.18)$$

and

$$V_B = \frac{5\pi}{8} \frac{\alpha s}{C_f} \sqrt{g z_B} \, (s \sin \theta_B) \qquad (3.19)$$

respectively, where s is the beach slope.

As a result of this formulation, a family of semi-theoretical profiles of expected longshore current velocity across the surf zone can be established. These profiles (Figure 3.1) contain a single maximum located between the breaker line and the shore. Both the location of the maximum velocity as well as the shape of the longshore current velocity profile across the surf zone are dependent upon the lateral mixing parameter, P (Figure 3.1) where $P = (\pi/2)(sN/\alpha C_f)$. P is directly proportional to beach slope and to N, a dimensionless constant, and inversely proportional to α, the ratio of wave amplitude to breaker depth, and C_f, the coefficient of drag on the bottom. Hence, for similar wave and bottom roughness conditions, an increase in beach

slope should produce a decrease in the maximum longshore current velocity and broaden the distribution of current velocities across the surf zone. A decrease in the coefficient of bottom friction should produce a similar response of the expected longshore current. The horizontal eddy viscosity takes the form

$$\mu_e = N\rho|x|\sqrt{gh}$$

and is dependent upon position across the surf zone. The adoption of this form of horizontal eddy viscosity provides solutions to the longshore current flow field, based on linear wave theory. These solutions are given in terms of the parameter, P. As P increases the expected one-dimensional longshore current mean velocity distribution across the surf zone broadens and the maximum velocity moves shoreward.

The need for the inclusion of a lateral mixing term in steady longshore current theory has been eliminated by the probability approach of Collins (1972). The monochromatic wave field is replaced by a random sea incident at the outer surf zone and a result is obtained which is similar in form, but different in absolute valve, to that of monochromatic mixing theory. The effect of a sea surface composed of waves of varying wave heights and lengths results in waves breaking at different locations and at slightly different angles across the surf zone. The result of this

process is to generate a well-mixed surf zone (Figure 3.2).

The probabilistic formulation of Collins (1972) predicts that longshore current velocity will generally increase with increases in wave height, length and angle of approach. However, in contrast to monochromatic mixing theory, this probabilistic formulation predicts an intensification and narrowing of the longshore current flow field with increases in beach slope. Although both the monochromatic mixing theory and the probabilistic sea surface approach, to the prediction of the distribution of longshore current velocity, are attempting to eliminate a discontinuous velocity profile across the breaker line, the physical principles employed in these formulations appear to be significantly different.

As a result of these considerations, it is hypothesized that the horizontal distribution of longshore current velocity across the surf zone should depend upon both the degree and type of mixing. Mixing across the surf zone appears to be the result of horizontal eddy viscosity as well as mixing resulting from differential wave breaking. The physical realization of these two processes should produce a mean longshore current velocity distribution across the surf zone which is exemplary of a very well-mixed zone near the breaker line.

Vertical Current Structure

The general practice of vertically integrating the equations of motion (Bowen, 1969; Thornton, 1969; Longuet-Higgins, 1970; Collins, 1972) eliminates any vertical variation in the longshore current flow field. The vertical velocity profile must be known, in order to provide estimates of velocity gradients which, in turn, are necessary for the understanding of surf zone processes and sediment transport. The vertical structure of the longshore current flow field has not been theoretically treated or experimentally observed, prior to this investigation.

The vertical structure of the longshore current flow field may possibly be characterized as an oscillating turbulent boundary layer. However, for conditions of this field investigation and from the formulation of Teleki (1970), the thickness of the oscillating turbulent boundary layer was approximately 0.81×10^{-2}m. Based on these calculations it, therefore, appears that the expected thickness of the oscillating turbulent boundary layer is far too small to produce significant vertical structure in the longshore flow field.

Time Dependent Structure

In the presence of an oscillatory wave field incident on a beach, it is somewhat unrealistic to expect a steady or slowly varying longshore current. Unsteadiness of longshore currents has been noted for quite some time. However, the

magnitude and dominance of the unsteadiness in the flow field has only recently been fully appreciated (Dette, 1974; Wood and Meadows, 1975). As Galvin (1967) states, one of the principal unknowns responsible for uncertainty in field data is: "The effect of substituting a mean value for the distribution of values of each measured variable." It, therefore, appears that a time-dependent analysis of the shallow water wave and current flow field is needed.

It should be anticipated that at a fixed point in the surf zone, variations in the mean longshore current would occur over relatively short time periods as a result of incident waves. This time dependent character of longshore currents should be expected to persist horizontally across the surf zone and vertically from the surface to the bottom. From theoretical considerations the primary period of these fluctuations should be anticipated to correspond to the incident wave period at each particular location in the surf zone.

If the wave particle velocity is conservative over one wave period, then the net contribution to the longshore current over that time interval is zero. Conventional longshore current theory suggests the contribution to the longshore current flow field resulting from the wave horizontal particle velocity is $c_B \sin \theta_B$. This implies that the wave is totally translational and hence, the particle velocity is not conservative. When time averaged, this translational

particle velocity component is assumed to generate a mean longshore current, $\bar{V} = f(c_B \sin \theta_B)$. A shoaling wave field is composed of both translational and oscillatory wave components; thus, a combination of conservative and non-conservation contributions to the longshore current velocity field should be expected. It should further be anticipated that as the characteristics of the breaking waves change from spilling to plunging, the translational components should dominate.

It, therefore, appears that the total longshore current velocity resulting from a breaking wave field should be composed of both a steady and a fluctuating velocity component, expressed as

$$V = \bar{V} + V_W.$$

The steady component $\bar{V}$ is proportional to the translational component of incident waves and the fluctuating component V_W is directly proportional to the magnitude and periodicity of the first order horizontal particle velocity.

Long-period velocity fluctuations should also be anticipated to be present in the longshore current flow field. If a wave field incident at the outer surf zone is composed of more than one frequency, interactive wave phenomena may be anticipated. This type of wave field should result in periodic amplitude modulation of the wave heights to produce beats.

If the incident wave amplitude is periodically growing and decaying as a result of a beat, it should also be anticipated that the radiation stress will vary in magnitude at the beat frequency, $f(1/\Delta\sigma)$. In a group of high waves, both $S_{x'x'}$ and E will be large, causing $\bar{\eta}$ to be depressed (becomes negative). A relative depression should, therefore, be anticipated in the mean surface level, forcing a mean flow away from the region of high waves. However, beneath groups of small waves the opposite situation should be anticipated. Specifically, the mean surface level $\bar{\eta}$ is raised (becomes positive) and a mean flow occurs toward the region at low waves.

Longuet-Higgins and Stewart (1962) explain the balance of forces for this response of the free surface in the following way. Associated with a group of large waves, the radiation stress S_{xx} is large. The applied force to the surrounding fluid $- \partial S_{xx}/\partial x$ is positive in advance of the group of large waves and negative behind the wave group. The applied force, therefore, tends to act in opposition to the restoring force resulting from the free surface deformation. The sign of the restoring force should be anticipated to be negative in advance of the large wave group and positive behind the group. Preceeding the arrival of the wave group the mean surface should acquire an upward tilt, and should acquire a corresponding downward tilt following the wave group (Figure 3.3).

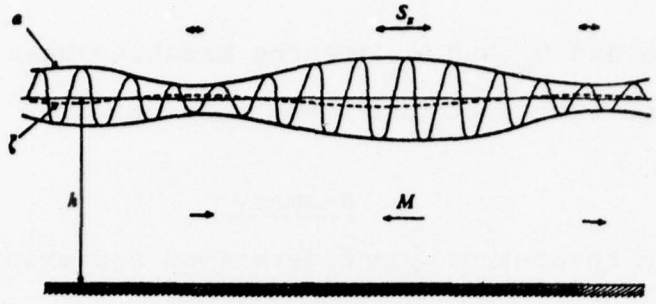

Figure 3.3

The theoretical expectation of the radiation stress to depress the mean surface beneath a group of high waves and to elevate the mean surface beneath a group of low waves (after Longuet-Higgins and Stewart, 1962).

Therefore, long-period fluctuations in the longshore current velocity field should be anticipated as a result of short-period wave interactions independent from any long-period swell present in the incident wave field.

As a result of these considerations, it is hypothesized that the total longshore current velocity is composed of at least three major components that are the direct result of the incident wave field. This total longshore current velocity vector should be composed of a mean longshore current velocity component and two fluctuating components, which are directly related to the incident breaking wave horizontal particle velocity and the long-period fluctuations resulting from wave interaction. Hence, the total longshore current velocity vector can be expressed as

$$V = \bar{V} + V_W + V_L$$

where $\bar{V}$ is the contribution by the steady longshore current

flow field and V_W and V_L are the breaking-wave period and long-period beat contributions, respectively.

Summary

From theoretical considerations and existing field and laboratory data, it should be anticipated that the total longshore current flow field should be composed of both a steady and a time-dependent component. Semi-theoretical considerations suggest that the steady component of the longshore current vector should vanish at both the shoreline and far offshore and contain a maximum between the breaker line and shore. The statistical representation of a random wave field appears to be the most reasonable representation of the nearshore environment. Use of the random sea concept appears to eliminate the need for inclusion of a horizontal mixing term in the momentum balance.

The practice of vertical integration of the conservation equations has precluded a theoretical expectation for vertical longshore current variability. Furthermore, prior to this investigation, no published observations of the vertical longshore current structure existed.

Application of the temporal dependency of longshore currents had previously received little theoretical attention and no experimental verification existed with regard to the time-dependent nature of the longshore current flow field. From physical considerations, it seems reasonable

to expect that significant time-dependent contributions to the longshore current flow field may arise from both direct velocity contributions associated with the longshore component of the wave horizontal particle velocity and from variations of the velocity field induced by interactive wave phenomena.

CHAPTER IV

FIELD EXPERIMENTS AND RESULTS

Introduction

Numerous semi-empirical and semi-theoretical formulations have been proposed for steady longshore current flow, however, experimental verification of these formulations are extremely limited. The model studies of Galvin and Eagleson (1965) and Eagleson (1965) provide the primary data by which these formulations have been tested. Although longshore currents have been generated and their velocities recorded in model basins, artificial barrier and basin constraints must be considered integral factors affecting the generation of these flow fields. Likewise, observations of longshore currents under field conditions have been extremely sparse and have lacked adequate experimental control. The employment of Lagrangian velocity measurements in early field studies as well as little or no simultaneous measurement of the incident wave field, have rendered these studies of little value to the theoretician. Recent Eulerian field investigations of longshore currents (Dette, 1974; Huntley

and Bowen, 1974) have also failed to provide simultaneous measurements of both the total longshore current velocity and incident wave fields. The dominant approach of these studies has been to install flow meters and wave probes on a tidal beach at low tide and allow the installation to become inundated with the rising tide. Longshore current velocities and water surface elevations were recorded over a tidal cycle. It is then argued that the distribution of measured current velocities across the surf zone, is not only representative of an instantaneous velocity profile obtained at fixed positions and known constant depths but is, in fact, equivalent to such measurements. Hence, it is apparent that comprehensive and well-documented sets of observations of longshore currents and wave conditions across the surf zone do not exist.

In order to avoid the restrictive nature and unavoidable boundary effects of model studies and to eliminate the ambiguity of previous field observations of longshore currents, two field investigations were conducted on an essentially tideless coast of Lake Michigan. The purpose of these investigations was to provide a complete and well-controlled set of observations of the horizontal and vertical distribution of longshore current. An Eulerian frame of reference was chosen for these observations to allow the best possible comparison with existing theoretical formulations.

The site of the field experimentation was chosen along the eastern shore of Lake Michigan, centrally located between the cities of Ludington and Pentwater, Michigan. This thirteen kilometer section of shoreline, extending approximately north-south is characterized by a multiple barred bathymetry with nearly straight and parallel contours. The beach in this region is composed of medium quartz sand with a mean diameter of 0.25 mm. The average tidal range is from 0 to 4.3 cm.

Monitoring of longshore current velocities and wave characteristics for both field experiments was only conducted when specific selected conditions existed. Specifically, a straight coastline, with parallel bathymetry, resulting in long-crested waves was required. In addition, only meteorological conditions which generated waves from either the west-southwest or west-northwest directions were acceptable for experimental monitoring.

These meteorological conditions generally produced waves with incident angles of twenty-five degrees or less. These wind wave fields consisted primarilly of

spilling breakers, hence, the complication of dealing with surf conditions composed of both spilling and plunging breakers was eliminated. It was also found that waves greater than approximately one meter in height may break at multiple locations offshore. Hence, a wave height limitation was imposed such that only conditions of waves breaking on the inner bar were considered for this investigation.

1974 Field Experiment

The first longshore current experiment, conducted on September 21, 1974, utilized three ducted impeller flow meters which were oriented parallel to the shoreline and were positioned at equally spaced vertical intervals (Figure 4.1). The upper meter was placed below the level of the lowest wave trough so that it was continuously submerged. The lower meter was placed adjacent to the bottom and the middle meter was placed half way between the upper and lower meters. Sequential measurements were made with this vertical current meter array at three locations across the surf zone. The outermost current monitoring station, was located

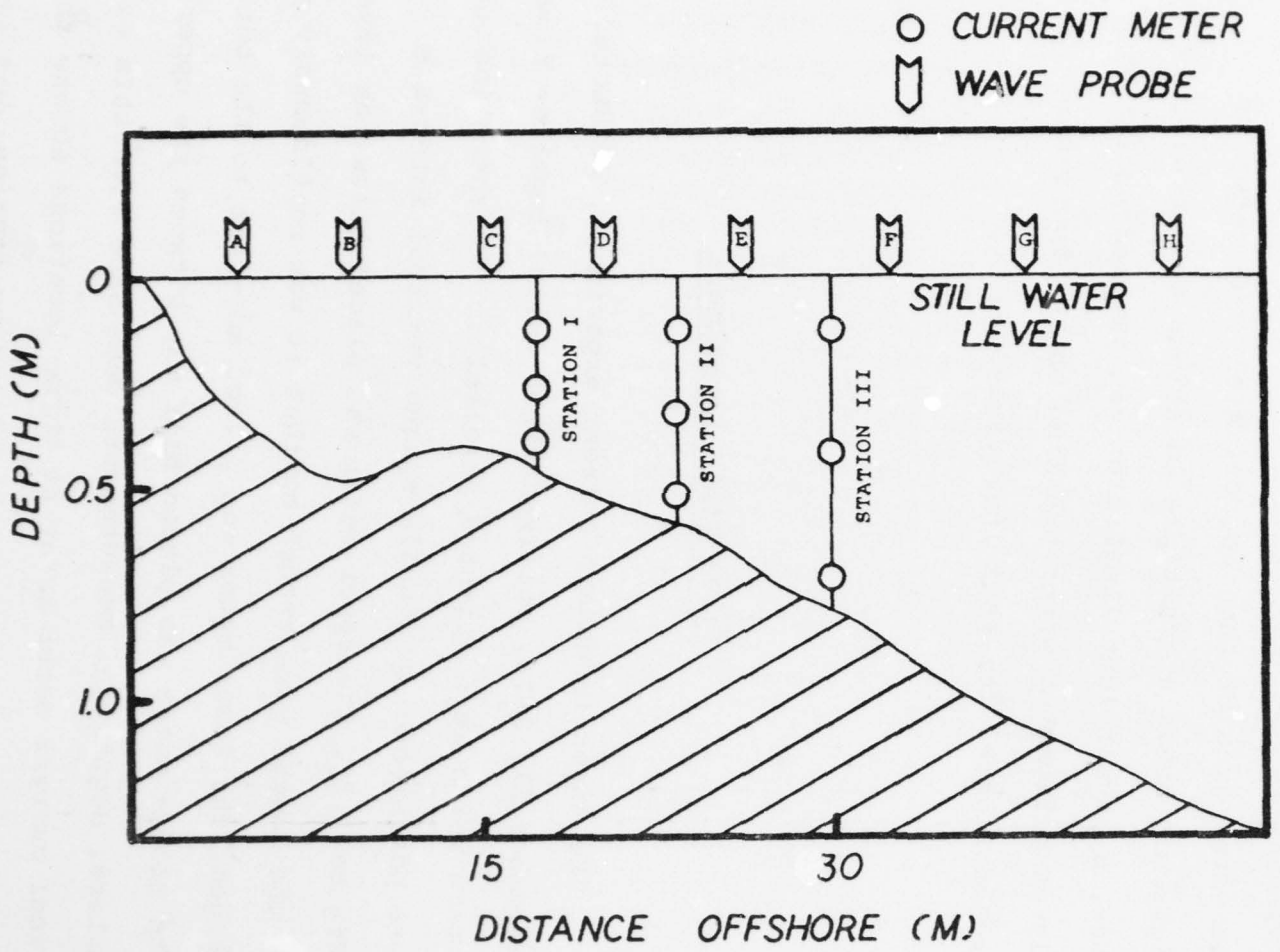

Figure 4.1 Bathymetric profile showing current meter locations and wave monitoring stations for Experiment I.

within the zone of active breaking. The inner stations, were located five and ten meters, respectively, shoreward of the deep water station. Maximum wave breaking occurred at the center station, hence, all three meter arrays were within the breaker zone. The total distance from the outer limit of the breaker zone to the shore was approximately forty-five meters.

Wave characteristics were monitored simultaneously at eight wave monitoring stations spaced approximately five meters apart from deep water to the shore. Incident wave period and celerity measurements were made with a series of surface piercing point gauges positioned at each wave monitoring station, oriented on a line perpendicular to the shoreline (Wood, 1973). The passage of a wave crest was recorded as an event for each sensor on an analog recorder. From the arrival times of an individual wave crest at two successive wave monitoring stations, mean wave celerity over that spatial interval can be calculated. These calculations were performed at wave monitoring station F, where visual breaking wave height observations were made. Breaking wave heights were recorded visually from shore with tripod mounted ten power binoculars focused on a survey level rod mounted on wave monitoring station F. Between ninety-two to one hundred fifty observations of breaking wave heights were made for each data run.

During constant sea state conditions, longshore current velocities and wave characteristics were simultaneously monitored, continuously for fifteen minute periods separated by fifteen minute intervals. During these interval periods, the array of three current meters was relocated at a predetermined position within the surf zone. These longshore current monitoring positions were chosen in an effort to investigate the anticipated maximum longshore current velocity near breaking. Before and after each monitoring period the sensors were inspected and their operation checked. Following relocation of the longshore current sensing array, the vertical spacing of the meters was re-established such that the vertical water column was equally partitioned. Wave and longshore current data were recorded on analog recorders as discrete on-off signals. These recorders were housed in a mobile shore based installation.

Hydrographic surveys were conducted, at close spatial intervals, offshore to a position outside the surf zone and alongshore to a distance of one surf zone width. The mean beach slope in the nearshore region was approximately one to forty. Slopes in the offshore region decrease to as shallow as one to one hundred.

Data Results

Experiment I resulted in the simultaneous acquisition of longshore current velocity data at three vertical

positions through the surf zone water column. Four successive fifteen-minute runs using this experimental configuration were conducted at three current meter array locations through the breaker zone. In addition, concurrent observations of wave period and wave height were made during each fifteen-minute longshore current monitoring period.

These data showed that significant temporal variability existed in the longshore current flow field. Hence, a second field investigation, designed to provide a complete time synchronous documentation of time-dependent longshore current velocities and surface wave time histories throughout the surf zone was initiated.

1976 Field Experiment

The second longshore current experiment, conducted November 1, 1976, along the same section of Lake Michigan shoreline used in the 1974 experiment, consisted of the simultaneous monitoring of the outputs of eight step resistance wave probes and twelve ducted impeller flow meters (Figure 4.2).

Simultaneous measurements of wave height and period were made with surface piercing wave staffs on a line perpendicular to the shoreline. Six wave monitoring stations were placed at ten meter intervals from the outer surf zone to the shore. Two additional wave probes were oriented at right angles to the continuous line of wave probes to determine the incident wave angle at breaking (Figure 4.3).

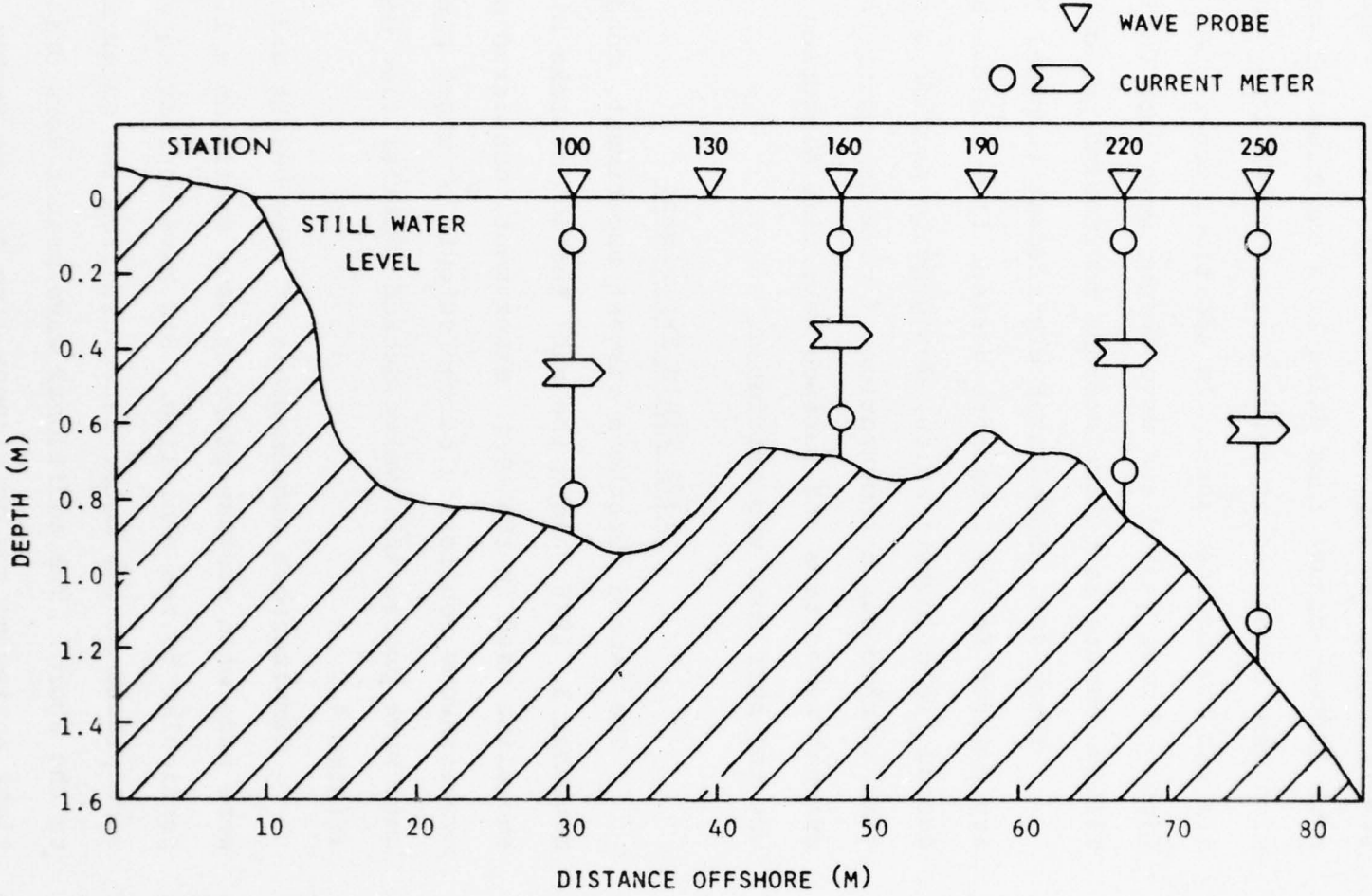

Figure 4.2 Bathymetric profile showing current meter locations and wave monitoring stations for Experiment II.

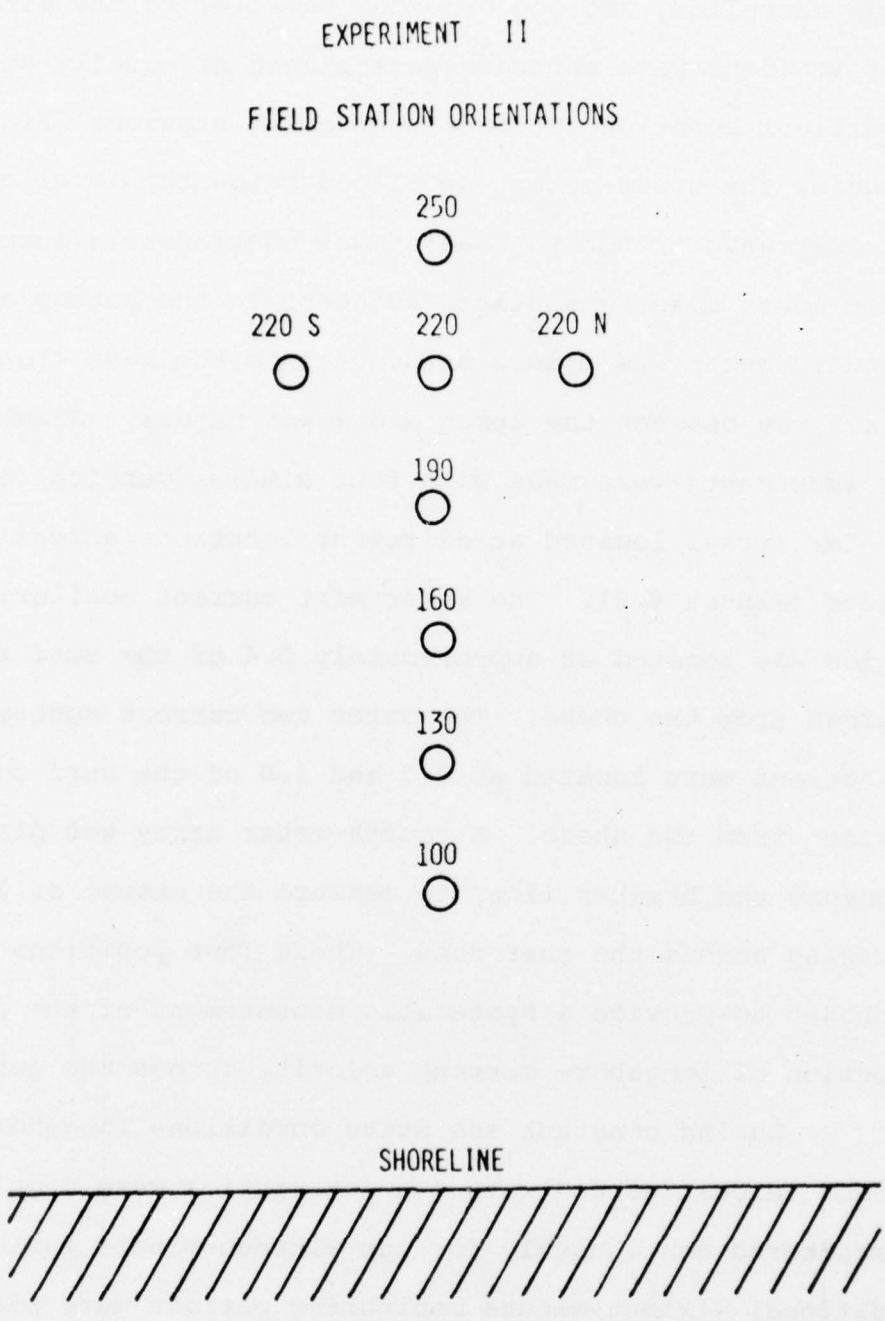

Figure 4.3 Plan view of field station orientation for Experiment II.

Two ducted impeller flow meters oriented parallel to the shoreline, and one oriented parallel to the direction of incident wave approach were placed at equally-spaced vertical positions at four monitoring stations (Figure 4.2). Again, the upper meter was placed below the level of the lowest wave trough so that it was continuously submerged. The lower meter was placed adjacent to the bottom and the middle meter was placed orthogonal to the wave crests and half way between the upper and lower meters. Simultaneous measurements were made with four similar vertical current meter arrays located at different locations across the surf zone (Figure 4.2). The inner most current monitoring station was located at approximately 0.4 of the surf zone width from the shore. The outer two current monitoring stations were located at 0.7 and 1.0 of the surf zone width from the shore. A fourth meter array was placed beyond the breaker line, to measure the extent of lateral mixing across the surf zone. These four positions were chosen to provide a systematic measurement of the distribution of longshore current velocity across the surf zone.

During constant sea state conditions longshore current velocities and wave characteristics were simultaneously monitored continuously for one sixteen-minute period. Additional sixteen-minute monitoring periods were planned for this experiment; however, they were not conducted due to severe storm conditions which destroyed the instrument arrays.

Hydrographic surveys were conducted, at close spatial intervals, offshore to a position outside the surf zone and alongshore to a distance of one surf zone width. The mean beach slope in the nearshore region was approximately one to forty. Slopes in the offshore region decrease to as shallow as one to one hundred.

Although the mean nearshore beach slopes were similar for both experiment I and II, the relative importance of the offshore bar is markedly different. The subaqueous bar present during experiment I, appears as a minor inflection in the offshore profile. In contrast, the bar present during experiment II was a major feature of the nearshore bathymetry. It should, therefore, be anticipated that results obtained from experiment I may be more likely related to conditions of a planer beach. Bathymetric conditions existing during experiment II were typical of a well-developed barred beach.

Data Results

During the course of experiment II the step resistance wave probe at station 220 became inoperative. In addition to the loss of the surface time history at station 220, this failure resulted in the loss of the ability to resolve the angle of approach of each individual wave as it passed through the sensor grid. Incident wave angles were measured relative to the known positions of the station grid.

The continuous observations of the onshore component of wave horizontal particle velocity obtained from the four meters oriented parallel to the direction of wave approach could not be used. The sampling interval of these meters was not sufficient to adequately resolve continuous breaking wave horizontal particle velocity. However, these meters did provide a measure of the maximum onshore component of the breaking wave horizontal particle velocity.

Experiment II resulted in the simultaneous acquisition of: longshore current velocities at two elevations at each of four stations across the surf zone; the maximum onshore component of breaking wave horizontal particle velocity at four locations across the surf zone; and water surface elevation time histories at seven locations across the surf zone. All data were recorded simultaneously and continuously for sixteen minutes. A summary of all data collected during both field experiments is presented in Tables 4.1 and 4.2.

Instrumentation and Calibration

Longshore current velocity and breaking wave horizontal particle velocity measurements were obtained with ducted impeller flowmeters (Wood, 1968). Modifications of these meters to sense impeller rotation utilizing a light emitting diode system was employed to remove any magnetic coupling between impeller and meter housing. These unidirectional flowmeters provide a rapid response time (0.1 second) and an excellent resolution of velocities from 0.04 m/sec. to 2.8 m/sec. The response of this flow meter is linear to

Table 4.1

DATA COLLECTED, EXPERIMENT I

Experiment I 21 September, 1974

	Run I	Run II	Run III	Run IV
Surface longshore currents measured *	X	X	X	X
Mid-depth longshore currents measured *	X	X	X	X
Bottom longshore currents measured *	X	X	X	X
Visual breaking wave height observations	X	X	X	X
Incident breaking wave period measured *	X	X	X	X
Incident breaking wave celerity measured	X	X	X	X
Incident breaking wave angle visually observed	X	X	X	X

* Fifteen minute time histories

Table 4.2

DATA COLLECTED, EXPERIMENT II

Experiment II 1 November, 1976

	Run I							
	ST 100	ST 130	ST 160	ST 190	ST 220S	ST 220	ST 220N	ST 250
Surface longshore currents measured *	X		X			X		X
Bottom longshore currents measured *	X		X			X		X
Maximum incident wave horizontal particle velocity *	X		X			X		X
Free surface elevation (height and period) *	X	X	X	X	X		X	X
Incident breaking wave angle visually observed	X		X			X		X

* Sixteen minute time histories

axial flow. These flow meters also have a cosine response to off-axis flow, satisfying the relationship

$$v_\theta = v \cos \theta$$

where v is the free stream velocity and θ is the angle between the axis of the sensor and the axis of the flow (Wood, 1968). Cosine response to off-axis flow is a necessary requirement for any investigation in which the principal flow axes of interest do not either coincide or form right angles with each other.

The output signal from the impeller sensors are discrete on-off signals which are recorded as an event on an analog recorder. The resulting data record is composed of a series of full scale deflections and zero level intervals. The interval between pulses represents the time average velocity of the flow field for a discrete time interval.

Each flow meter used in this investigation was calibrated both before and after the field experiments. Static calibration tests were carried out to determine the response of each flow meter to axial flow. The tow tank facilities of the Department of Civil Engineering, Purdue University, were utilized for these calibrations. Each meter was towed at sixteen constant speeds ranging from 0.12 to 1.82 m/sec. for the total 45 m length of the facility. The time required to travel the last 33 m was recorded with an electronic timer. From this calibration test data a velocity calibration curve was constructed for each current meter.

A least squares polynomial regression was performed on each calibration curve to determine the "best fit" equation for the response of that meter. These regression equations were then utilized to convert the recorded impeller rotation rate of the meter to an average velocity over that interval. These calibration curves were compared before and after the field experimentation to insure the response of each meter did not vary.

Surface time histories throughout the surf zone were obtained by utilizing conventional step resistance wave probes (e.g., Caldwell, 1956; Russell, 1963; and Wood, 1970). These wave probes consist of a series of equally spaced sensing electrodes and a ground electrode. Each electrode is individually wired to a circuit of known resistance. Hence, a voltage drop across the circuit occurs as each successive electrode is immersed in water. The output signal from these wave probes is then recorded on an eight-channel analog recorder. Hence, a nearly continuous, synchronous time history of the water surface elevations at each wave probe location is available.

Summary

As a result of these field investigations, an integrated time synchronous, set of water surface elevations and longshore current velocity measurements exist under natural controlled conditions. Velocity profiles of the

mean longshore current across the surf zone as well as vertically through the water column have now been measured. The current monitoring system employed in this investigation allowed acquisition of data on a sufficiently short time interval to document the time dependent character of the flow field at each sensing location. To supplement the longshore current velocity data, characteristics of the shallow water surface wave field were synchronously measured, thus, allowing direct comparison between longshore current velocity and incident wave characteristics.

CHAPTER V

ANALYSIS AND RESULTS

Introduction

Previous field and laboratory observations of longshore currents have provided good, qualitative descriptions of nearshore circulation. These observations have aided in determining those processes important to the surf zone as well as in development of theoretical models of the longshore current flow field. However, few of these observations were accompanied by simultaneous observations of the incident wave field throughout the surf zone. Obviously, determination of driving forces of longshore currents, independent of a detailed knowledge of the surf zone wave field, is difficult.

In addition, the horizontal and vertical distribution of the longshore current flow field has not been observed in the field. No complete two-dimensional mapping of this nearshore flow structure is available. Yet, a detailed knowledge of this flow structure is necessary in order to predict sediment transport rates and coastal response to severe storms.

This investigation was conducted to obtain simultaneous and continuous measurements of longshore current velocity

and incident wave parameters, necessary to determine horizontal and vertical longshore current velocity distributions and their variability with time. These measurements were also designed to provide information about the total longshore current flow field and its relationship to surf zone driving forces, initiated by the incident wave field.

Preliminary Data Reduction and Analysis

Data obtained in both experiments from the ducted impeller flow meter arrays were recorded on analog recorders. The time intervals between discrete on-off signals of the meters were digitized and converted to an average velocity over each interval. These continuous velocity data were then smoothed and interpolated on 0.25 second time intervals. Data from surface piercing wave sensors were also recorded on an analog recorder. These records were digitized and interpolated to equal, 0.25 second, time intervals.

A preliminary analysis of both the wave and longshore current data was performed to determine the mean, range and standard deviation of each measured variable. This analysis was necessary to identify those data which met the criteria of a constant sea state. Conditions acceptable for further data analysis precluded growth or decay of either the mean incident wave height or the mean longshore current velocity.

The mean, range and standard deviation of incident wave height fields for both experiments are presented in Tables 5.1 and 5.2.

Table 5.1

BREAKING WAVE HEIGHT STATISTICS

Experiment I	$\bar{H}$(M)	Range (M)	S(M)
Run I	0.59	0.34 - 0.75	0.07
Run II	0.58	0.42 - 0.77	0.06
Run III	0.58	0.45 - 0.77	0.06
Run IV	0.52	0.29 - 0.80	0.11

Table 5.2

WAVE HEIGHT STATISTICS ACROSS THE SURF ZONE

Experiment II	$\bar{H}$(M)	Range (M)*	S(M)
Station 250	0.23	0.10 - 0.65	0.12
Station 220	--	Inoperative	--
Station 220N	0.23	0.10 - 0.54	0.14
Station 220S	0.24	0.10 - 0.74	0.16
Station 190	0.18	0.10 - 0.42	0.11
Station 160	0.12	0.10 - 0.40	0.07
Station 130	0.12	0.10 - 0.38	0.05
Station 100	0.11	0.10 - 0.34	0.06

*Lower limit of range represents actual smallest wave height used in analysis

Probability distributions of incident breaking wave height were constructed for data obtained during each run of Experiment I (Figures 5.1 - 5.4). The means of these incident wave height distributions were statistically

Figure 5.1 Observed breaking wave height probability distribution of Run I, Experiment I.

Figure 5.2 Observed breaking wave height probability distribution of Run II, Experiment I.

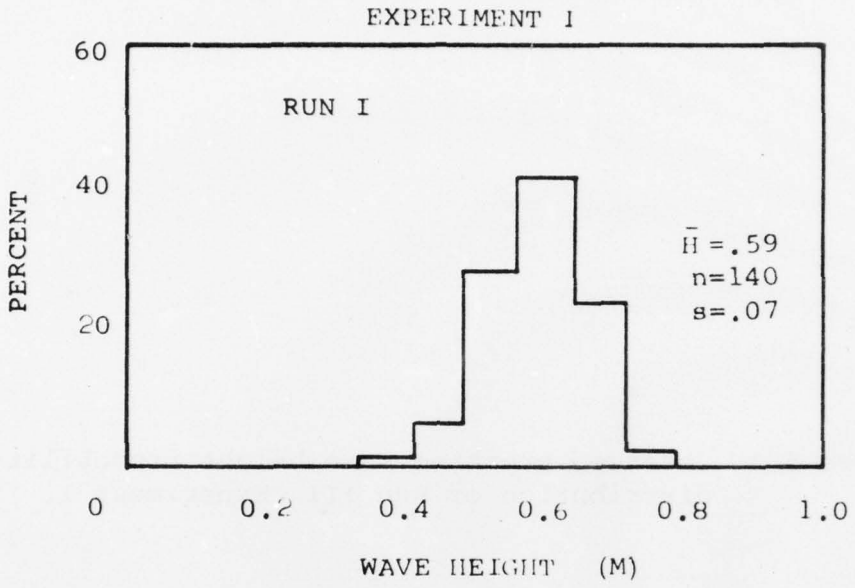

Figure 5.1

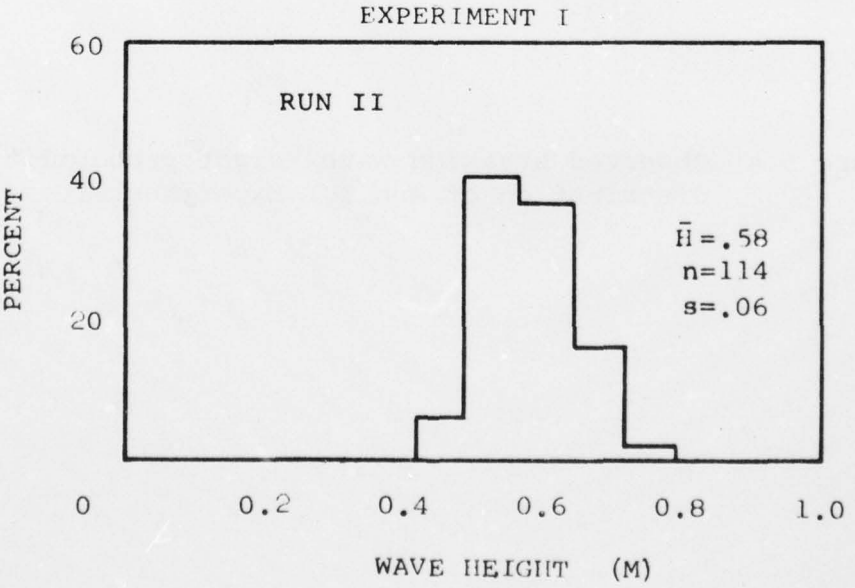

Figure 5.2

Figure 5.3 Observed breaking wave height probability distribution of Run III, Experiment I.

Figure 5.4 Observed breaking wave height probability distribution of Run IV, Experiment I.

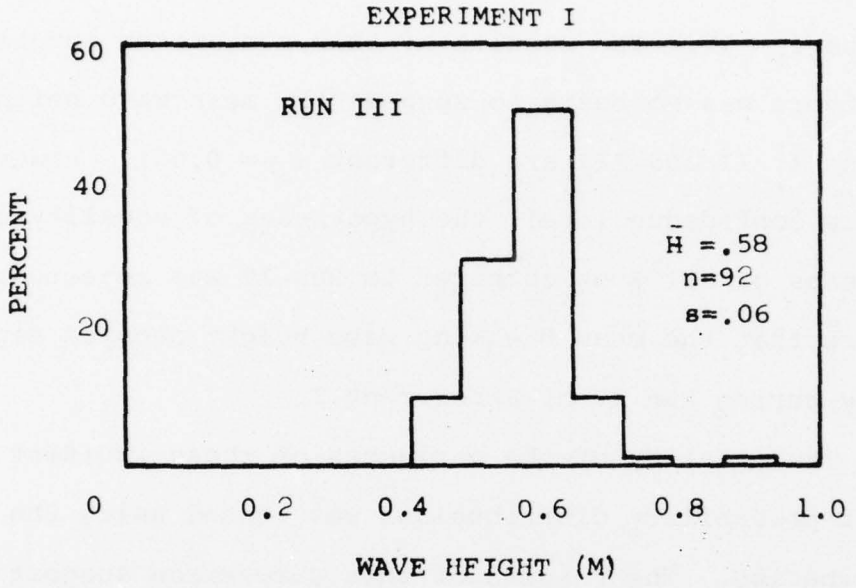

Figure 5.3

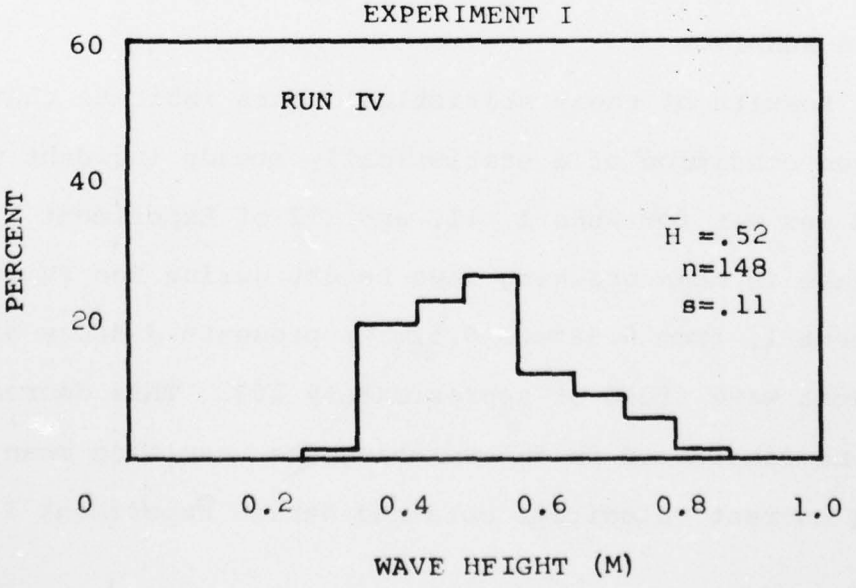

Figure 5.4

compared to test the hypotheses that each pair of samples could be members of the same population. The t-test was used for this comparison of the mean breaking wave heights of Runs I - IV. The results of this comparison suggested that there was no basis to suggest the mean wave heights of Runs I, II and III are different ($\gamma = 0.05$). However, at this confidence level, the hypotheses of equality of the means of all Runs compared to Run IV was rejected. It appears that the mean breaking wave height decayed significantly during Run IV of Experiment I.

The equality of the variances of these incident wave height probability distributions was tested using the F-distribution. The results of this comparison suggest that samples obtained during Runs I, II and III were drawn from populations having equal variances ($\gamma = 0.05$). This hypothesis was rejected for the wave height distribution obtained during Run IV.

Results of these statistical tests indicate that the desired condition of a statistically steady incident wave field was met for Runs I, II, and III of Experiment I. The decrease in mean breaking wave height during Run IV of Experiment I, from 0.58m to 0.52m, represents a decay of the incident wave field of approximately 10%. This decrease must be considered in interpreting the resulting mean longshore current velocities obtained during Experiment I, Run IV.

Probability distributions of observed incident wave height were also constructed for data obtained at Station 250 during the one sixteen-minute run of Experiment II. In order to evaluate the hypothesis that the incident wave field remained statistically steady in its mean during Experiment II, a probability distribution constructed from the first eight minutes of the experiment was compared with a distribution from the last eight minutes (Figures 5.5 and 5.6). The t-test was used for this comparison of the mean breaking wave heights at Station 250. The results of this comparison indicated that there was no basis to suggest the mean wave heights of the first eight minutes differed from the mean wave heights of the last eight minutes at all values of γ. The equality of the variances of these incident wave height probability distributions was also tested using the F-distribution. The results of this comparison suggest that samples obtained from both distributions were drawn from populations having equal variances, at all values of γ. An additional statistical comparison of these distributions was made using the Kolmogorov-Smirnov Test. The purpose of this test is to determine the equality of two sample distributions and is considered a more severe test than the t-test (Chapman 1959). Results of this analysis suggest that the hypothesis that the two samples came from the same distribution may be rejected with probability of 99.999 of being incorrect. Hence, there is

Figure 5.5 Observed incident wave height probability distribution at Station 250, Experiment II, first 480 seconds.

Figure 5.6 Observed incident wave height probability distribution at Station 250, Experiment II, last 480 seconds.

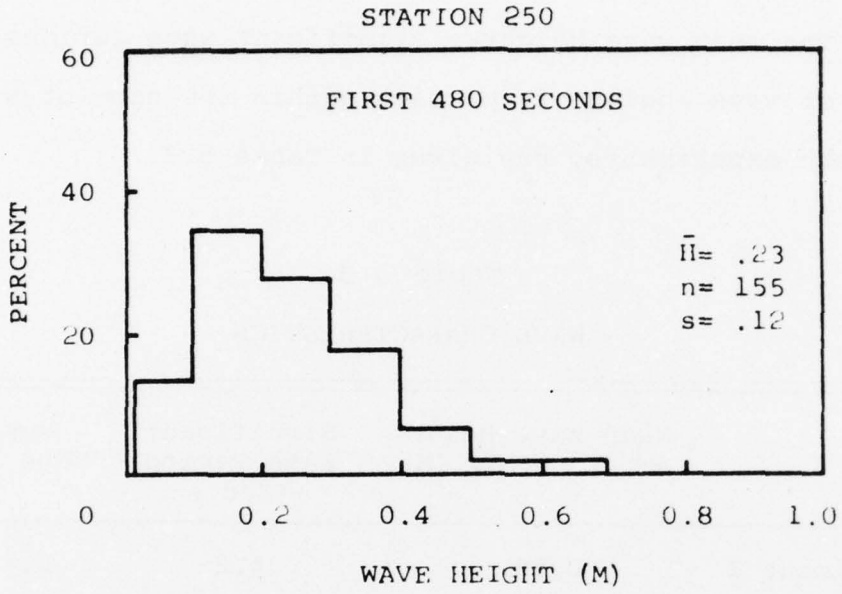

Figure 5.5

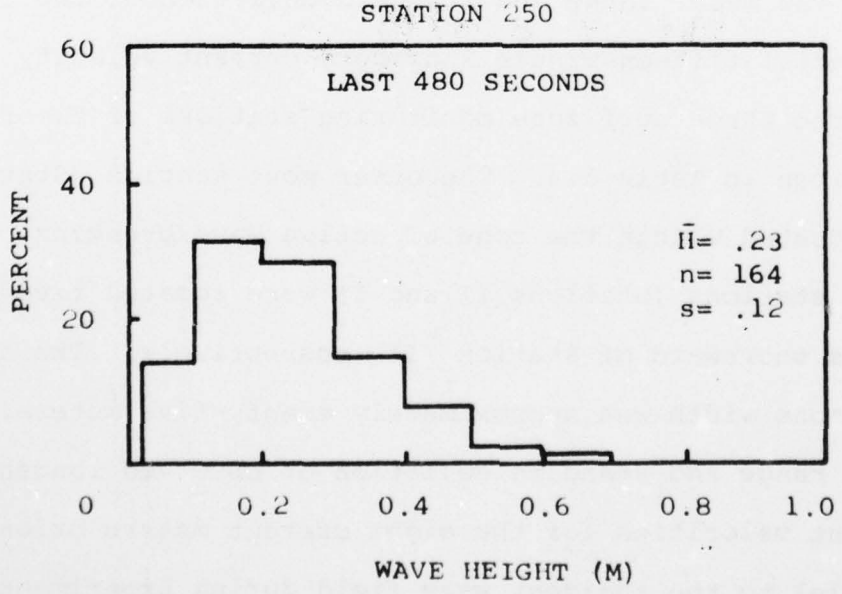

Figure 5.6

no basis to suggest that the mean wave height and distribution of wave heights were not statistically steady during Experiment II.

The mean wave heights, significant wave periods and range of wave angles of approach within the zone of study for both experiments, are given in Table 5.3.

Table 5.3

WAVE CHARACTERISTICS

	Mean Wave Height at Breaking (M)	Significant Wave Period (Sec.)	Range of Wave Angles
Experiment I	0.58	4.2	21° ± 5°
Experiment II	0.23	3.45, 3.73	15° ± 5°

The mean, range and standard deviation of the four sequential fifteen-minute longshore current velocity records from the three surf zone monitoring stations of Experiment I are given in Table 5.4. The outer most station (Station III) was located within the zone of active wave breaking. The inner stations (Stations II and I) were located five and ten meters shoreward of Station III, respectively. The total surf zone width was approximately twenty-five meters. The mean, range and standard deviation of observed longshore current velocities for the eight current meters oriented parallel to the incident wave field during Experiment II are given in Table 5.5. The range of observed maximum

Table 5.4

LONGSHORE CURRENT DATA,
EXPERIMENT I
(m/sec)

	Station II Run I	Station II Run II	Station I Run III	Station II Run IV
SURFACE METER				
mean velocity	0.66	0.63	0.69	0.64
range of velocities	2.08 - 0.30	1.92 - 0.30	1.28 - 0.30	1.43 - 0.30
standard deviation	0.22	0.25	0.21	0.22
MIDDLE METER				
mean velocity	0.64	0.60	0.62	0.61
range of velocities	1.94 - 0.31	1.13 - 0.30	1.13 - 0.31	1.24 - 0.31
standard deviation	0.26	0.20	0.18	0.20
BOTTOM METER				
mean velocity	0.60	0.61	0.54	0.63
range of velocities	1.36 - 0.31	1.15 - 0.31	1.05 - 0.31	1.15 - 0.31
standard deviation	0.20	0.19	0.18	0.26

Table 5.5

LONGSHORE CURRENT DATA,
EXPERIMENT II
(m/sec)

	Station 100	Station 160	Station 220	Station 250
SURFACE METER				
mean velocity	0.21	0.30	0.19	0.33
range of velocities	1.13 - 0.0	0.75 - 0.15	0.34 - 0.12	1.64 - 0.18
standard deviation	0.12	0.08	0.03	0.18
MIDDLE METER				
range of velocities	1.69 - 0.0	1.77 - 0.0	1.62 - 0.0	1.63 - 0.0
BOTTOM METER				
mean velocity	0.25	0.30	0.19	0.26
range of velocities	1.23 - 0.0	1.18 - 0.16	0.44 - 0.14	1.05 - 0.14
standard deviation	0.16	0.09	0.03	0.12

horizontal particle velocities for each of the four flow meters oriented into the incident wave field, during Experiment II, are also shown in Table 5.5.

A summary of all analyses performed on data collected during this investigation is presented in Tables 5.6 and 5.7. Longshore current and incident wave data analyzed from Experiment I is summarized in Table 5.6. Longshore current velocities, wave particle velocities and incident wave data analyzed from Experiment II are summarized in Table 5.7.

Longshore Currents Across the Surf Zone

Time averaged, steady state, longshore current velocities, calculated from the total longshore current velocity series, provide the only direct means of comparing observations with existing longshore current theory. Theoretically derived, one-dimensional, steady state, longshore current velocity profiles across the surf zone have been suggested by several authors. However, the theory of Longuet-Higgins (1970 a and b) remains the most widely accepted formulation to date. Alternative formulations have been suggested by: Collins (1972), to represent the incident wave field statistically; Thornton (1971), to incorporate a variable horizontal eddy viscosity into the longshore current formulation; and James (1974 a&b), to include a slightly non-linear hyperbolic free surface expression. The formulation of Collins (1972) provides an alternative approach to Longuet-Higgins (1970 a and b) longshore current prediction while

Table 5.6

DATA ANALYZED EXPERIMENT I (9/21/74)

Total Available Data	Mean Values Calculated	Range of Values Calculated	Standard Deviation Calculated	Spectra Calculated	Time Series Decomposed
Run I					
Wave Data	X	X	X	X	-
Surface Meter (V)	X	X	X	X	X
Middle Meter (V)	X	X	X	X	X
Bottom Meter (V)	X	X	X	X	X
Run II					
Wave Data	X	X	X	X	-
Surface Meter (V)	X	X	X	X	X
Middle Meter (V)	X	X	X	X	X
Bottom Meter (V)	X	X	X	X	X
Run III					
Wave Data	X	X	X	X	-
Surface Meter (V)	X	X	X	X	X
Middle Meter (V)	X	X	X	X	X
Bottom Meter (V)	X	X	X	X	X
Run IV					
Wave Data	X	X	X	X	-
Surface Meter (V)	X	X	X	X	X
Middle Meter (V)	X	X	X	X	X
Bottom Meter (V)	X	X	X	X	X

(-) Indicates data analysis not available.

Table 5.7

DATA ANALYZED EXPERIMENT II (11/1/76)

Total Available Data	Mean Values Calculated	Range of Values Calculated	Standard Deviation Calculated	Spectra Calculated	Time Series Decomposed
Station 250					
Wave Data	X	X	X	X	X
Surface Meter (V)	X	X	X	X	X
Middle Meter (U)	X	X	X	X	-
Bottom Meter (V)	X	X	X	X	X
Station 220					
Wave Data	-	-	-	-	-
Surface Meter (V)	X	X	X	X	X
Middle Meter (U)	X	X	X	X	-
Bottom Meter (V)	X	X	X	X	X
Station 190					
Wave Data	X	X	X	X	X
Station 160					
Wave Data	X	X	X	X	X
Surface Meter (V)	X	X	X	X	X
Middle Meter (U)	X	X	X	X	-
Bottom Meter (V)	X	X	X	X	X
Station 130					
Wave Data	X	X	X	X	X
Station 100					
Wave Data	X	X	X	X	X
Surface Meter (V)	X	X	X	X	X
Middle Meter (U)	X	X	X	X	-
Bottom Meter (V)	X	X	X	X	X

(-) Indicates data analysis not available.

AD-A064 079 PURDUE UNIV LAFAYETTE IND GREAT LAKES COASTAL RESEAR--ETC F/G 8/3
A FIELD INVESTIGATION OF THE SPATIAL AND TEMPORAL STRUCTURE OF --ETC(U)
DEC 78 G A MEADOWS N00014-75-C-0716
UNCLASSIFIED TR-6 NL

2 OF 2
AD
A064078

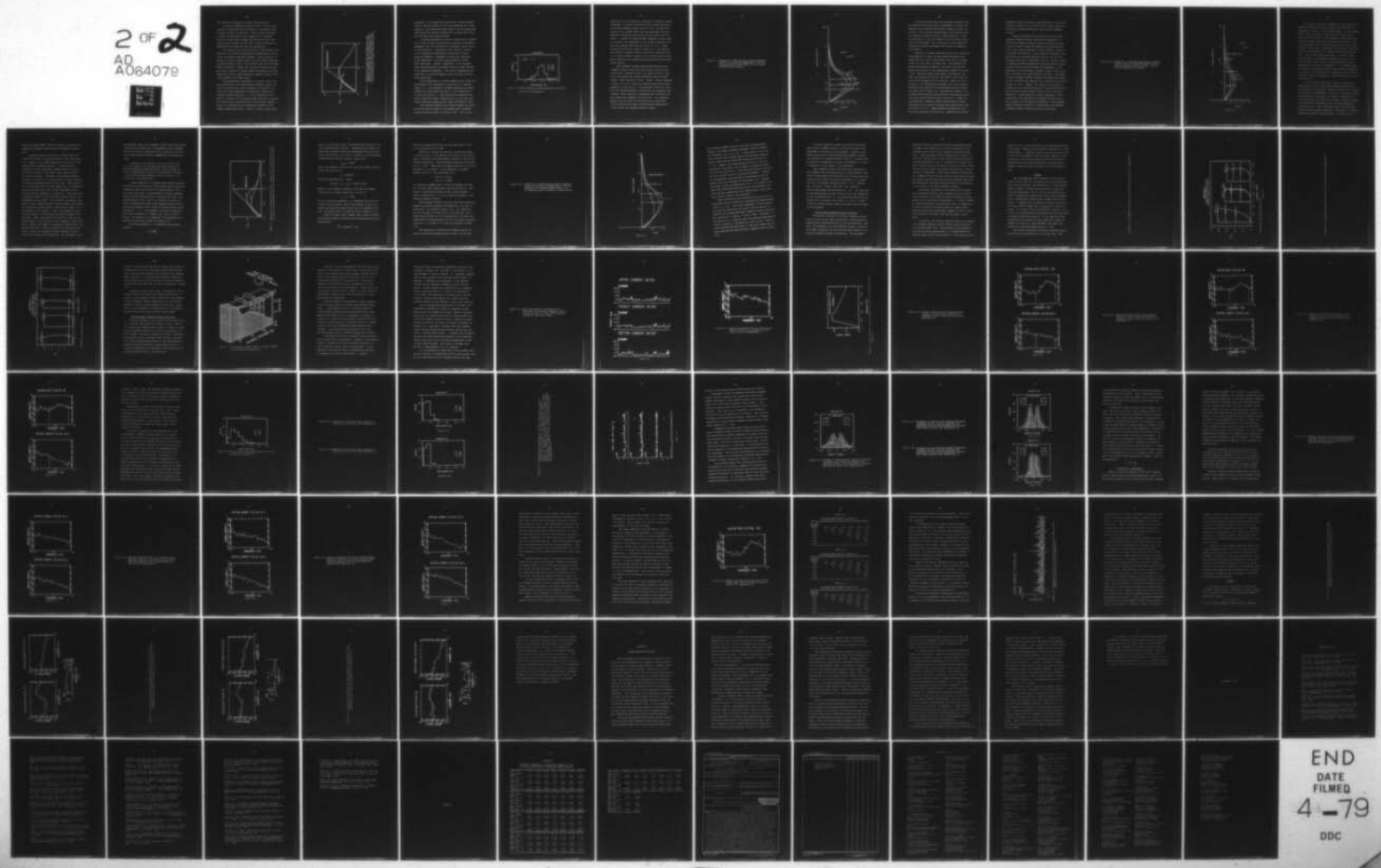

END
DATE FILMED
4-79
DDC

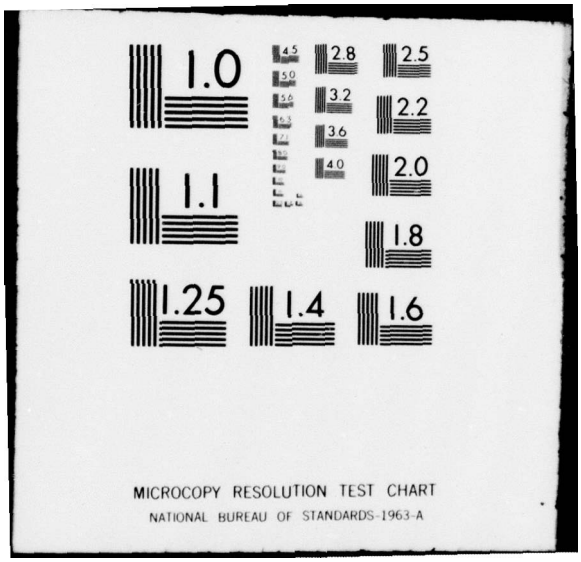
1.0
1.1
1.25
1.4
1.6
1.8
2.0
2.2
2.5
2.8
3.2
3.6
4.0
4.5
5.0
5.6
6.3
MICROCOPY RESOLUTION TEST CHART
NATIONAL BUREAU OF STANDARDS-1963-A

the theories of Thornton and James simply modify it.

Solutions suggested by Thornton (1971) rely on an estimation of magnitude and distribution of horizontal eddy viscosity across the surf zone. Thornton shows solutions in which the magnitude of the kinematic eddy viscosity varies by three orders of magnitude across the surf zone. This variation across the surf zone is very influential in determining the resulting velocity distribution.

The slightly non-linear solutions of James produce two effects on the profiles generated by Longuet-Higgins (1970). First, the predicted maximum longshore current velocity is reduced as much as eighty percent from the values suggested by Longuet-Higgins (1970), for the same input wave and bathymetric conditions. Second, the location at which the maximum velocity occurs is shifted toward the breaker line thus, producing slightly higher predicted longshore current velocities seaward of the break point.

The probabilistic formulation of Collins (1972), for the distribution of the mean surface longshore current velocity across the surf zone, represents an attempt to include the random properties of natural wave fields into longshore current prediction. In this formulation, the need for inclusion of a horizontal eddy viscosity to account for lateral mixing across the surf zone has been removed. Mixing is accounted for by differential breaking of the random incident wave field. Figure 5.7 shows a generalized

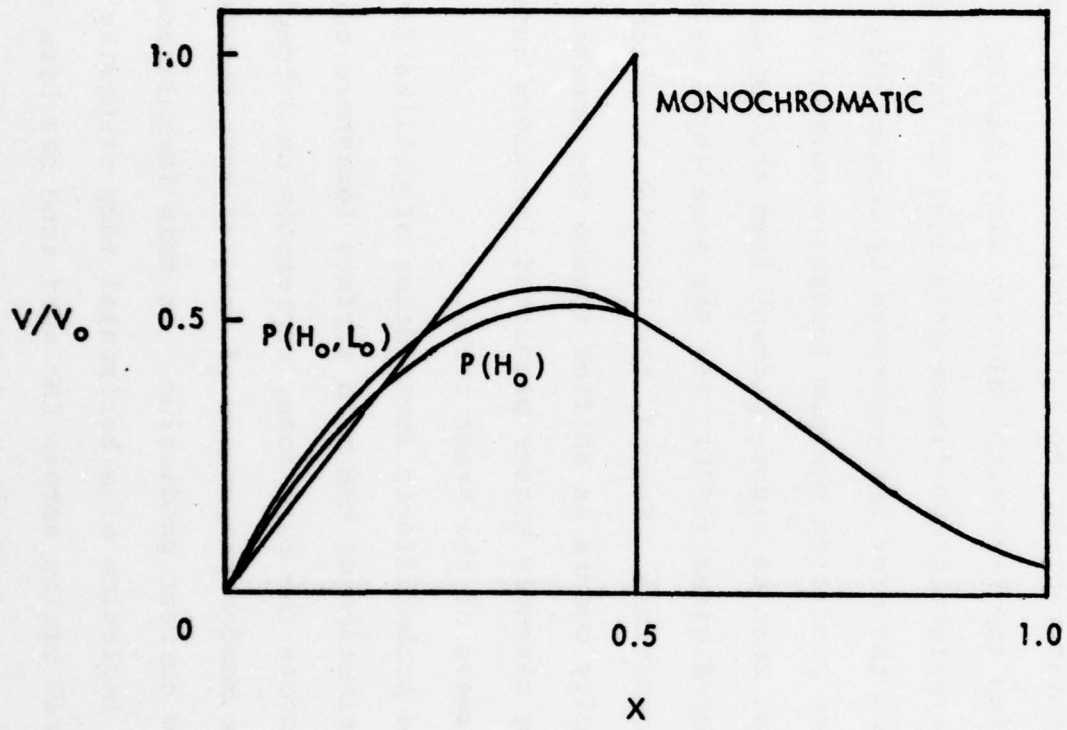

Figure 5.7 Comparison of predicted non-dimensional surface mean longshore current velocity profiles across the surf zone for, monochromatic, one-, and two-dimensional incident wave distributions.

comparison of the predicted distribution of mean longshore current velocity across the surf zone generated for a monochromatic, one-dimensional (wave height) and two-dimensional (wave height and length) probabilistic incident wave field with the same total energy content.

A further advantage of Collins' probabilistic formulation is the ability to incorporate variations in nearshore bathymetry into the calculation of longshore current velocity distributions. Furthermore, this numerical solution is not necessarily restricted to conditions of gently sloping bathymetry. Bathymetric conditions prevailing during Experiment I are best approximated by a planar beach topography. However, Experiment II was conducted under conditions where an offshore bar was a major feature of the nearshore bathymetry. This latter bathymetric configuration is the more commonly occurring form of natural sandy coastlines.

During Experiment I the mean breaking wave height was determined to be 0.58 meters at a period of 4.2 seconds (Table 5.3). The cumulative incident breaking wave height probability distribution for Runs I - IV of Experiment I is given by Figure 5.8. This distribution possesses the nearly symetrical shape, characteristic of surf zone wave height probability distributions (Wood and Meadows, 1975).

This observed breaking wave height probability distribution was used as input to the probabilistic longshore current prediction model of Collins (1972). Due to the

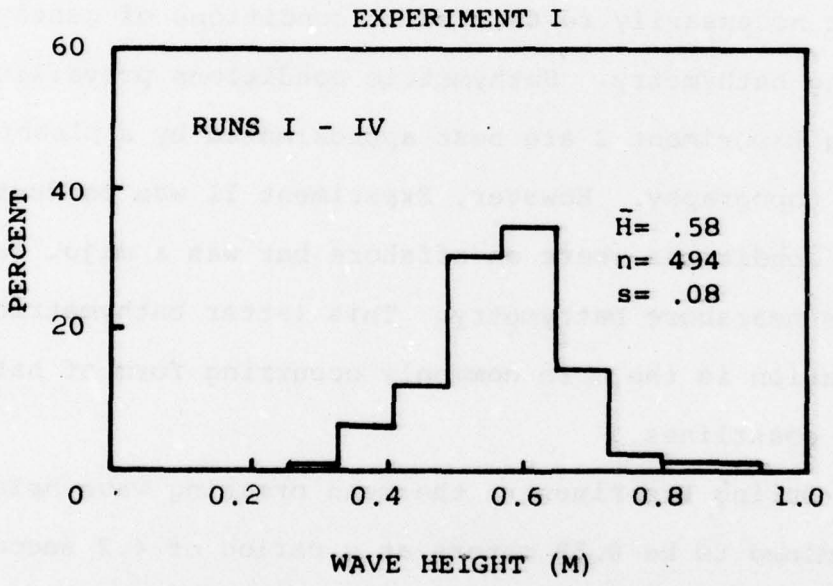

Figure 5.8 Observed breaking wave height probability distribution for Runs I-IV of Experiment I.

sensitivity of this numerical technique to irregular bottom topography, the beach configuration was assumed equivalent to the mean offshore planer slope of 1:40. The mean wave length of the incident wave field was calculated from the observed significant wave period and was found to be 25.0 meters. A family of predicted mean longshore current velocity profiles was generated for the range of observed incident wave angles within the surf zone, $21° \pm 5°$. These predicted profiles are shown in Figure 5.9. The observed mean surface longshore current velocities, from Experiment I, are also plotted on Figure 5.9, as vectors with vertical marks indicating one standard deviation from the mean longshore velocity.

Best agreement between observed and predicted mean longshore current velocities was achieved by setting the coefficient of bottom friction, C_f, equal to 0.032. This value lies between the values suggested by both Longuet-Higgins (1970) and Miller (1968). Longuet Higgins suggested a value of 0.01 for a beach of constant slope while Miller suggested a value of 0.04. Bretschneider (1954) has found that the observed damping of swell which is propagated over a smooth, level, sea bed is consistent with a bottom friction coefficient between 0.034 and 0.097. It, therefore, appears that the value of derived friction coefficient (0.032) obtained from data collected during Experiment I is well within the expected range of values.

Figure 5.9 Comparison of observed mean surface longshore current velocities from Experiment I with the formulation of Collins (1972), for the range of observed wave angles.

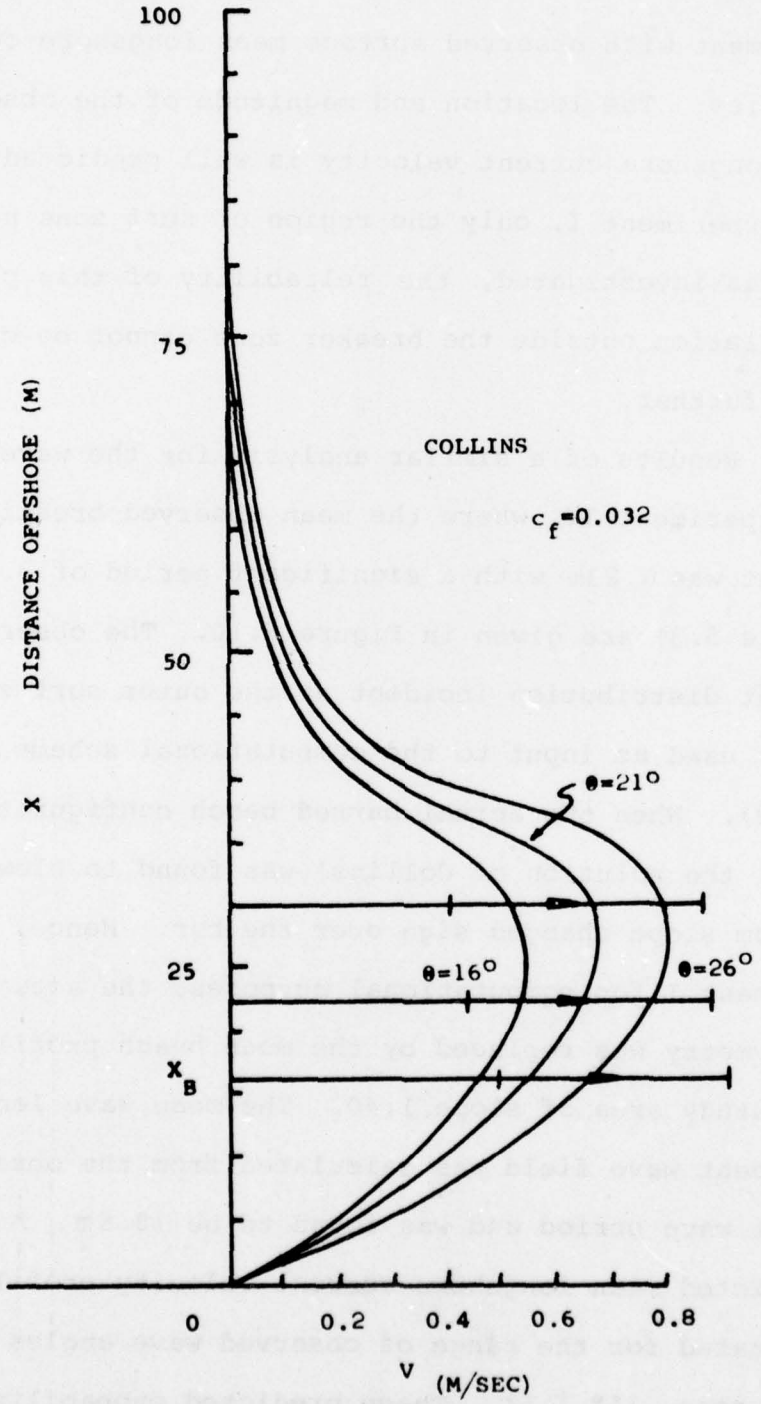
100
75
50
25
X_B
X DISTANCE OFFSHORE (M)
COLLINS
c_f=0.032
θ=21°
θ=16°
θ=26°
0
0.2
0.4
0.6
0.8
V (M/SEC)

Figure 5.9

Calculations made using this numerical technique and the observed field conditions of Experiment I provide good agreement with observed surface mean longshore current velocities. The location and magnitude of the observed maximum longshore current velocity is well predicted. Since, for Experiment I, only the region of surf zone near breaking was investigated, the reliability of this prediction formulation outside the breaker zone cannot be commented upon further.

Results of a similar analysis for the wave conditions of Experiment II, where the mean observed breaking wave height was 0.23m with a significant period of 3.7 seconds (Table 5.3) are given in Figure 5.10. The observed wave height distribution incident at the outer surf zone was again used as input to the computational scheme of Collins (1972). When the actual barred beach configuration was used, the solution of Collins' was found to blow up as the bottom slope changed sign over the bar. Hence, as in Experiment I for computational purposes, the actual offshore bathymetry was replaced by the mean beach profile through the study area of slope 1:40. The mean wave length of the incident wave field was calculated from the observed significant wave period and was found to be 18.6m. A family of predicted mean longshore current velocity profiles were generated for the range of observed wave angles within the surf zone, $15° \pm 5°$. These predicted probabilistic solutions are presented on Figure 5.10. Observed mean surface

longshore current velocities, from Experiment II, are also plotted on Figure 5.10, as vectors with vertical marks indicating one standard deviation from the mean longshore velocity.

Comparisons between the predicted profiles and the observed longshore current velocities of Experiment II could only be made by altering the wave breaking criteria to allow a match between the observed and predicted location of the highest frequency of wave breaking. Calculations made using Collins' (1972) numerical technique, with and without the altered breaking criteria, and with the observed field data of Experiment II do not produce as good an agreement between observed and predicted mean longshore current velocity as was achieved for Experiment I. The magnitude of predicted mean longshore current velocity compares favorably with observed mean velocities. Once again the best agreement between observed and predicted longshore current velocities was obtained with a bottom friction coefficient of 0,032. However, the location of the velocity maximum as well as the distribution of predicted mean longshore current velocity across the surf zone is not well predicted. As was previously stated, Experiment II was conducted in the presence of an offshore bar which was a major feature of the nearshore bathymetry. Good agreement between predicted values for a planar beach and observed longshore current velocities was not anticipated.

Figure 5.10 Comparison of observed mean surface longshore current velocities from Experiment II with the formulation of Collins (1972), for the range of observed wave angles.

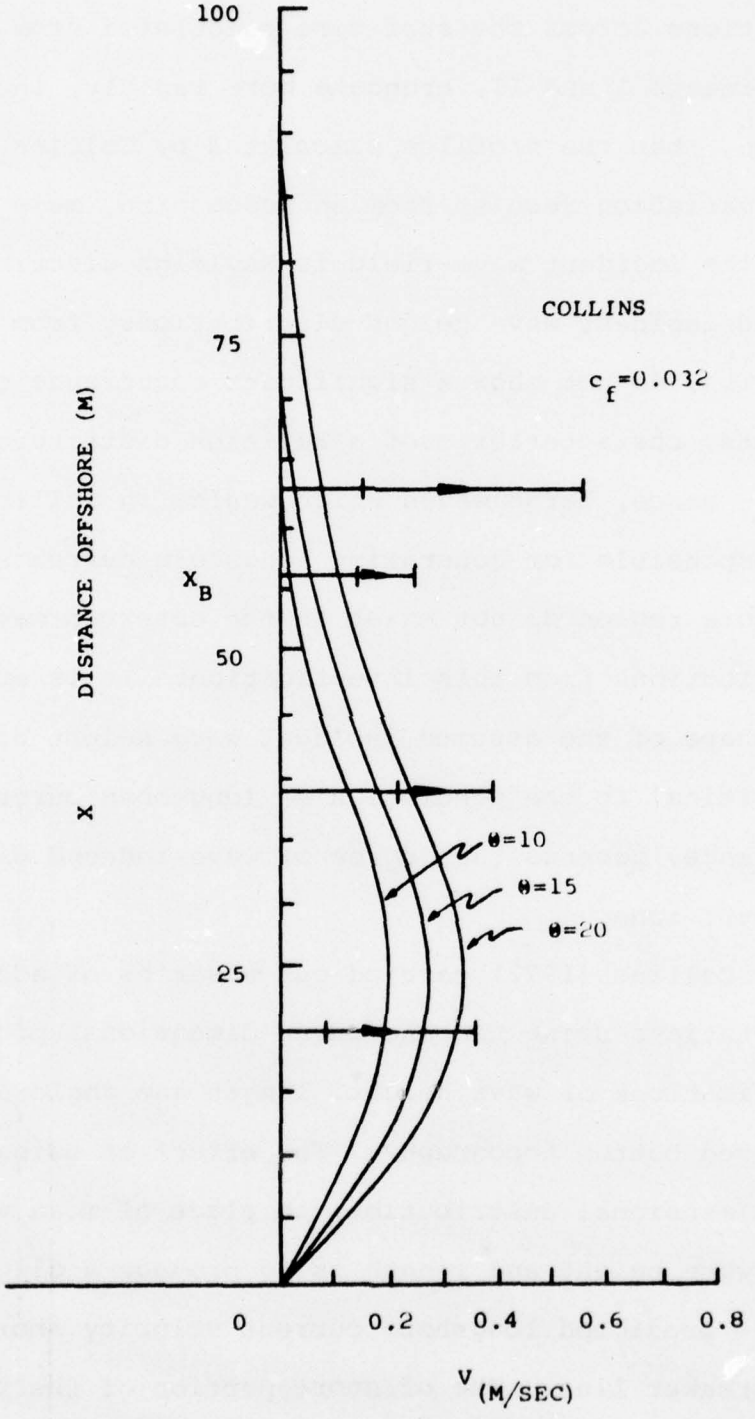
100
75
50
25
0
0.2
0.4
0.6
0.8
COLLINS
c_f=0.032
X_B
X DISTANCE OFFSHORE (M)
θ=10
θ=15
θ=20
V (M/SEC)

Figure 5.10

The shape of predicted longshore current velocity distributions across the surf zone calculated from data of Experiments I and II, truncate more rapidly, in the offshore region, than the profiles calculated by Collins (1972). This variation results from an assumption, made by Collins, that the incident wave field is Rayleigh distributed. Observed incident wave height distributions, from this investigation, do not show a significant occurrence of large wave heights, characteristic of a Rayleigh distributed sea surface. Hence, large waves which would, in Collins' model, be responsible for generating longshore currents in the offshore region do not exist in the observed wave height distributions from this investigation. It is evident that the shape of the assumed incident wave height distribution is critical to the prediction of longshore current velocity and hence, governs the degree of wave-induced mixing across the surf zone.

Collins (1972) carried out a series of additional computations using two and three-dimensional probability distributions of wave height, length and angle and included a barred bottom topography. The effect of using an incident two-dimensional distribution, in place of mean values, of both wave height and length is to produce a slight increase of the predicted longshore current velocity shoreward of the breaker line. The offshore portion of the predicted velocity profile remains unchanged. The effect of a three-dimensional probability distribution, in place of mean

values, of wave height, length and angle is to depress the predicted longshore current velocity throughout the surf zone.

Longshore current velocity for a barred beach configuration results in a double maximum in the current profile. However, this double maximum is an artifact of the computational procedure employed. A discontinuity is introduced into the predicted longshore current velocity profile as a result of the bottom slope changing sign at the crest of the bar. Therefore, the predicted velocity minimum, over the bar, is not the result of actual modeling of physical processes within the surf zone. The existence of a low velocity zone over the offshore bar in the observed longshore current flow field is well documented by data collected during Experiment II (Table 5.4). Each mean value presented in Table 5.4 was calculated from the output of an independent current meter. The extremely reproducible estimates of mean longshore current velocity between the surface and the bottom current meters at each station (Table 5.4) is attributable to two factors. First, the longshore current structure appears to be uniform with depth throughout the surf zone. Hence, the observed low velocity zone over the offshore bar is a real feature of the longshore current flow field. Second, the number of estimates of mean velocity was sufficiently great to have eliminated most temporal variability. Hence, the estimates of mean longshore current velocity are stable and reproducible. The existence of the

low velocity zone in the longshore current flow field associated with the offshore bar is documented by mean longshore current velocities calculated from the outputs of six adjacent current meters operating independently and simultaneously.

In addition, the existence of a low velocity zone over the longshore bar has been previously observed by Wood and Meadows (unpublished data). Along the same section of Lake Michigan shoreline, they observed a reduction of 32% of the maximum longshore current velocity in the region over the submarine bar.

A second comparison of observed mean surface longshore current velocities from this investigation with the predicted longshore current velocities from Longuet-Higgins (1970 a and b) was also made. A generalized set of mean longshore current velocity distributions, across the surf zone, from Longuet-Higgins (1970 a and b) are plotted in Figure 5.11. These representative steady state longshore current distributions correspond to three values of the horizontal mixing parameter, P. P = 0, corresponds to the case of monochromatic waves incident at a breaker line, with no lateral mixing. An increase in the parameter, P, corresponds to increased lateral mixing across the breaker line.

The mixing parameter, P, is dependent upon several factors,

$$P = \frac{\pi}{2} \frac{sN}{\alpha C_f}$$

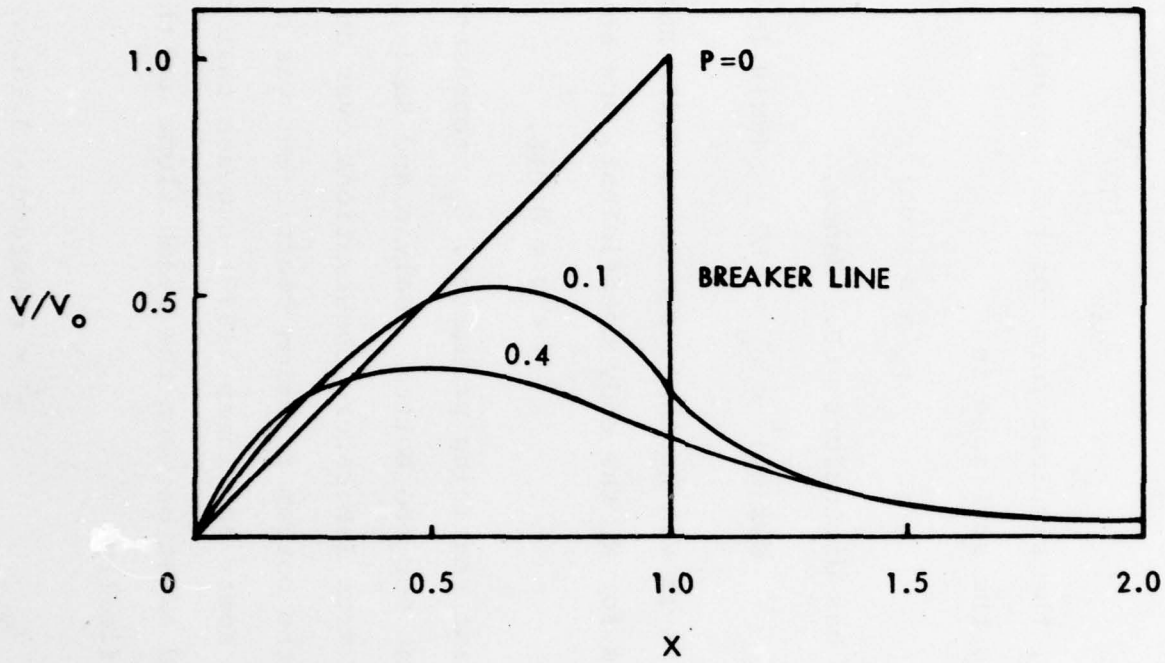

Figure 5.11 Comparison of non-dimensional mean surface longshore current velocity profiles across the surf zone for monochromatic (P=0), and increasing later mixing (P=0.1) and (P=0.4).

where s is the beach slope, C_f the bottom friction and α and N are dimensionless constants. Longuet-Higgins (1970 b) suggests that turbulent velocities responsible for mixing within the surf zone are not likely to exceed 0.1 of the maximum wave horizontal particle velocity (U_{max}) where

$$U_{max} = \alpha (gh)^{\frac{1}{2}}.$$

Hence, the simplest form for the variation of eddy viscosity across the surf zone is

$$\mu_e = N\rho x (gh)^{\frac{1}{2}},$$

which has dimensions ρLU. Hence,

$$N\rho x (gh)^{\frac{1}{2}} = \mu_e = \rho LU \leq \rho (Kx) 0.1\alpha (gh)^{\frac{1}{2}}.$$

Where K is von Karman's constant, 0.40, and the probable limits for N, the eddy coefficient, are set at

$$0 < N < 0.016.$$

The last remaining parameter, C_f, represents the drag coefficient for the bottom. Galvin and Eagleson (1965) calculated from laboratory observations over an impermeable bed, that the bottom friction coefficient was a constant, 0.01.

Komar and Inman (1970) suggest that a simple relation should exist between the beach slope and the drag coefficient. Specifically,

$$\frac{C_f}{s} = \text{constant} \approx 0.15.$$

Using the average beach slope for the study area of 1:40, C_f is calculated to be 0.0038.

Results of fitting the numerical calculation scheme of Collins (1972) to the observed field data of the investigation resulted in two independent estimates of the bottom friction coefficient. Both estimates placed the coefficient at, $C_f = 0.032$. Using the two extreme values for C_f and the values of $\alpha = 0.41$ and $N = 0.016$ suggested by Longuet-Higgins (1970 b), P was calculated to be

$$0.05 \quad (C = 0.032)$$

$$0.41 \quad (C = 0.0038)$$

It, therefore, appears that P should lie between 0.05 and 0.4, for the field conditions of this investigation. This result is satisfying considering that Longuet-Higgins (1970 b) states that $P \geq 0.4$; the velocity gradient at the shoreline becomes infinite.

Mean longshore current velocities and their respective standard deviations, obtained from Experiment I of this investigation, are plotted on Figure 5.12. For comparison, the mean longshore current velocity distributions, calculated from field data of this investigation, utilizing the formulation of Longuet-Higgins (1970 b) for mixing parameter values of $P = 0.05$ and $P = 0.4$ are also plotted on Figure 5.12.

The comparison of theoretical longshore current velocity profiles from Longuet-Higgins (1970 a and b) with

Figure 5.12 Comparison of observed mean surface longshore current velocities from Experiment I with the formulation of Longuet-Higgins (1970), for the expected range of values of lateral mixing.

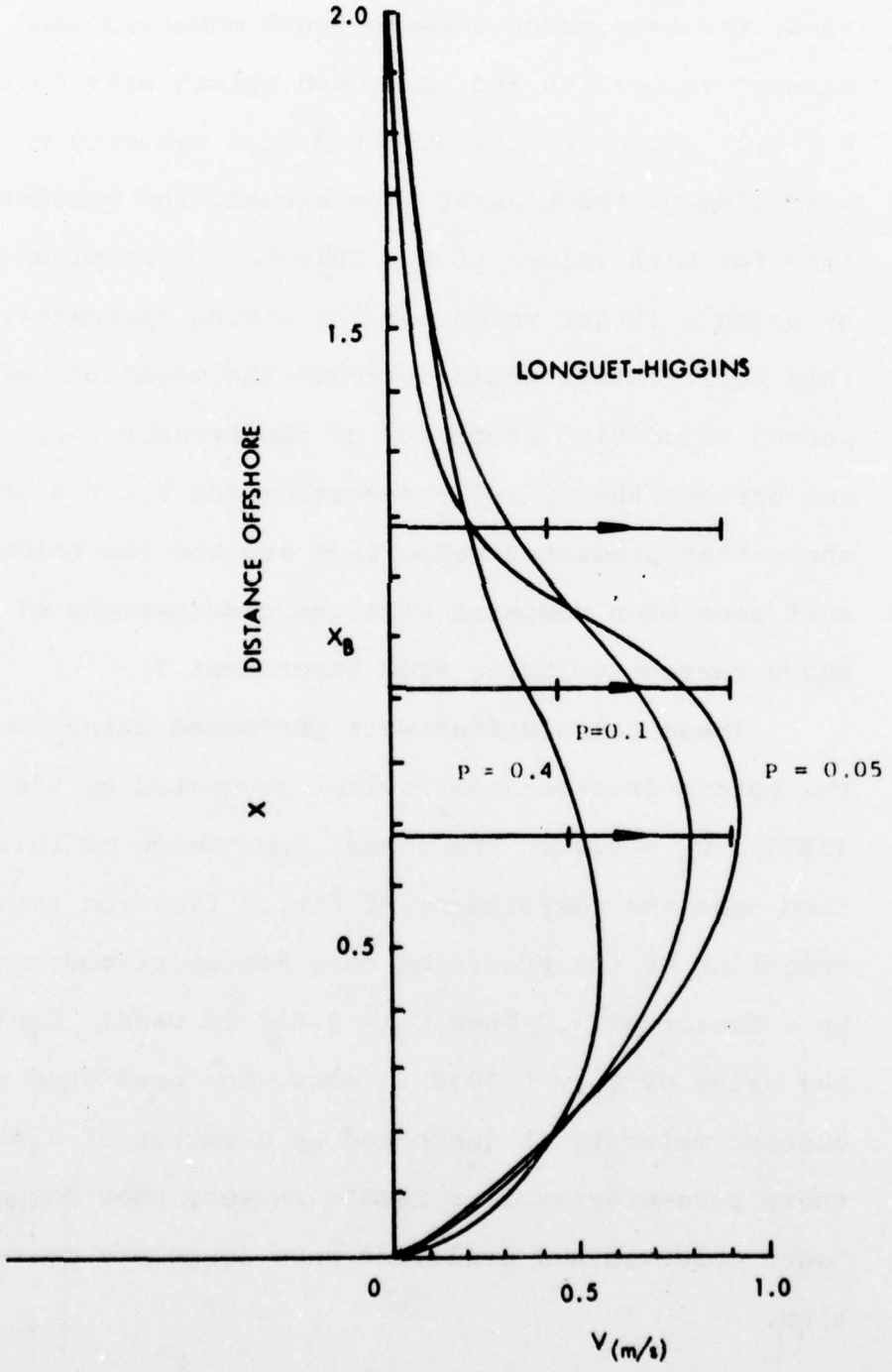
2.0
1.5
LONGUET-HIGGINS
DISTANCE OFFSHORE
X
X_B
P=0.1
P = 0.4
P = 0.05
0.5
0
0.5
1.0
V(m/s)

Figure 5.12

mean surface longshore current velocities from Experiment I (Figure 5.12) shows reasonable agreement, from the breaker line shoreward, for a P = 0.05. In this region of the surf zone, the best match between these observed mean longshore current velocities and predicted values were obtained for P = 0.1. However, the observed mean velocity on the seaward side of the breaker line exceeds the predicted velocities for both values of P. This difference might be corrected by using a larger value for the mixing parameter. However, this modification would decrease the magnitude of the expected velocities shoreward of the breaker line. Comparison between theory and observation for P = 0.4 (Figure 5.12) shows that predicted velocities are too low throughout the surf zone when compared with the observations of mean longshore current velocity from Experiment I.

These calculations were performed using the value of the bottom friction coefficient suggested by Longuet-Higgins (1970), $C_f = 0.01$. The linear dependence of this formulation upon the coefficient of bottom friction results in a reduction of the predicted mean longshore current velocities by a factor of 3.2 when $C_f = 0.032$ is used. Similarly, if the value of $C_f = 0.0038$ is used, the predicted magnitude of current velocity is increased by a factor of 2.6. Both of these parameterizations result in very poor comparisons between observed and predicted mean longshore current velocities.

A similar comparison between predicted and observed mean surface longshore current velocities using data from Experiment II resulted in poor agreement. However, under these conditions of a barred bathymetry, agreement between the formulation of Longuet-Higgins (1970) for a planer beach and results of Experiment II was not anticipated. In fact, a comparison of this nature is not applicable.

Mean longshore current data from this investigation has suggested that the formulation of Longuet-Higgins (1970) tends to best predict the distribution of current velocities across the surf zone if the mixing parameter, P, is specified near its maximum reasonable value (≈ 0.4). However, best agreement between predicted and observed velocity magnitudes was obtained for $P = 0.1$. The magnitude of the observed mean current velocity is not well predicted by this formulation for a $P = 0.4$ unless the bottom friction coefficient is allowed to be $0.0038 < C_f < 0.01$. A coefficient of bottom friction within this range does not appear to be reasonable.

Vertical Mean Longshore Current Structure

The vertical structure of the mean longshore current velocity field has not been theoretically investigated, nor experimentally determined prior to this investigation. However, the assumption that the longshore current is uniform with depth throughout the surf zone has been applied to all existing longshore current formulations. Time averaged

longshore current velocities from this investigation tend to support this assumption of vertical uniformity of the longshore current flow field, outside the bottom boundary layer. These longshore current observations (Figures 5.13 and 5.14) indicate that at each current monitoring station, for both Experiments I and II, variation of the mean longshore current velocity with depth is relatively small. These average velocities were calculated from the total (fifteen minutes for Experiment I and sixteen minutes for Experiment II) longshore current velocity series at each meter location. This result implies that large velocity gradients and hence, correspondingly large shear stresses should be anticipated in the region of the water-sediment interface.

Continuous, overlapping thirty-second time averages were calculated from the total longshore current velocity series for each of the three vertically positioned current meters for all data sets of Experiment I. A typical example of these calculations is presented for Run I, in Appendix A. For each successive averaging period the current meter nearest the sea bed recorded mean longshore current velocities from 18 to 50 percent less than the upper current meter.

In addition, the vertical profile of the thirty-second time averaged longshore current velocity oscillates about its long-term mean value. Thirty-second time averaged velocities oscillate approximately ±0.1 m/second about the long-term mean values (see Appendix A). The period for one

complete cycle of this oscillation is approximately seventy-five seconds. Results of this analysis, applied to all runs of Experiment I, indicated a similar long-period oscillation. As the vertical longshore current profile responds to this oscillation, the vertical structure of the flow field is preserved, but this thirty-second time averaged vertical longshore current velocity structure is not stationary in time.

Summary

The two-dimensional mean longshore current profile across the surf zone and with depth has now been documented under field conditions. The distribution of observed mean surface longshore current velocity across the surf zone from both Experiments I and II are not well predicted by either a probabilistic description of surf zone processes or by a deterministic theory which considers only lateral mixing. It appears that the degree of mixing across the surf zone is more intense than is predicted by either approach. As a result of this investigation, further verification of the magnitude of the bottom friction coefficient on natural beaches was supplied. It was empirically determined that the bottom friction coefficient should lie between 0.03 and 0.04. Best agreement with theory was achieved for both Experiments with $C_f = 0.032$.

The vertical structure of the mean longshore current flow field has been observed for the first time. The

Figure 5.13 Longshore current mean vertical velocity profiles, Experiment I.

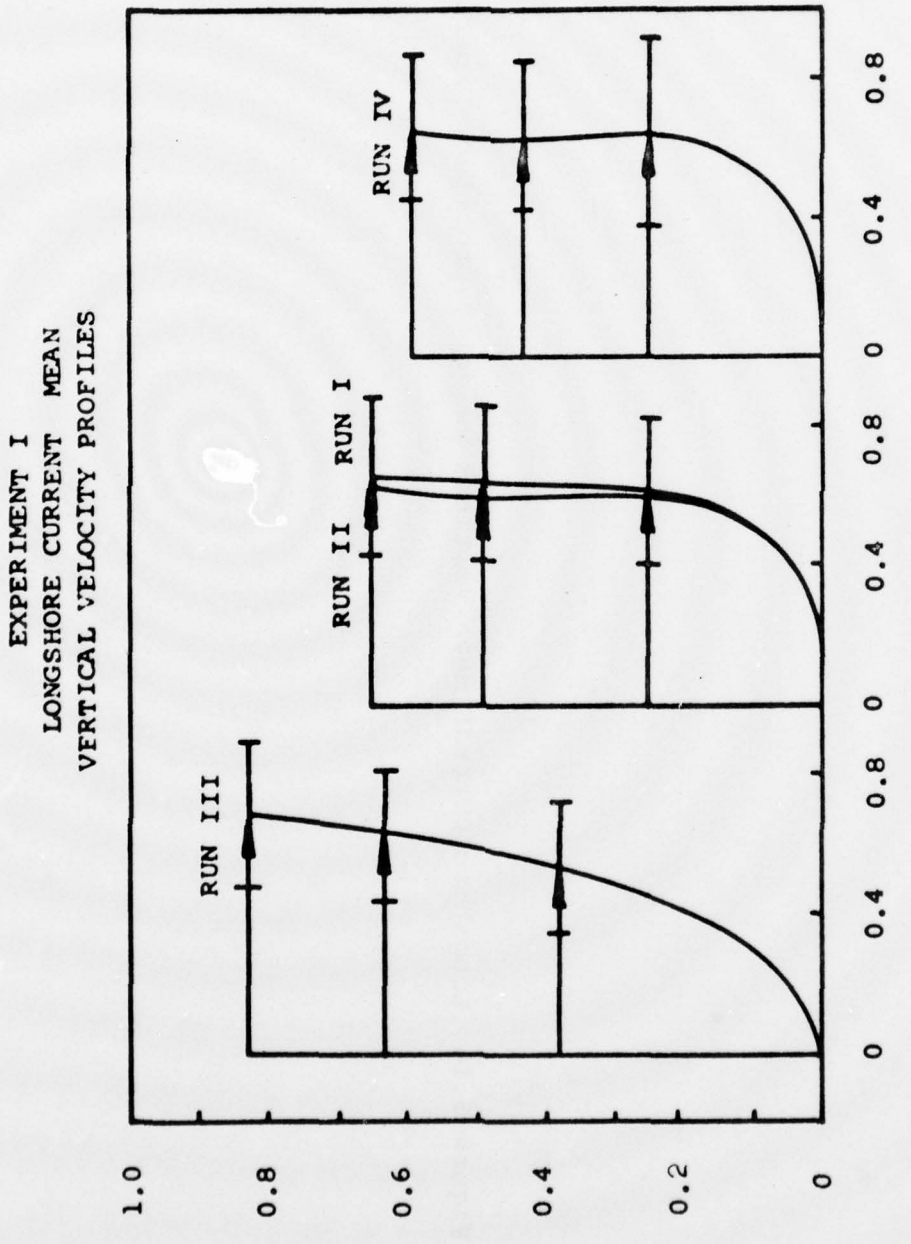
EXPERIMENT I
LONGSHORE CURRENT MEAN
VERTICAL VELOCITY PROFILES
RUN III
RUN II
RUN I
RUN IV
1.0
0.8
0.6
0.4
0.2
0
z/h_x
0
0.4
0.8
VELOCITY (M/SEC)
One Standard Deviation

Figure 5.13

Figure 5.14 Longshore current mean vertical velocity profiles, Experiment II.

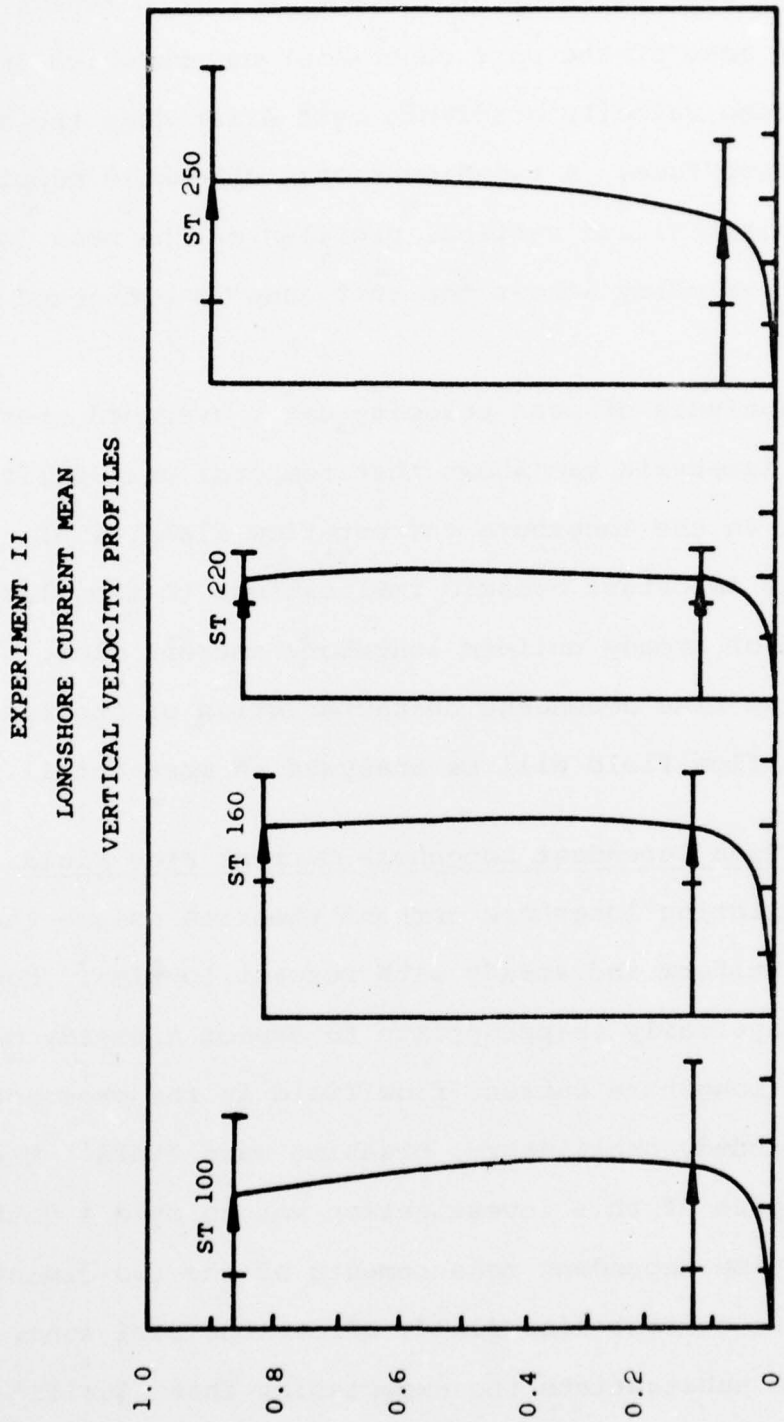
EXPERIMENT II
LONGSHORE CURRENT MEAN
VERTICAL VELOCITY PROFILES
ST 100
ST 160
ST 220
ST 250
1.0
0.8
0.6
0.4
0.2
0
z/h_x
0
0.2
VELOCITY (M/SEC)
One Standard Deviation

Figure 5.14

vertical flow structure was found to remain nearly uniform through most of the surf zone water column which implies that steep velocity gradients must exist near the sediment-water interface. A two-dimensional schematic mapping of the horizontal and vertical profiles of the mean longshore current velocity across the surf zone is presented in Figure 5.15.

Analysis of mean velocity data, averaged over thirty-second intervals, has shown that temporal variability is present in the longshore current flow field. This observation has important dynamic implications to the classical concept of steady uniform longshore current flow. Therefore, the time dependent characteristics of the longshore current flow field will be analyzed in more detail.

Time Dependent Longshore Current Flow Field

Existing longshore current theories assume that velocity is uniform and steady with respect to time. However, it is physically inappropriate to expect a steady or slowly varying longshore current flow field in the presence of a broad banded, oscillatory, breaking wave field. Therefore, one purpose of this investigation was to make a detailed set of time dependent measurements of the two-dimensional longshore current flow field, across the surf zone, in order to substantiate the expectation that significant unsteadiness should exist in the flow field.

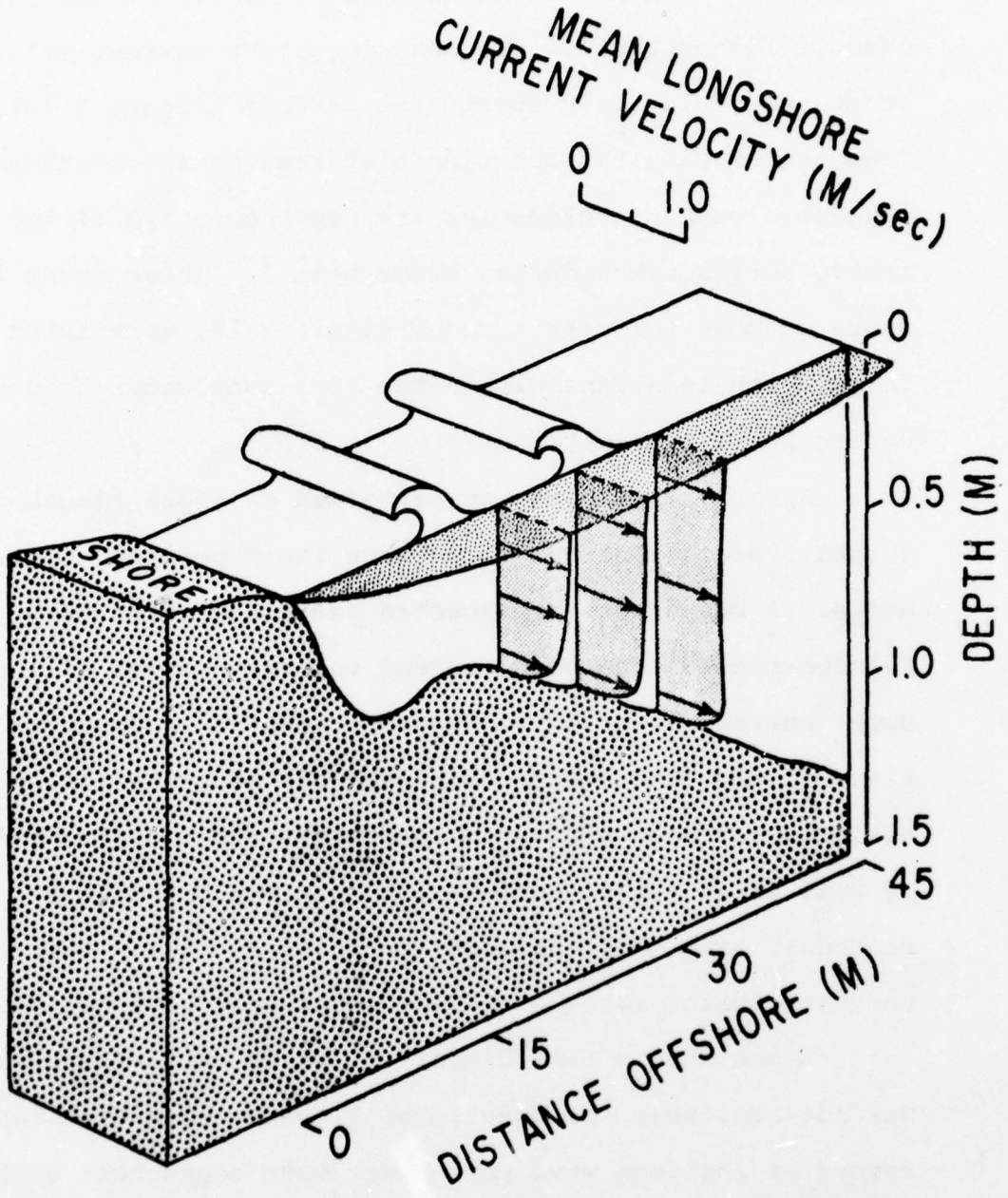

Figure 5.15 Two-dimensional schematic mapping of the mean longshore current velocity from Experiment I.

Analysis of field measurements, from this study, show that, at a fixed point in the surf zone, variations in excess of 150 percent of the mean longshore current velocity occur over relatively short time periods (Figure 5.16). These three simultaneous time histories of fluctuating longshore current velocities are representative of the twelve series taken during Experiment I. These three longshore current velocity series, Figure 5.16, were taken at three depth locations within the surf zone water column during Run I of Experiment I.

Spectral analysis was performed on these longshore current velocity series to isolate their periodic components. A representative spectra calculated from the fifteen-minute longshore current velocity series of the upper current meter of Run I, Experiment I is shown in Figure 5.17. Results of this analysis indicate that significant variance exists in the range from 4 to 6 seconds as well as at longer periods (the maximum being 78.8 seconds). The short-periods fluctuations fall within the anticipated range of incident breaking wave periods.

A continuous time history of water surface elevation was not available for Experiment I, however, a simultaneous record of incident wave period was made concurrent with these longshore current velocity observations. It was, therefore, necessary to employ an approximate technique to estimate the incident wave spectra. A spectra

calculated using the technique suggested by Collins (1967) is shown in Figure 5.18. The peak in the spectra is in a range between 4.0 and 6.0 seconds. It, therefore, appears that the mean period of the incident breaking waves, 4.2 seconds, is resolved, as anticipated, in the spectral analysis of the concurrent longshore current velocity series. Similar results were obtained for all longshore current series for Runs II, III and IV of Experiment I. In all cases, the existence of fluctuations at the mean incident breaking wave period was evident from the spectral analysis of the longshore current time histories.

Data collected during Experiment II provides time synchronous information on both the longshore current velocity and the incident wave field. Spectra calculated from these time synchronous records of water surface elevation and longshore current velocity, measured at three positions across the surf zone, are shown in Figures 5.19 through 5.21. Each pair of incident wave and longshore current spectra exhibits several similar peaks within the range of incident wave periods. It appears that throughout the surf zone short-period fluctuations in the longshore current flow field occur at periods corresponding to the incident breaking waves. This range of incident wave periods is approximately 3.0 to 6.2 seconds.

It is reasonable to assume that if the incident wave particle velocity is conservative over one wave period, then the net contribution to the longshore current over that

Figure 5.16 Three representative simultaneous time histories of fluctuating longshore current velocities taken at three depth locations through the surf zone column.

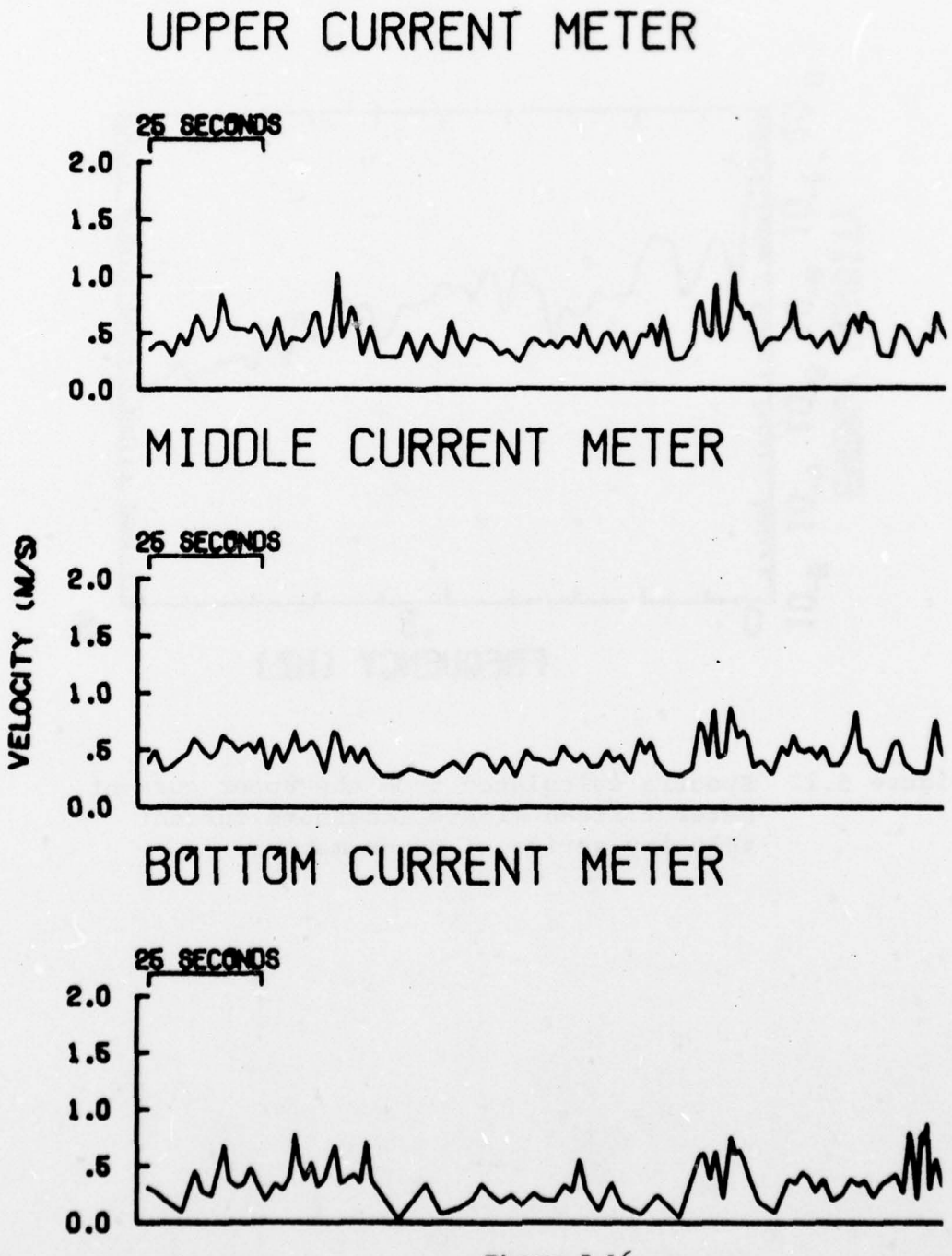
UPPER CURRENT METER
25 SECONDS
2.0
1.5
1.0
.5
0.0
MIDDLE CURRENT METER
VELOCITY (M/S)
25 SECONDS
2.0
1.5
1.0
.5
0.0
BOTTOM CURRENT METER
25 SECONDS
2.0
1.5
1.0
.5
0.0

Figure 5.16

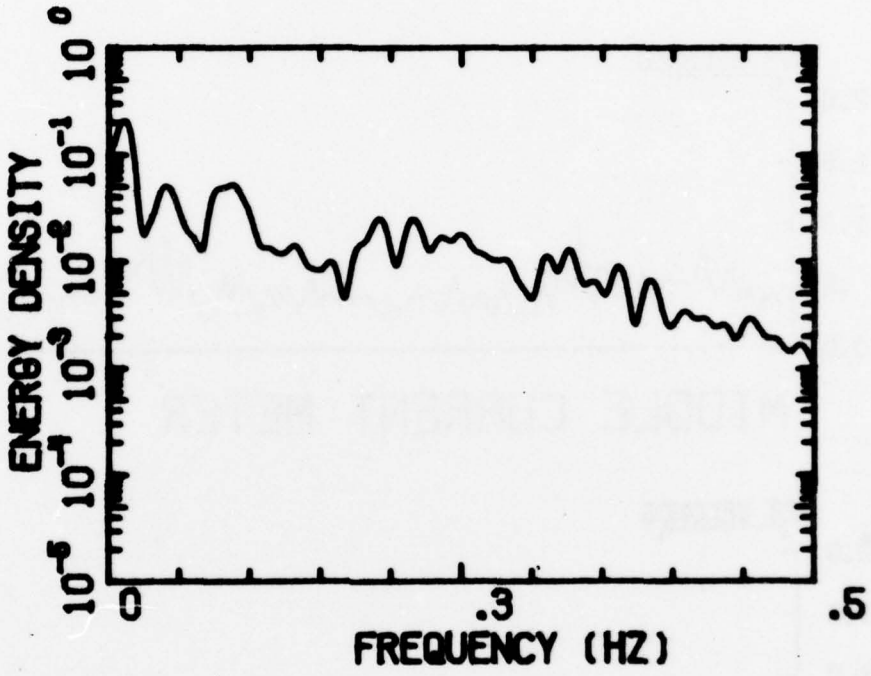

Figure 5.17 Spectra calculated from the upper current meter fifteen minute longshore current velocity series of Experiment I.

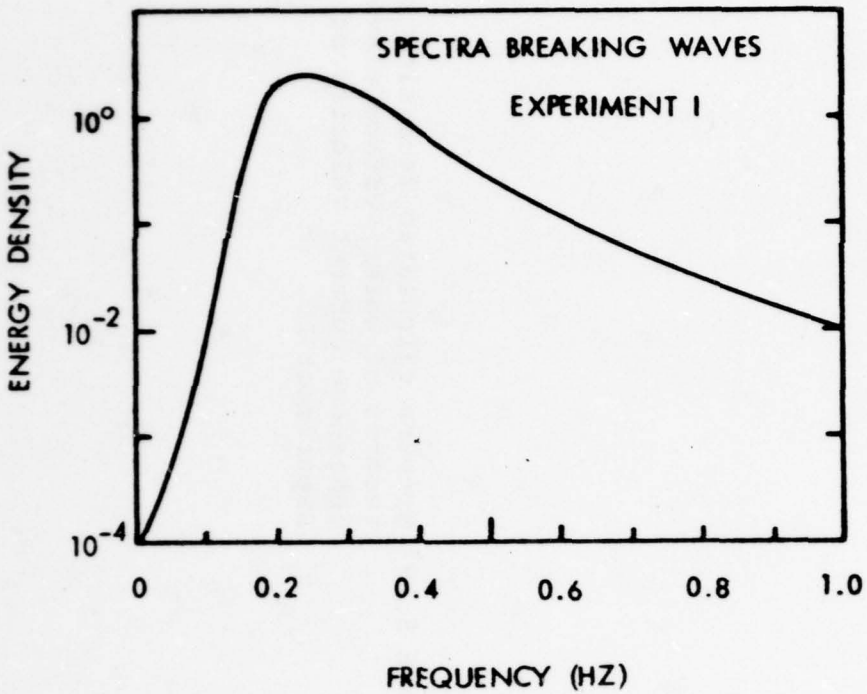

Figure 5.18 Spectra calculated using the technique of Collins (1967) and the wave data of Experiment I.

Figure 5.19 Spectra calculated from time synchronous records of water surface elevation and longshore current velocity at Station 250, Experiment II.

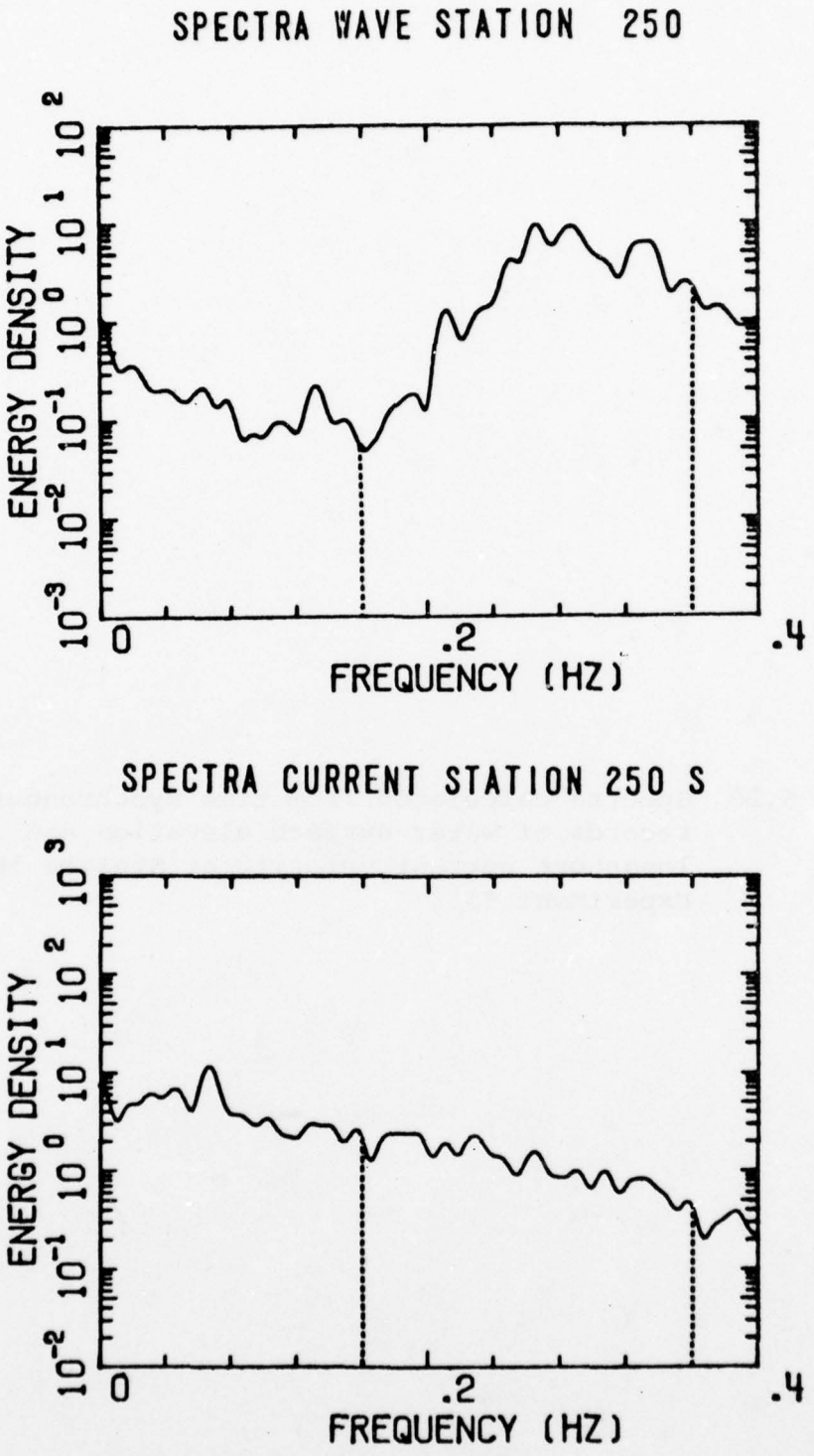
SPECTRA WAVE STATION 250
ENERGY DENSITY
10^{-3} 10^{-2} 10^{-1} 10^{0} 10^{1} 10^{2}
0
.2
.4
FREQUENCY (HZ)
SPECTRA CURRENT STATION 250 S
ENERGY DENSITY
10^{-2} 10^{-1} 10^{0} 10^{1} 10^{2} 10^{3}
0
.2
.4
FREQUENCY (HZ)

Figure 5.19

Figure 5.20 Spectra calculated from time synchronous records of water surface elevation and longshore current velocity at Station 160, Experiment II.

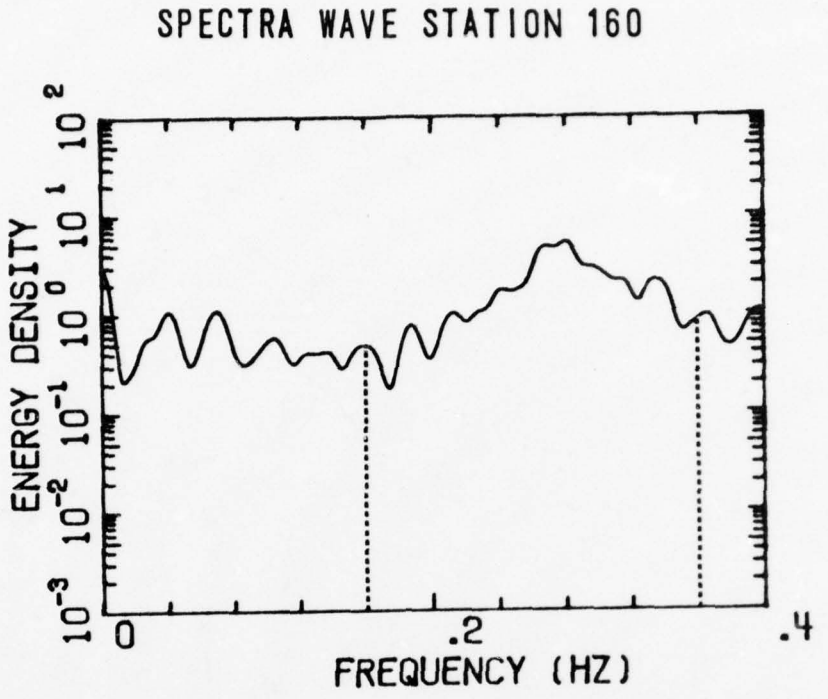
SPECTRA WAVE STATION 160
ENERGY DENSITY
10^{-3} 10^{-2} 10^{-1} 10^{0} 10^{1} 10^{2}
0
.2
.4
FREQUENCY (HZ)

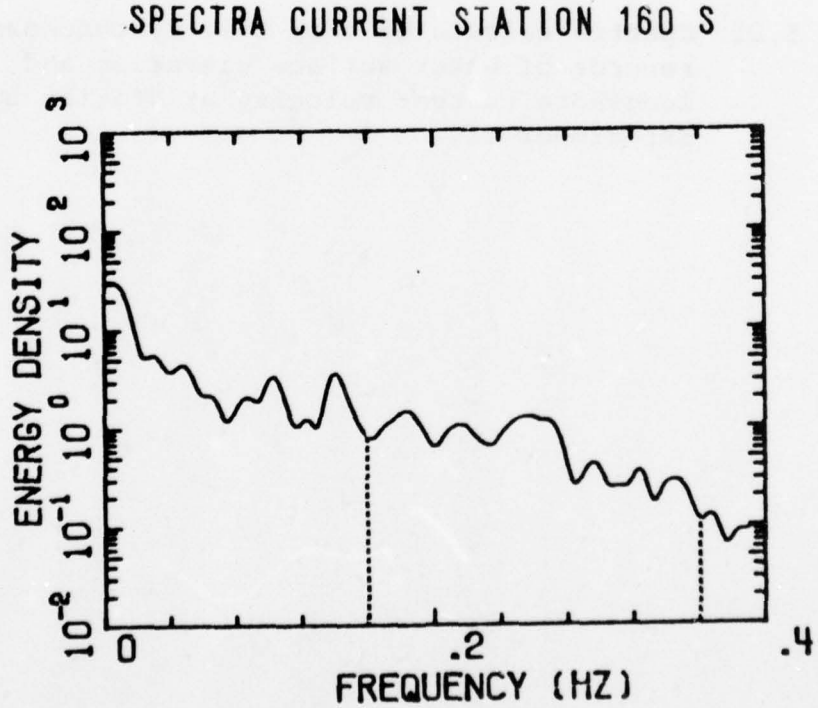
SPECTRA CURRENT STATION 160 S
ENERGY DENSITY
10^{-2} 10^{-1} 10^{0} 10^{1} 10^{2} 10^{3}
0
.2
.4
FREQUENCY (HZ)

Figure 5.20

Figure 5.21 Spectra calculated from time synchronous records of water surface elevation and longshore current velocity at Station 100, Experiment II.

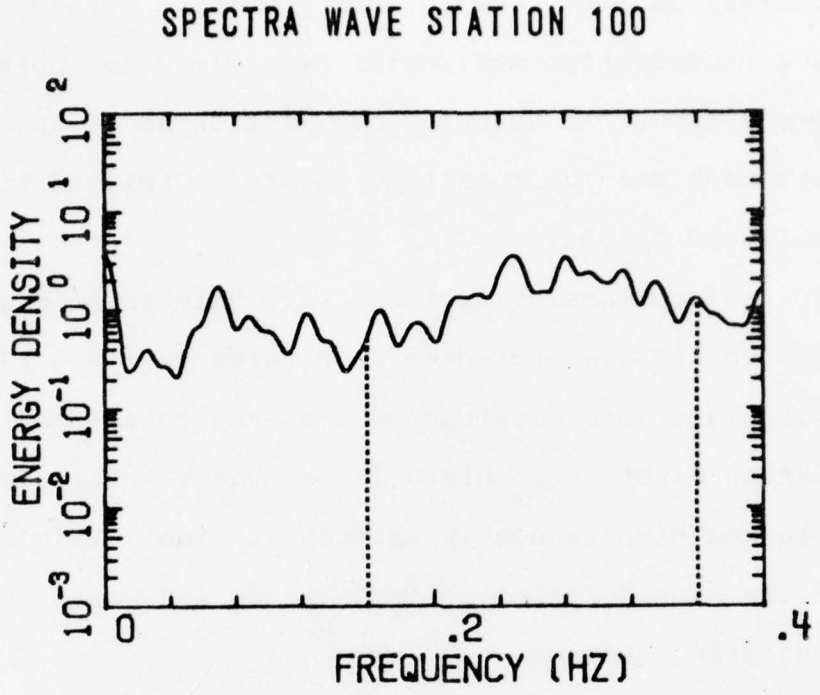
SPECTRA WAVE STATION 100
ENERGY DENSITY
10^{-3} 10^{-2} 10^{-1} 10^{0} 10^{1} 10^{2}
0
.2
.4
FREQUENCY (HZ)

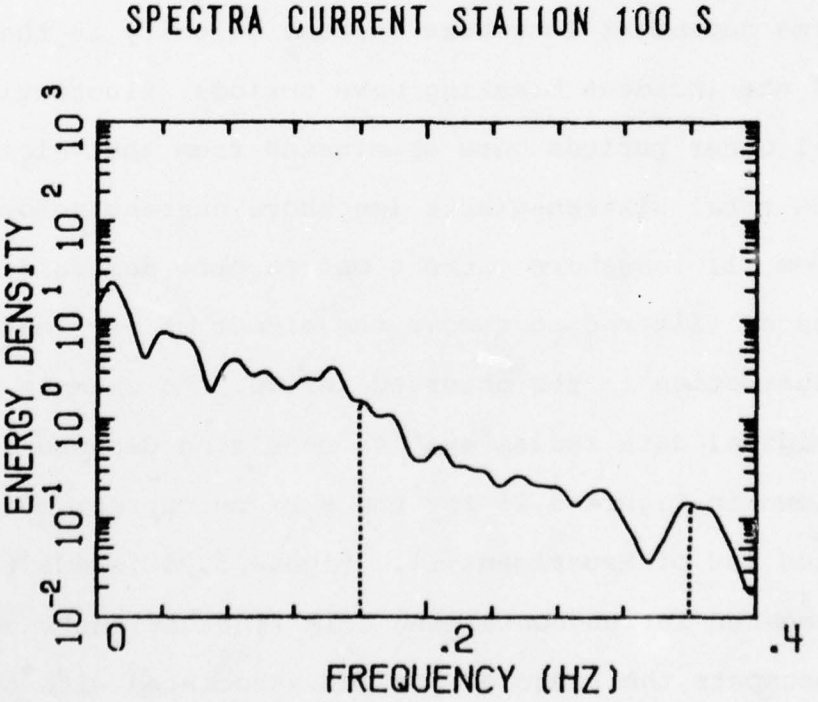
SPECTRA CURRENT STATION 100 S
ENERGY DENSITY
10^{-2} 10^{-1} 10^{0} 10^{1} 10^{2} 10^{3}
0
.2
.4
FREQUENCY (HZ)

Figure 5.21

interval is zero. Hence, the resulting longshore component of a conservative horizontal particle velocity should produce a symmetric velocity oscillation about an abssissa of zero mean and its magnitude should be related to the incident wave height.

Histograms of incident wave heights at Stations 250, 160 and 100 are presented in Figures 5.22 - 5.24. These histograms were constructed from the total continuous sixteen-minute time histories of water level elevation, obtained simultaneously at each station. This resulted in the consideration of from 319 to 459 waves at each monitoring station.

In order to evaluate only the contribution to the time dependent longshore current velocity in the range of the incident breaking wave periods, fluctuations of all other periods were eliminated from the velocity record. The total sixteen-minute longshore current velocity records from all longshore current meters were demeaned and band passed filtered to remove the effect of any long-period fluctuation in the observed series. An example of the original data series and its resulting decomposition is shown in Figure 5.25 for the surface current meter at Station 160 of Experiment II. Figure 5.25C shows the filtered, demeaned series containing only fluctuations whose periods encompass the range of periods associated with the incident wave field. This series should contain the observed longshore current velocity component resulting from the oscillatory

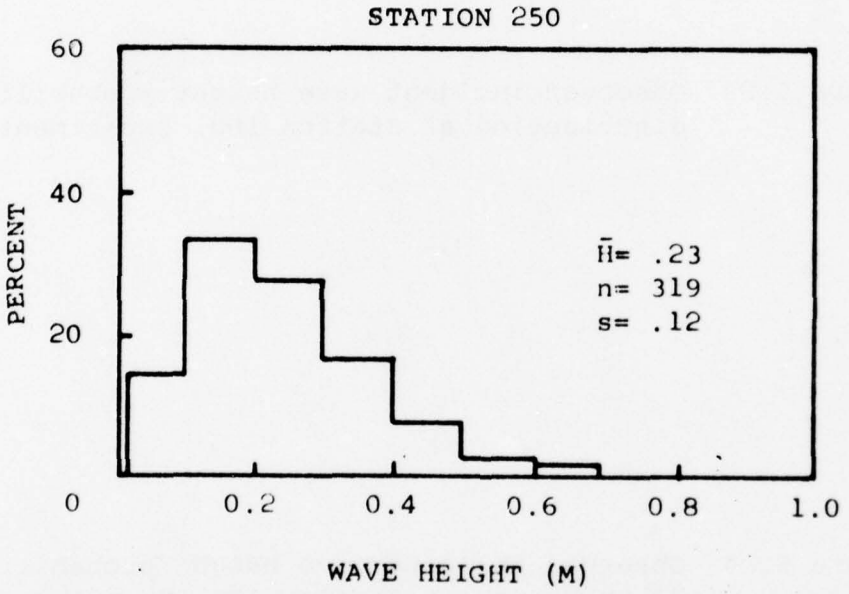

Figure 5.22 Observed incident wave height probability distribution at Station 250, Experiment II.

Figure 5.23 Observed incident wave height probability distribution at Station 160, Experiment II.

Figure 5.24 Observed incident wave height probability distribution at Station 100, Experiment II.

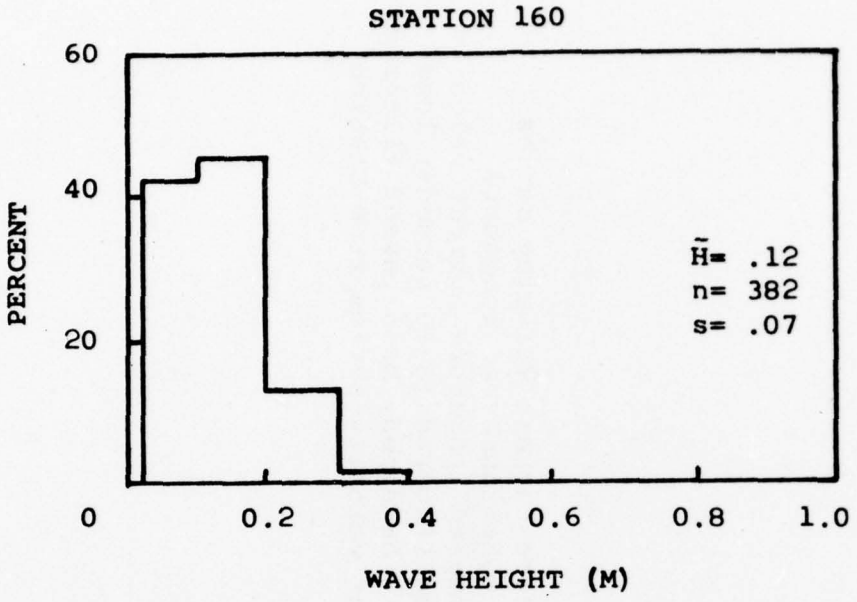

Figure 5.23

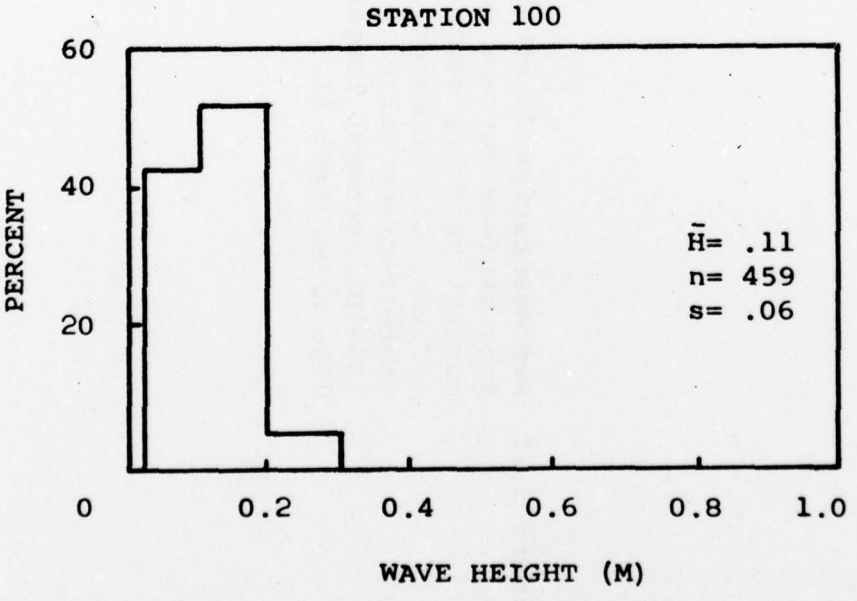

Figure 5.24

Figure 5.25 Representative fluctuating longshore current velocity series from surface current meter: A) total observed longshore current velocity series; B) demeaned longshore current velocity series; C) demeaned, band passed filtered (3-10 seconds) longshore current velocity series; D) demeaned, band passed filtered (25-100 seconds) longshore current velocity series, from Station 160, Experiment II.

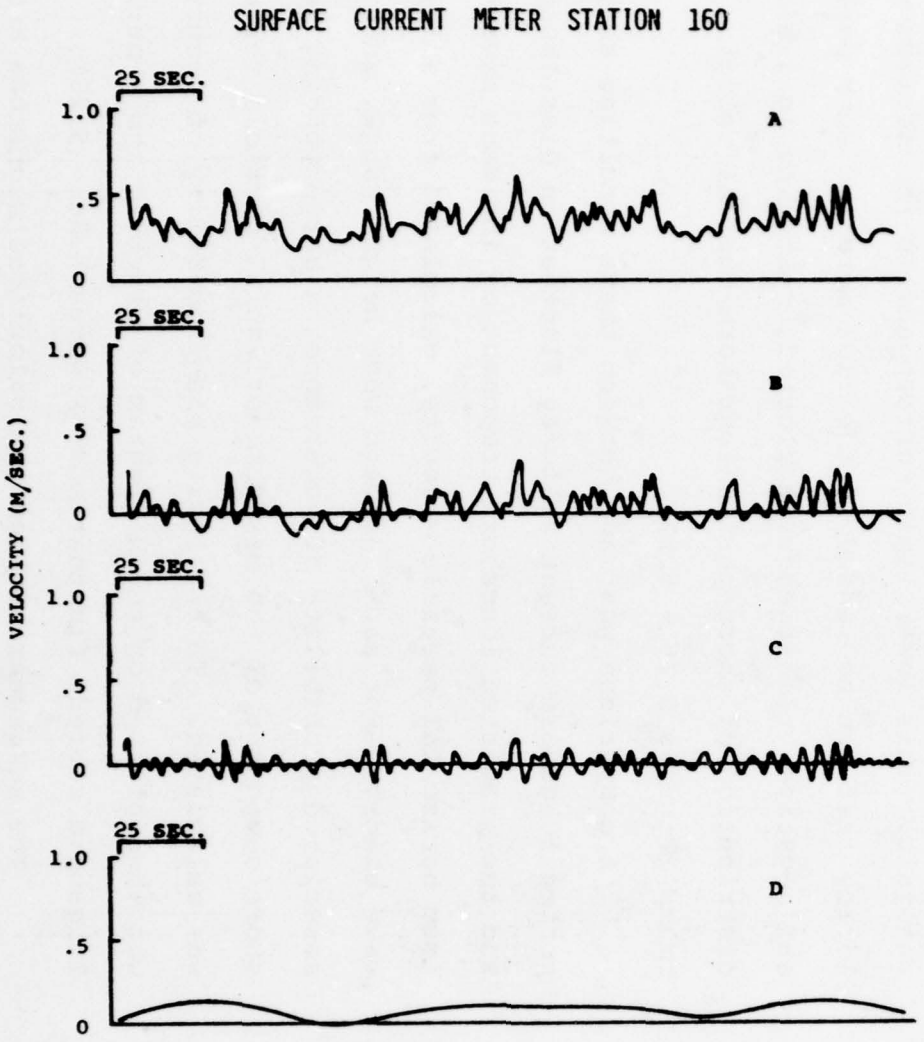
SURFACE CURRENT METER STATION 160
25 SEC.
1.0
.5
0
A
B
C
D
VELOCITY (M/SEC.)

Figure 5.25

portion of the breaking wave horizontal particle velocity.

Histograms of this short-period fluctuating longshore current velocity component were constructed from the demeaned, short-period, band passed filtered, velocity series from each of the surface longshore current meters. Only velocities greater than 0.04 m/sec. were considered in this analysis. This lower limit corresponds to the minimum velocity that can be sensed by the flow meters. Both positive and negative velocities were plotted, resulting in a bimodal distribution of short-period longshore current velocity maximums (Figures 5.26 - 5.28).

A comparison was made between these resulting short-period longshore current velocity fluctuation distributions and the predicted longshore component of incident wave maximum horizontal particle velocity, calculated from solitary wave theory. For each incident wave height range, and its associated probability of occurrence, a corresponding longshore component of the maximum horizontal particle velocity was calculated. This velocity and probability of occurrence was then plotted on the histogram of observed short-period longshore current fluctuations (Figures 5.26 - 5.28).

The agreement between the calculated magnitude and distribution of the longshore component of incident wave particle velocity and the observed short-period longshore current fluctuations is remarkably good for each surf zone monitoring station. It, therefore, appears that short-period fluctuations in the longshore current flow field

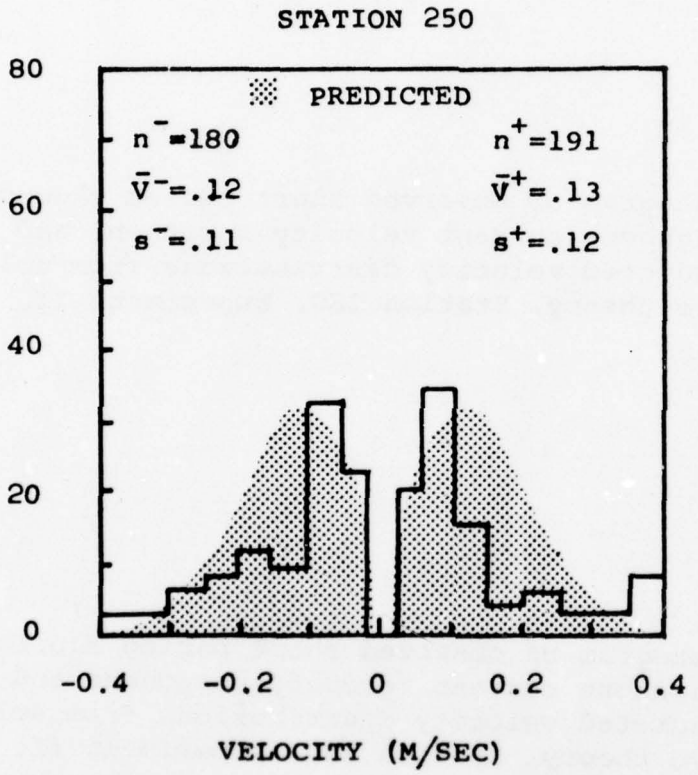

Figure 5.26 Histogram of observed short period fluctuating longshore current velocity component and predicted velocity distributions from solitary wave theory, Station 250, Experiment II.

Figure 5.27 Histogram of observed short period fluctuating longshore current velocity component and predicted velocity distributions from solitary wave theory, Station 160, Experiment II.

Figure 5.28 Histogram of observed short period fluctuating longshore current velocity component and predicted velocity distributions from solitary wave theory, Station 100, Experiment II.

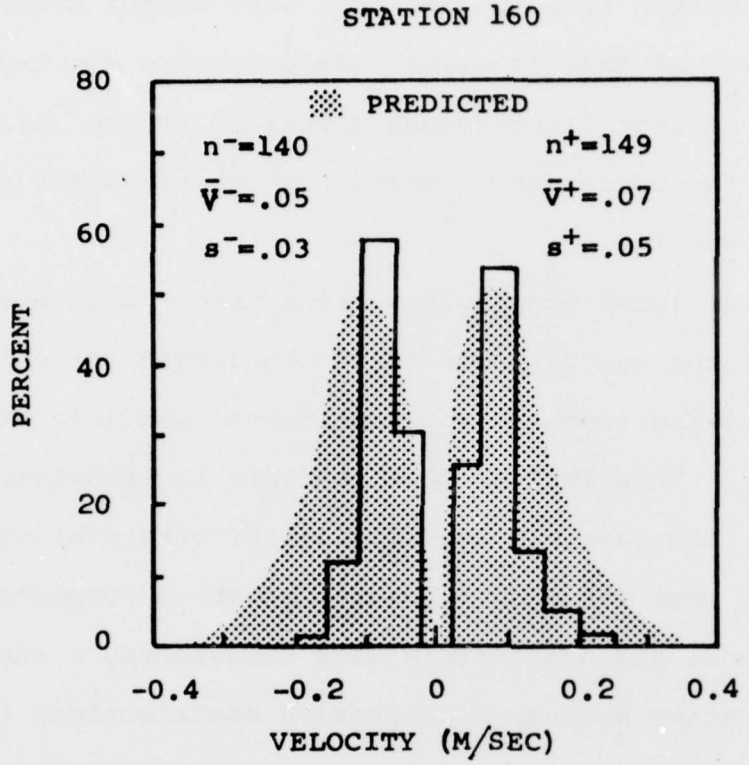

Figure 5.27

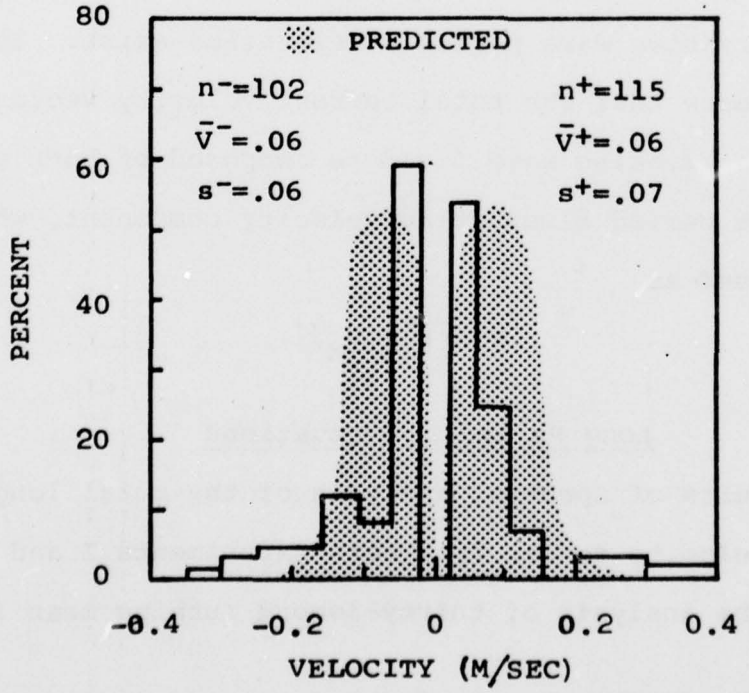

Figure 5.28

can be predicted from the incident wave height probability distribution at that location. Hence, these short-period longshore current fluctuations appear to be the anticipated result of the conservative portion of the incident wave particle velocity.

Conventional longshore current theory suggests, however, that the contribution to the longshore current flow field resulting from the wave horizontal particle velocity is $c_B \sin\theta_B$. This implies that the wave is translational and hence, the particle velocity is not conservative. Since a shoaling wave field on a natural beach is composed of both translational and oscillatory wave components, a combination of conservative and non-conservative contributions to the longshore current velocity field should be expected. For the case of pure two-dimensional motion the existence of a mean longshore current velocity component is required if non-conservative wave particle velocities exist. It, therefore, appears that the total current velocity vector resulting from a breaking wave field is composed of both a steady and a wave period fluctuating velocity component, which can be expressed as

$$V = \overline{V} + V_W.$$

Long Period Fluctuations

Results of spectral analysis of the total longshore current velocity series from both Experiments I and II, as well as the analysis of thirty-second running mean longshore

current velocities suggests that significant long-period fluctuations are present in the longshore current flow field. To evaluate the contribution to the time dependent longshore current velocity at periods longer than those associated with the incident wave field, the total longshore current velocity records from each current monitoring station of both experiments were demeaned and decomposed to remove any steady or wave period fluctuations from the observed series. An example of this decomposition is shown in Figure 5.25 which is a representative portion of the total sixteen-minute longshore current velocity record from the surface current meter at Station 160 of Experiment II. The filtered, demeaned series (Figure 5.25 D) contains only fluctuations whose periods are between 25 and 100 seconds. This series represents the long-period component of the longshore current flow field.

To further evaluate the long-period velocity components spectra were calculated from the total, simultaneously measured, longshore current velocity records from the upper and lower current meters at Stations 250, 160 and 100 of Experiment II (Figures 5.29 - 5.31). All spectra show well defined high and low frequency peaks which can be associated with surf zone driving forces.

There are several possible explanations for the existence of low frequency variance in the longshore current spectra. Among these is the possibility of long-period

Figure 5.29 Spectra calculated from total, simultaneously measured, longshore current velocity records from the upper and lower current meters at Station 250, Experiment II.

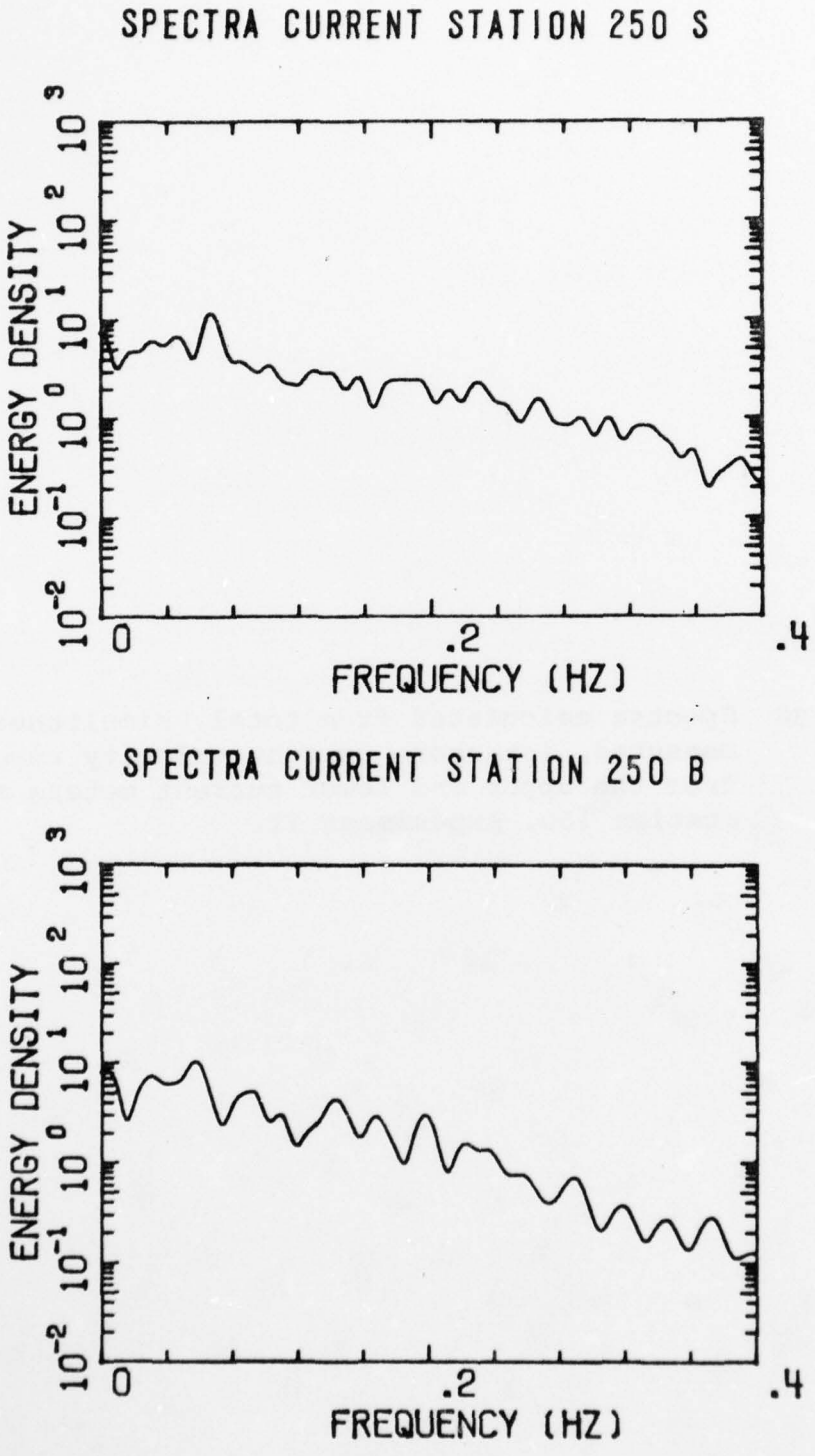
SPECTRA CURRENT STATION 250 S
ENERGY DENSITY
10^{-2} 10^{-1} 10^{0} 10^{1} 10^{2} 10^{3}
0
.2
.4
FREQUENCY (HZ)
SPECTRA CURRENT STATION 250 B
ENERGY DENSITY
10^{-2} 10^{-1} 10^{0} 10^{1} 10^{2} 10^{3}
0
.2
.4
FREQUENCY (HZ)

Figure 5.29

Figure 5.30 Spectra calculated from total, simultaneously measured, longshore current velocity records from the upper and lower current meters at Station 160, Experiment II.

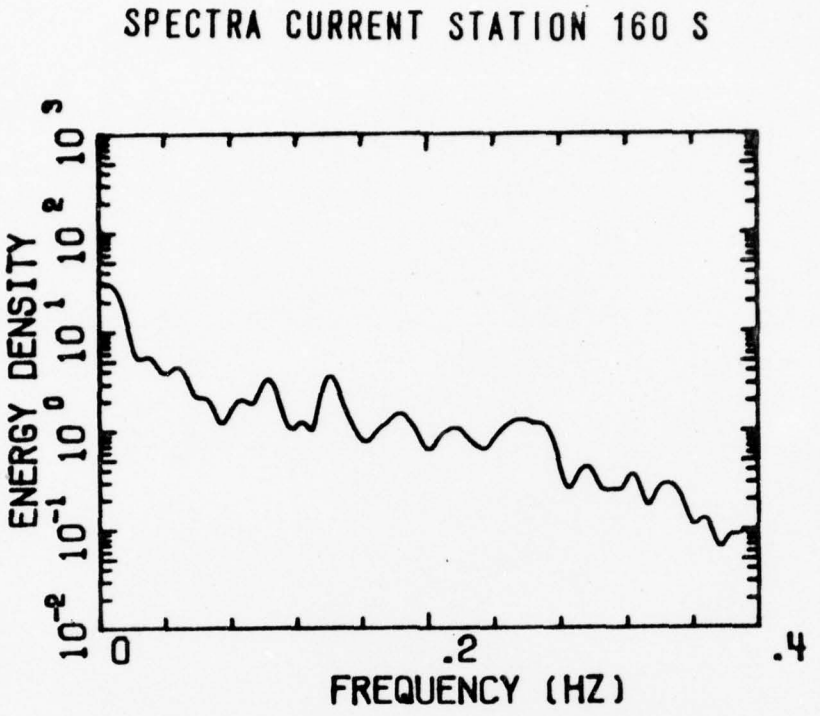
SPECTRA CURRENT STATION 160 S
ENERGY DENSITY
10^{-2} 10^{-1} 10^{0} 10^{1} 10^{2} 10^{3}
0
.2
.4
FREQUENCY (HZ)

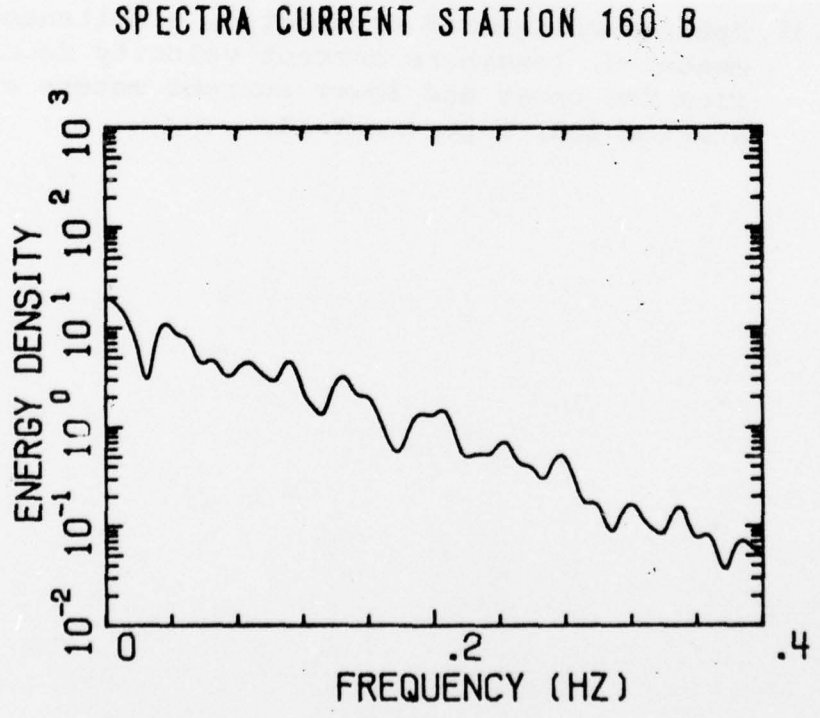
SPECTRA CURRENT STATION 160 B
ENERGY DENSITY
10^{-2} 10^{-1} 10^{0} 10^{1} 10^{2} 10^{3}
0
.2
.4
FREQUENCY (HZ)

Figure 5.30

Figure 5.31 Spectra calculated from total, simultaneously measured, longshore current velocity records from the upper and lower current meters at Station 100, Experiment II.

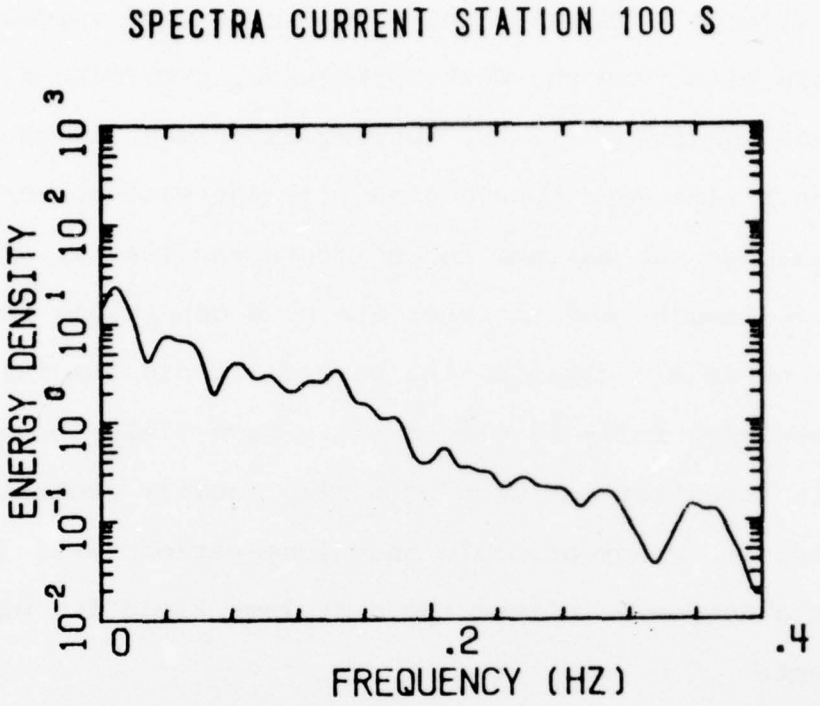
SPECTRA CURRENT STATION 100 S
ENERGY DENSITY
10^{-2} 10^{-1} 10^{0} 10^{1} 10^{2} 10^{3}
0
.2
.4
FREQUENCY (HZ)

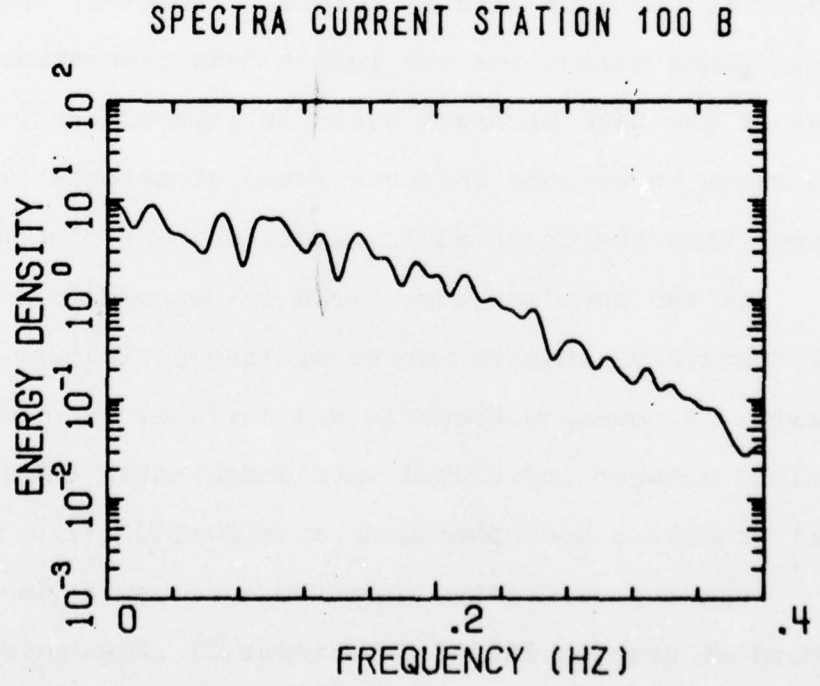
SPECTRA CURRENT STATION 100 B
ENERGY DENSITY
10^{-3} 10^{-2} 10^{-1} 10^{0} 10^{1} 10^{2}
0
.2
.4
FREQUENCY (HZ)

Figure 5.31

swell being a component of the incident wave field. During Experiment I the wave and wind fields were approaching the field site from the west-north-west, providing a maximum fetch length of 110 km. During Experiment II the wave and wind fields were approaching from the west-south-west; for this case the maximum fetch length was 104 km. For these fetch lengths and the moderate wind conditions necessary to run these experiments, the wave field did not reach the state of a fully developed sea. Wave fields observed during this investigation were primarily locally generated. Therefore, it is not probable that long-period swell (8-17 sec.) was a component of the incident wave field for either experiment.

Another possible cause of long-period wave motion incident at the surf zone is seiches. However, the minimum anticipated period for the lowest made transverse oscillation of the Lake Michigan basin is approximately five hours. The range of periods characteristic of seiches is much longer than the observed longshore current fluctuations.

If the incident wave field is composed of more than one frequency, another source of long-period wave motion exists. A non-monochromatic sea surface can produce interactions between individual wave components. This interaction will produce a beat phenomena at a period $f(1/\Delta\sigma)$.

Spectra calculated from the outer surf zone wave record at Station 250 of Experiment II shows several spectral

peaks in the wind wave range (Figure 5.32). These peaks correspond to periods of 3.02, 3.45, 3.73, 4.74, 5.26 and 7.58 seconds. This incident wave field is clearly non-monochromatic in the wind wave range.

The linear addition of two wave trains of similar period will produce a beat phenomena. As an example of the generation of beat frequencies, wave components of frequencies corresponding to those resolved by the spectral analysis of wave Station 250, in the wind wave range, were combined to produce their respective beat frequencies (see Table 5.8). It can be seen from Table 5.8 that appropriate combinations of incident wave periods can produce long-period fluctuations of periods resolved by the spectral analysis. A similar analysis was performed for the incident wave periods resolved by spectral analysis of wave records from Stations 160 and 100 of Experiment II (Tables 5.9 and 5.10, respectively). The results of this analysis also suggest wave interactions are occurring within the surf zone.

The linear addition of two sinusoidal wave components of periods 3.45 and 3.73 seconds, resolved by the spectral analysis of the wave record from Station 250, Experiment II, produce a wave envelope with a beat period of 45.9 seconds. Spectral analysis was then preformed on this synthetic two-component times series. The results of this spectral analysis resolved the two-input sinusoidal components, however,

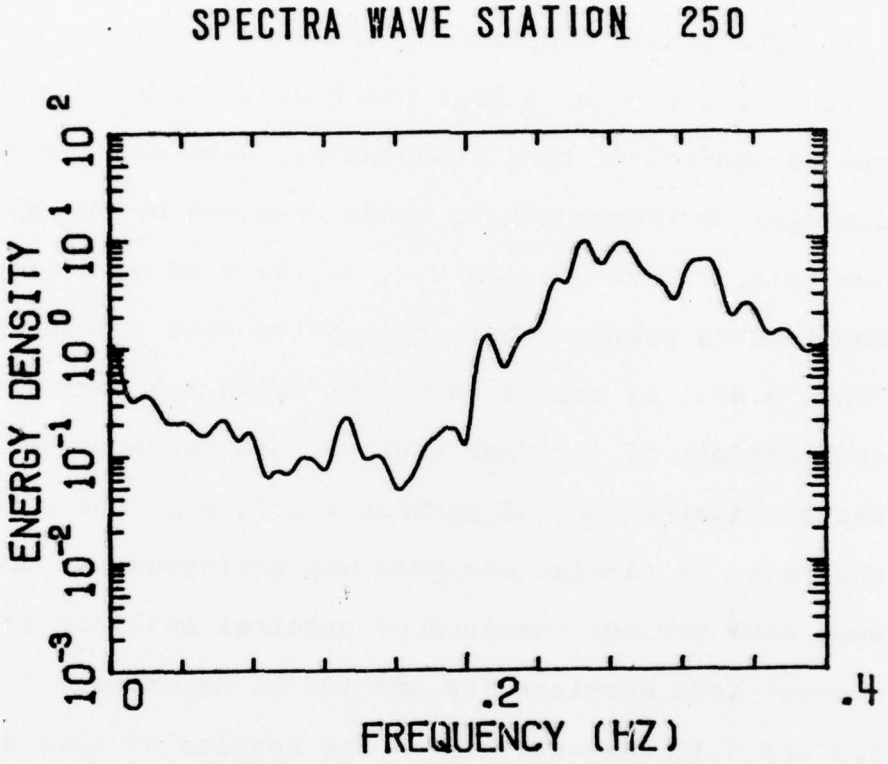

Figure 5.32 Spectra calculated from the total sixteen minute water surface elevation record at Station 250, Experiment II.

Table 5.8

CALCULATED BEAT PERIODS, STATION 250

Resolved Periods (sec.)	3.02	3.45	3.73	4.74	5.26	7.58
3.02	∞	24.2	15.9	9.3	7.1	5.0
3.45		∞	45.9	12.7	10.0	6.3
3.73			∞	17.5	12.8	7.3
4.74				∞	48.0	12.7
5.26					∞	17.2
7.58						∞

Table 5.9

CALCULATED BEAT PERIODS, STATION 160

Resolved Periods (sec.)	3.00	3.56	3.73	4.76	5.35	7.19
3.00	∞	19.1	15.3	8.1	6.8	5.2
3.56		∞	78.1	14.1	10.6	7.1
3.73			∞	17.2	12.3	7.8
4.76				∞	43.2	14.1
5.35					∞	20.9
7.19						∞

Table 5.10

CALCULATED BEAT PERIODS, STATION 100

Resolved Periods (sec.)	2.99	3.23	3.57	4.00	5.26	6.05
2.99	∞	40.2	18.4	11.8	6.9	5.9
3.23		∞	33.9	16.8	8.4	6.9
3.57			∞	33.2	11.1	8.7
4.00				∞	16.7	11.8
5.26					∞	40.3
6.05						∞

no variance was resolved at the beat frequency. This result should be expected, since no wave phenomena exist at the beat frequency.

An examination of the original time series from Station 250, Experiment II, reveals very well defined wave groups (Figure 5.33). This periodic amplitude modulation of the incident wave field appears to be the result of the formation of a beat from at least two incident wave components. The period of the beat tends to correspond with the calculated period of 45.9 seconds. However, this observed incident wave field is not simply the result of a two-component interaction. As additional wave components are included in the analysis, beats are generated at multiple frequencies and are not stationary in time.

However, the spectra calculated from the water surface elevation record at Station 250 does resolve variance at this theoretical beat period, 45.9 seconds. For a spectral response at this period to exist, wave motion at that frequency must be present since periodic amplitude modulation of the time series is known not to result in a spectral response at that period. It, therefore, appears that this long period fluctuation in the free surface elevation is driven by a locally generated beat.

As has been suggested by Longuet-Higgins and Stewart (1962), for a non-monochromatic sea, that the effect of an increase in the radiation stress associated with a group of

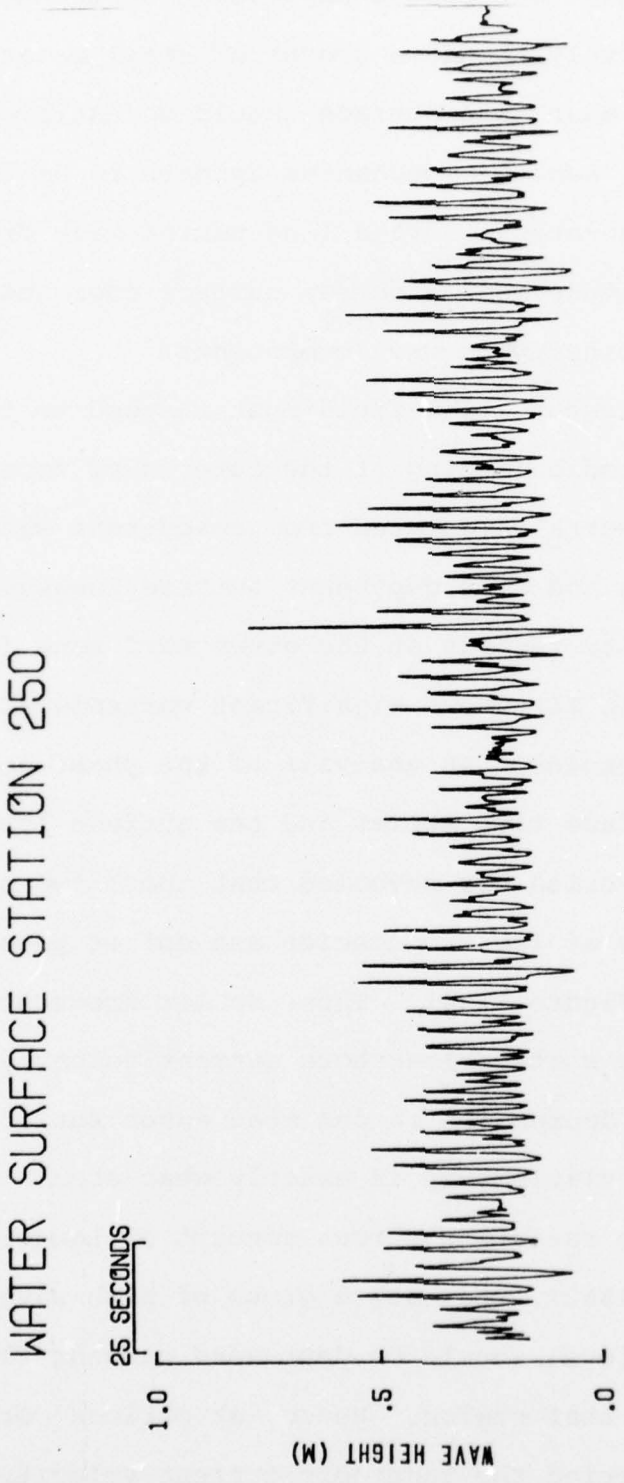

Figure 5.33 Representative portion of the total sixteen minute water surface elevation record at Station 250, Experiment II.

high waves tends to create a depression in the mean water level. Conversely, beneath groups of small waves an elevation in the mean free surface should be anticipated (Figure 3.3). Hence, a mechanism appears to be in operation which generates a forced long-period wave from a periodic amplitude modulated sea surface composed of at least two distinct wind wave components.

The longshore flow field must respond to this low frequency periodic forcing at the outer surf zone. Comparison of spectra calculated from concurrent water surface elevation and time dependent surface longshore current velocity records at the outer surf zone (Station 250, Experiment II) shows significant variance at particular low frequencies. An analysis of the phase lag between the water surface time series and the surface longshore current time series has revealed that these two series tend to be in-phase at low frequencies and out of phase at high frequencies (Figure 5.34). Thus, at low frequencies, a maximum in the surface longshore current velocity is associated with a depression in the mean water surface, and vice versa. This relationship is exactly what should be anticipated from the radiation stress concept of Longuet-Higgins and Stewart (1962). Beneath a group of high waves the mean free surface level should be depressed causing fluid to be expelled from that region. Hence, at periods corresponding to the beat period the longshore current velocity should reflect this pulsation. Therefore, maxima in long-period

longshore current velocity fluctuations should be associated with the arrival of groups of large waves. These large waves have been shown to produce large magnitude fluctuations in the longshore current flow field at periods associated with the incident wave field. It, therefore, appears that fluctuations in the longshore current flow field can be induced by successive wave groups (beats) which can drive observed long-period oscillations in the nearshore zone.

Results of similar phase comparisons between the surface longshore current velocity and concurrent water surface elevation records at Stations 160 and 100 are presented in Figures 5.35 and 5.36, respectively. Once wave breaking has occurred, the pattern of forced oscillations in the longshore current flow field is not as clear as it was prior to breaking. Non-linearities associated with wave breaking, wave transformations, and wave interactions through the surf zone appear to alter the expected phase relationships.

Summary

As a result of this investigation, three primary longshore current velocity components have been isolated which contribute to the total instantaneous longshore current flow vector,

$$V = \bar{V} + V_W + V_L$$

$\bar{V}$, is the steady longshore current velocity component

Figure 5.34 Outer surf zone spectra and phase computed from sixteen minute simultaneous time histories of water level elevation and surface longshore current velocity at Station 250, Experiment II.

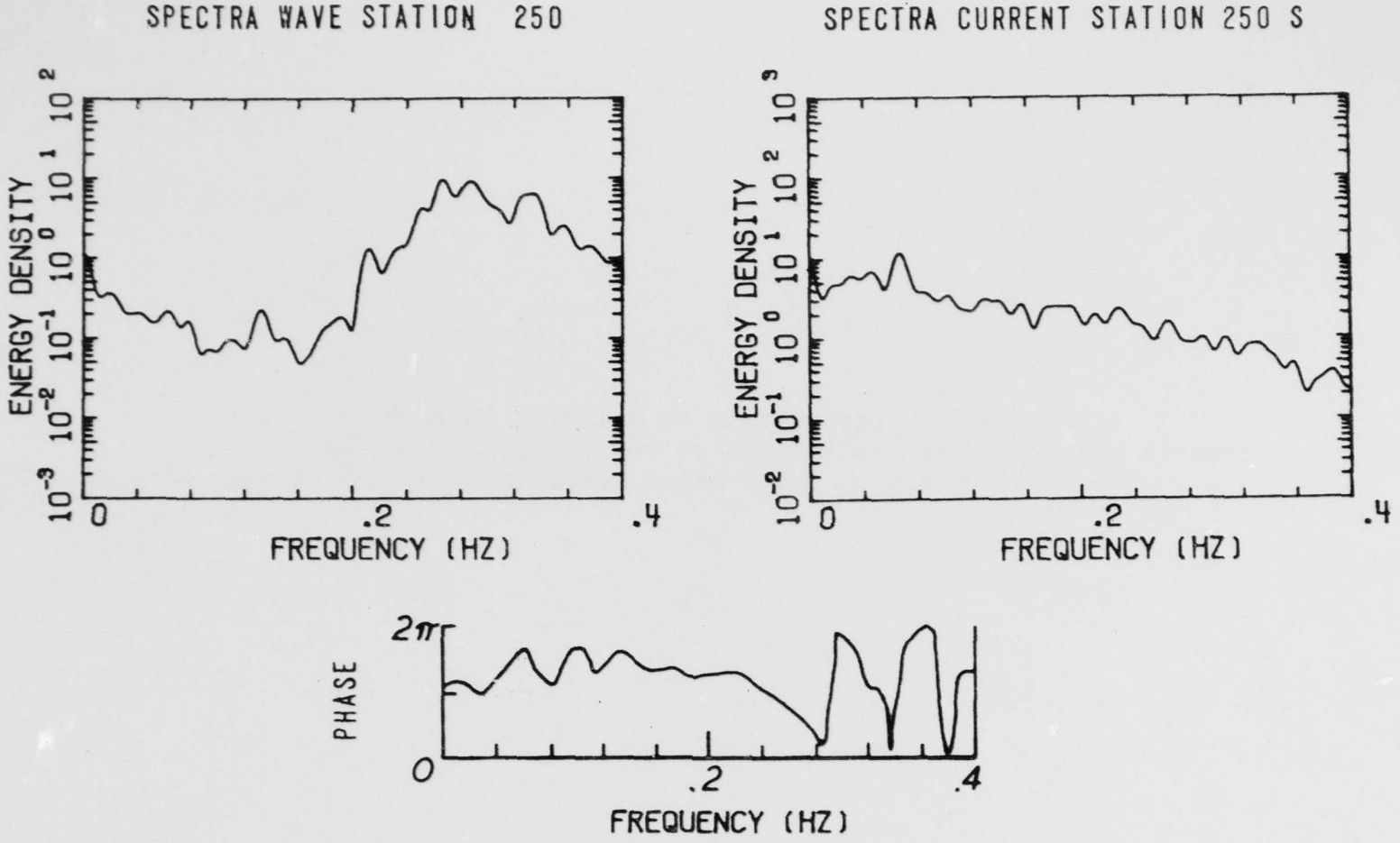
SPECTRA WAVE STATION 250
ENERGY DENSITY
10^{-3} 10^{-2} 10^{-1} 10^{0} 10^{1} 10^{2}
0
.2
.4
FREQUENCY (HZ)
SPECTRA CURRENT STATION 250 S
ENERGY DENSITY
10^{-2} 10^{-1} 10^{0} 10^{1} 10^{2} 10^{3}
0
.2
.4
FREQUENCY (HZ)
PHASE
2π
0
.2
.4
FREQUENCY (HZ)

Figure 5.34

Figure 5.35 Mid surf zone spectra and phase computed from sixteen minute simultaneous time histories of water level elevation and surface longshore current velocity at Station 160, Experiment II.

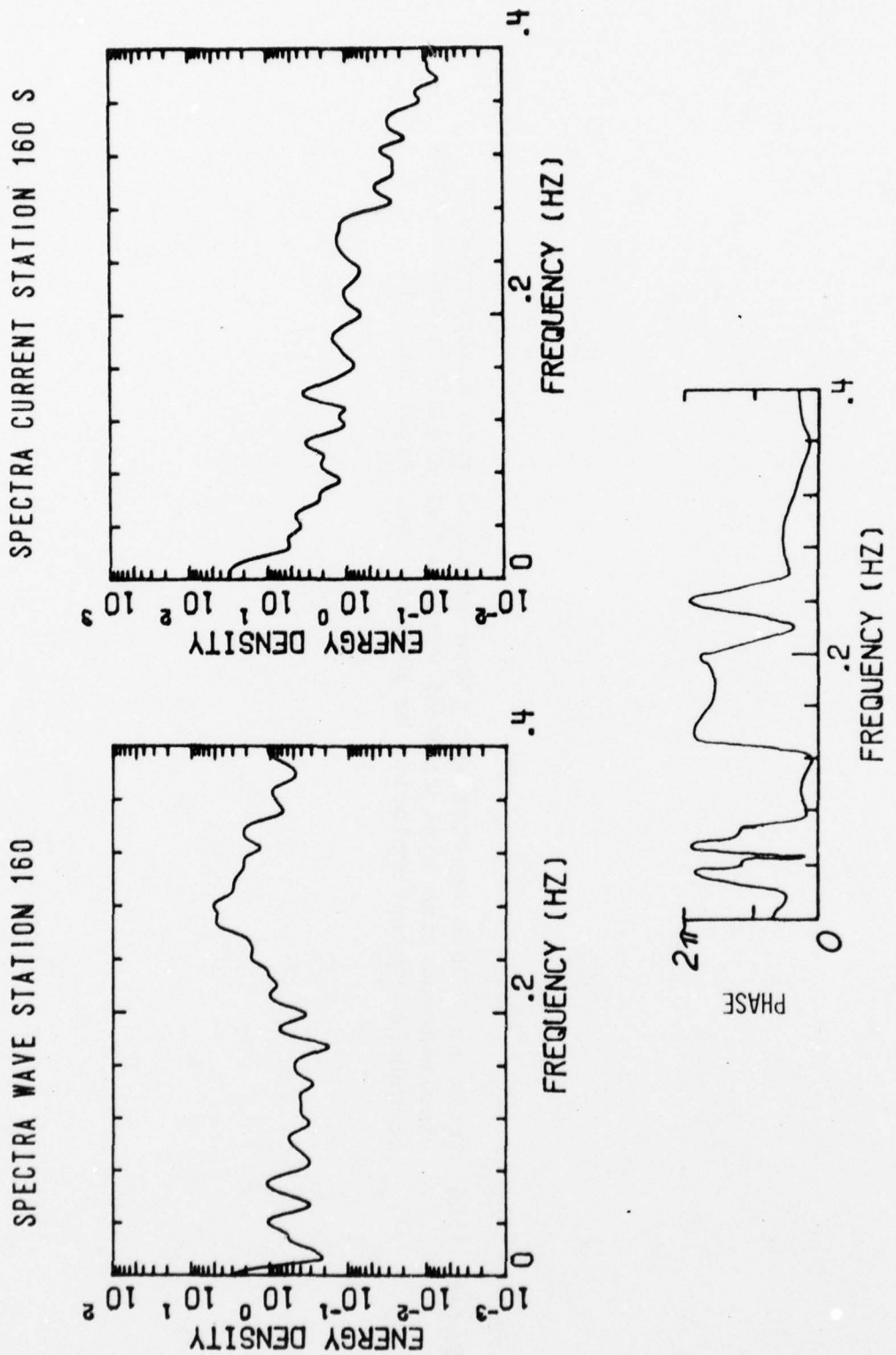
SPECTRA CURRENT STATION 160 S
ENERGY DENSITY
FREQUENCY (HZ)
SPECTRA WAVE STATION 160
ENERGY DENSITY
FREQUENCY (HZ)
PHASE
FREQUENCY (HZ)

Figure 5.35

Figure 5.36 Inner surf zone spectra and phase computed from sixteen minute simultaneous time histories of water level elevation and surface longshore current velocity at Station 100, Experiment II.

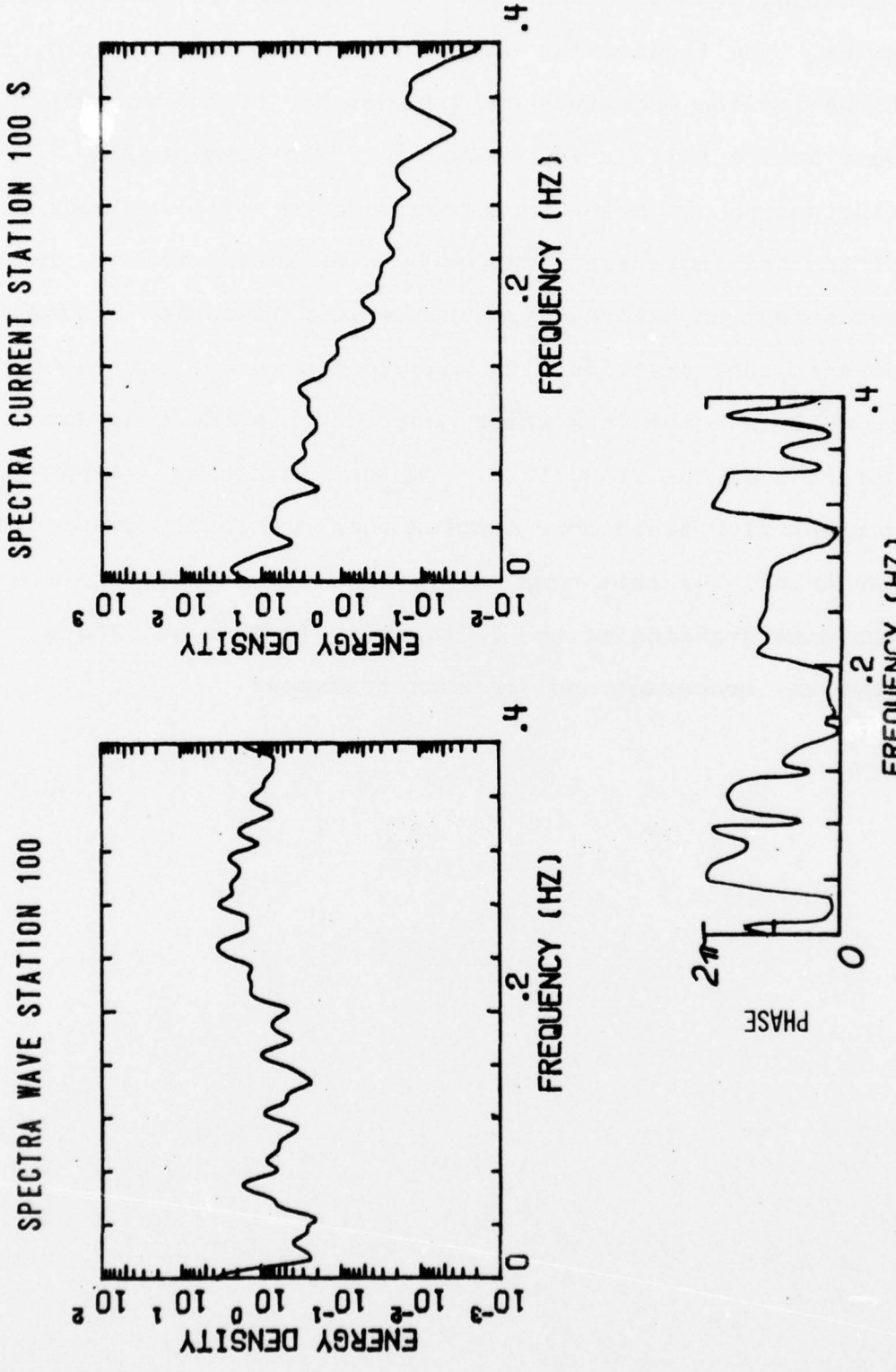
SPECTRA WAVE STATION 100
ENERGY DENSITY
FREQUENCY (HZ)
SPECTRA CURRENT STATION 100 S
ENERGY DENSITY
FREQUENCY (HZ)
PHASE
FREQUENCY (HZ)

Figure 5.36

resulting from the translational component of the incident waves. The fluctuating component, V_W, is directly proportional to the magnitude and periodicity of the incident wave horizontal particle velocity. The long-period fluctuating component, V_L, results from periodic loading of the nearshore zone induced by wave interactions. This investigation has resulted in the identification of components that contribute to mean longshore current velocity as well as components which contribute to the time dependent portions of the flow field. The net result is a longshore current flow field more complex than previously considered. Recognition of this complexity, however, may lead to a better understanding of the factors involved in nearshore physical processes and sediment transport.

CHAPTER VI

CONCLUSIONS AND DISCUSSION

This investigation has made several essential contributions to the understanding of longshore current dynamics and may lead to a greater understanding of nearshore physical processes on natural beaches. Specifically, a two-dimensional mapping, across the surf zone and with depth, of the longshore current flow field has now been established under field conditions. This mapping has also been established for two types of commonly occurring natural bathymetries; one in which the offshore bar is a major feature and another in which the bar is a minor feature of the nearshore bathymetry. This investigation has established a temporal structure for the longshore current flow field, which should aid in the understanding of sediment transport as well as circulation within the coastal zone. It is anticipated that, as a result of this study, the response of both engineering and natural structures within the nearshore region to wave-induced current motions may be better understood.

It can be concluded from this study that the vertical structure of the mean longshore current flow field is uniform with depth except for a narrow bottom boundary layer.

This observation is in agreement with previous theoretical assumptions on the vertical structure of the longshore current flow field. Vertical uniformity of the flow field throughout most of the surf zone water column implies sharp velocity gradients, and hence large shear stresses at the sediment-water interface. Likewise, the magnitude of these shear stresses varies widely in response to longshore current velocity fluctuations.

From this investigation it can also be concluded that the total, instantaneous longshore current velocity vector at any point across the surf zone is composed of three primary components. These components are: i) a steady longshore current velocity component; ii) a long-period fluctuating velocity component which tends to be out-of-phase with the incident wave field; and iii) a short-period fluctuating longshore current velocity component which tends to be in-phase with the incident wave field.

The mean longshore current velocity component has been attributed, in a two-dimensional context, to the non-conservative portion of breaking wave horizontal particle velocity. However, three-dimensional flow on a natural beach may result in additional driving forces of longshore currents. Lake Michigan was chosen as the field site for these experiments to eliminate the contribution to the mean longshore current velocity resulting from the tide. However, variations of the incident wave field in the alongshore direction can be expected to result in a slope of the

nearshore water surface, causing a mean longshore flow. This effect cannot be evaluated because of the two-dimensional nature of this study, but the resulting flow may still have been measured.

The long-period fluctuating longshore current velocity component results from the beat produced by interaction of a non-monochromatic incident wave field. Beneath groups of high waves the mean sea surface is depressed resulting in a flow of fluid from that region. The opposite situation should be anticipated beneath groups of small waves. Hence, the long-period fluctuating longshore current velocity component should be out of phase with the induced long period component of the incident wave field. In a three-dimensional framework, an incident short-crested sea surface as well as the existance of edge waves may also contribute to the longshore current velocity vector. These contributions, however, cannot be evaluated within the two-dimensional context of this study.

Short-period longshore current fluctuations have been shown to result from the conservative portion of the incident breaking wave horizontal particle velocity. The surf zone, however, is a region of transition from nearly conservative wave particle velocities outside the surf zone to totally translational wave particle velocities near the shore. Hence, each wave-induced component of the total longshore current velocity vector should not necessarily contribute, in the same relative proportion, to the longshore

current flow field at any point across the surf zone. Any one of the three components contributing to the longshore current flow field could be dominant, depending upon position across the surf zone.

The results of this study have further indicated that neither the deterministic radiation stress approach to the prediction of longshore currents, Longuet-Higgins (1970), nor the probabilistic formulation of Collins (1972), provide adequate prediction of the magnitude and distribution of longshore current velocity across the surf zone. The probabilistic formulation of Collins (1972) appears to provide the most satisfying formulation in terms of observed incident wave fields; however, in order to provide good quantitative predictions of longshore current flow fields, a close examination of both the mixing parameter (P) and the coefficient of bottom friction (C_f) must be undertaken. In addition, the assumed incident wave height probability distribution at the outer surf zone must be in better agreement with actual observed distributions. For only in this way can an accurate parameterization of bottom friction and lateral mixing be obtained. Furthermore, it seems unrealistic to expect mixing across the surf zone to occur from only lateral mixing or from only the random breaking of a probabilistic incident wave field. On a natural beach both processes should be occurring simultaneously.

This investigation has also isolated the existence of a low velocity zone in the longshore current flow field over the

submarine bar, which is not present on a planer beach. This low velocity zone was not observed during Experiment I for several reasons. First, the bar was a minor feature of the surf zone bathymetry. Second, the surf zone was much broader during Experiment I with the zone of active breaking shifted further offshore. Third, only a limited portion of the surf zone was investigated during this preliminary experiment. It should, therefore, be anticipated that for waves breaking over a bar and experiencing an exponential decay of wave height shoreward. The longshore current should also monotonically decay shoreward, but this is not seen. Instead, the bar appears to produce a frictional retardation of the longshore current flow field directly over its crest.

The results of this investigation suggest several areas of future work. Observations of the total longshore current flow vector should be extended into the third dimension. This would provide a complete understanding of the spatial and temporal character of nearshore circulation and related physical processes. Specifically, it would assist in the evaluation of forcing functions which have a longshore dependency. It appears that existing analytic formulations for longshore current flow prediction should be re-evaluated in light of the findings of this study. Specifically, time dependent formulations should be derived and evaluated on the temporal scales suggested by this study.

As a result of this study, the two-dimensional spatial and temporal structure of the longshore current flow field has been measured on a natural beach. This achievement, however, only represents an initial step toward complete understanding of nearshore physical processes. Many more field investigations of this type are necessary before total understanding of beach processes is attained. Until that time, man will not be able to use this natural resource, the beach, without altering its natural processes and beauty.

REFERENCES CITED

REFERENCES CITED

Bowen, A.J., Rip Currents, Ph.D. Thesis, University of California at San Diego, 115 pp., 1967.

Bowen, A.J., The generation of longshore currents on a plane beach, Jour. Mar. Res., 27, 1969.

Bowen, A.J., D.L. Inman, and V.P. Simmons, Wave "set-down" and "set-up", Jour. of Geophys. Res., 73, No. 8, 1968.

Brebner, A., and J.W. Kamphuis, Model tests on relationship between deep-water wave characteristics and longshore currents, Queens University, Civil Eng. Res. Rep., 31, 1963.

Bretschneider, C.L., Field investigation of wave energy loss of shallow water ocean waves. U.S. Army, Beach Erosion Board, Tech. Mem. 46, 1954.

Brunn, P., Longshore currents and longshore troughs, Jour.of Geophys. Res., 68, No. 4, 1963.

Caldwell, J.M., The step-resistance wave gage, Costal Eng. Inst., Council on Wave Res., Berkeley, California, 44-60, 1956.

Chapman, D.G. "A comparative study of several one-sided goodness-of-fit tests", Ann. Math Stat., 29, 655, 1959.

Collins, J. I., "Wave statistics from Hurricane Dora", Jour. Waterways and Harbors Division, A.S.C.E., 1967.

Collins, J. I., Longshore currents and wave statistics in the surf zone, Tetra Tech. Inc., Report No. TC 149-2, 1972.

Dette, H.H., Uber brandungsstromungen im bereich hoher Reynolds-Zahlem, Heft 41. Leichtweiss-Institut Fur Wasserbau der Technischen Uniersitat Braunschweig, 1974.

Eagleson, P.S., Theoretical study of longshore currents on a plane beach, M.I.T., Hydrodynamics Lab Tech. Rept. 82, 1965.

Earl, M.D., Longshore currents generated by waves with a Rayleigh wave amplitude distribution, (Abs.), Trans. Amer. Geophys. Union, 55, No. 4, 1974.

Galvin, C.J., Longshore current velocity: A review of theory and data, Rev. Geophys., 5, 287-304, 1967.

Galvin, C.J., and P.S. Eagleson, Experimental study of longshore currents on a plane beach, U.S. Army Coast. Eng. Res. Center, Tech. Mem., 10, 80, 1965.

Harrison, W., Empirical equation for longshore current velocity, Jour. Geophys. Res., 73, 6929-6936, 1968.

Harrison,W., and W.C. Krumbein, Interactions of the beach-ocean-atmosphere system at Virginia Beach, Virginia, U.S. Army Costal Eng. Res. Center, Tech. Mem.,7, 1-102, 1964.

Huntley, D.A. and A.J. Bowen, Field measurements of near-shore velocities, Proc. Fourteenth Conf. Costal Eng. A.S.C.E., 1974.

Inman, D.I., and W.H. Quinn, Currents in the surf zone, Proc. 2nd Conf. on Cost. Eng. 24-36, 1951.

Inman, D.L., and Bagnold,R.A., Littoral processes 2. The Sea, 3, 529-533. M.N. Hill, (ed.), Interscience, New York.

James, I.D., Non-linear waves in the nearshore region: Shoaling and set-up, Estuarine and Coastal Mar. Sci., 2, 1974a.

James, I.D., A non-linear theory of longshore currents, Estuarine and Coastal Mar. Sci., 2, 1974b.

Komar, P.D., Nearshore cell circulation and distribution of giant cusps, Geol. Soc. Amer. Bull., 82, 1971.

Komar, P.D., and Inman, D.L., Longshore sand transport on beaches. Jour. Geophy. Res.,75, 5914-5927, 1970.

Longuet-Higgins, M.S., The statistical analysis of a random moving surface, Phil. Trans. Royal Soc. of London, A-966, 1957.

Longuet-Higgins, M.S., Longshore currents generated by obliquely incident sea waves 1, Jour. Geophys. Res., 75, No. 33, 6778-6789, 1970a.

Longuet-Higgins, M.S., Longshore currents generated by Obliquely incident sea waves 2, Jour. Geophys. Res., 75, No. 33, 6790-6801, 1970b.

Longuet-Higgins, M.S., Recent progress in the study of longshore currents. In: R.E. Meyer (ed.), Waves on beaches and resulting sediment transport. Academic Press, New York, N.Y., 203-248, 1972.

Longuet-Higgins, M.S. and Stewart, R.W., Change in the form of short gravity waves on long waves and tidal currents. Jour. Fluid Mech.,8, 565-583, 1960.

Longuet-Higgins, M.S. and Stewart, R.W., Radiation stress and mass transport in gravity waves. Jour. Fluid Mech.,13, 481-504, 1962.

Longuet-Higgins, M.S. and Stewart, R.W., A note on wave set-up. Jour. Mar. Res.,21,4-10,1963.

Longuet-Higgins, M.S. and Stewart, R.W., Radiation stresses in water waves; a physical discussion, with applications. Deep-Sea Res., 11, 529-562, 1964.

Miller, R.L., Experimental determination of run-up of undular and fully developed bores, Jour.Geophys. Res.,73, 4497-4510, 1968.

Noda, E.K., Wave induced nearshore circulation, Res., 79, No. 21, 1974.

Philips, O.M., On the dynamics of unsteady gravity waves of finite amplitude. Part 1. The elementary interactions. Jour. Fluid Mech.,9,193-217, 1960.

Putman, J.A., W.H. Munk, and M.A. Traylor, The prediction of longshore currents, Trans. Am. Geophys. Union, 30, 337-345, 1949.

Russell, T.L., A step-type recording wave gage, Ocean Wave Spectra, Prentice-Hall, New Jersey, 251-257, 1963.

Shepard, F.P., K.O. Emery, and E.C. LaFond, Rip currents: A process of geological importance, Jour. Geol.,49,No. 4, 1941.

Sonu, C.J., Field observation of nearshore circulation and meandering currents, Jour. Geophys. Res.,77,No. 18, 1972.

Sonu, C.J., Three dimensional beach changes, Jour. Geol.,81, 42-46, 1973.

Sonu, C.J., J.M. McCloy, and D.S. McArthur, Longshore currents and nearshore topographies, Proc. 10th Conf. on Coast. Eng., 525-549, New York, 1967.

Teleki, P.G., Wave Boundary Layers and their relation to sediment transport, 1970.

Thornton, E.B., Longshore currents and sediment transport, Tech. Report, No. 5, University of Florida, 1969.

Thornton, E.B., Variation of longshore currents across the surf zone, Proc. 12th Conf. on Cost. Eng., 1, 291-308, Washington, D.C., 1971.

Whitham, G.B., Mass, momentum and energy flux in water waves, Jour. Fluid Mech.,12,1962.

Wood, W.L., A ducted impellor flowmeter for shallow-water measurements of internal velocities in breaking waves, Michigan State University, Dept. of Geology, Tech. Report No. 1, 1968.

Wood, W.L., A shallow-water instrument system for monitoring wave and current parameters in the nearshore zone, Michigan State University, Dept. of Geology, Tech. Report No. 2, 1970.

Wood, W.L., A wave and current investigation in the nearshore zone, Michigan State University, Dept. of Geology, Final Report, 1973.

Wood, W.L., Three dimensional conditions of surf, Proc. 15th Conf. Costal Eng., A.S.C.E., 1, No.30, 1977.

Wood, W.L., and G.A. Meadows, Unsteadiness in longshore currents, Geophys. Res. Letts., 2, No.11, 1975.

APPENDIX

APPENDIX A

CONTINUOUS OVERLAPING 30 SECOND TIME AVERAGES OF THE VERTICAL DISTRIBUTION OF LONGSHORE CURRENT VELOCITY

Time (Sec.)	0-30	15-45	30-60	45-75	60-90	75-105	90-120
Upper Meter:							
Mean (v)	0.49	0.54	0.46	0.39	0.39	0.40	0.42
Std. Dev. (s)	0.11	0.13	0.15	0.09	0.07	0.07	0.09
Mid. Meter:							
Mean (v)	0.48	0.51	0.43	0.35	0.37	0.41	0.41
Std. Dev. (s)	0.08	0.08	0.11	0.07	0.06	0.05	0.08
Bottom Meter:							
Mean (v)	0.31	0.41	0.36	0.23	0.21	0.25	0.21
Std. Dev. (s)	0.12	0.12	0.17	0.14	0.06	0.08	0.11
Time (Sec.)	105-135	120-150	135-165	150-180	165-195	180-210	195-225
Upper Meter:							
Mean (v)	0.51	0.55	0.46	0.45	0.46	0.48	0.54
Std. Dev. (s)	0.17	0.15	0.11	0.11	0.12	0.16	0.17
Mid. Meter:							
Mean (v)	0.48	0.52	0.46	0.45	0.43	0.48	0.52
Std. Dev. (s)	0.16	0.13	0.10	0.13	0.14	0.15	0.14
Bottom Meter:							
Mean (v)	0.32	0.39	0.31	0.37	0.39	0.39	0.44
Std. Dev. (s)	0.20	0.16	0.20	0.16	0.20	0.18	0.17
Time (Sec.)	210-240	225-255	240-270	255-285	270-300	285-315	300-330
Upper Meter:							
Mean (v)	0.56	0.52	0.47	0.56	0.67	0.44	0.38
Std. Dev. (s)	0.15	0.12	0.10	0.14	0.17	0.14	0.11
Mid. Meter:							
Mean (v)	0.51	0.47	0.45	0.51	0.66	0.44	0.43
Std. Dev. (s)	0.13	0.11	0.10	0.13	0.16	0.12	0.11
Bottom Meter:							
Mean (v)	0.45	0.34	0.26	0.48	0.54	0.41	0.34
Std. Dev. (s)	0.15	0.14	0.14	0.18	0.21	0.18	0.14
Time (Sec.)	315-345	330-360	345-375	360-390	375-405	390-420	405-435
Upper Meter:							
Mean (v)	0.42	0.38	0.44	0.54	0.48	0.41	0.40
Std. Dev. (s)	0.13	0.10	0.14	0.16	0.14	0.12	0.12
Mid. Meter:							
Mean (v)	0.40	0.40	0.42	0.48	0.46	0.40	0.41
Std. Dev. (s)	0.10	0.10	0.12	0.13	0.13	0.12	0.12
Bottom Meter:							
Mean (v)	0.34	0.33	0.35	0.31	0.29	0.22	0.23
Std. Dev. (s)	0.10	0.18	0.12	0.20	0.18	0.13	0.13

Time (Sec.)	420-450	435-465	450-480	465-495	480-510	495-525	510-540
Upper Meter:							
Mean (v)	0.42	0.46	0.53	0.52	0.51	0.55	0.53
Std. Dev. (s)	0.13	0.14	0.16	0.14	0.13	0.16	0.14
Mid. Meter:							
Mean (v)	0.42	0.46	0.51	0.52	0.52	0.54	0.52
Std. Dev. (s)	0.12	0.14	0.15	0.15	0.13	0.15	0.11
Bottom Meter:							
Mean (v)	0.23	0.39	0.42	0.42	0.35	0.40	0.40
Std. Dev. (s)	0.15	0.16	0.16	0.15	0.14	0.15	0.15

Time (Sec.)	525-555	540-570
Upper Meter:		
Mean (v)	0.54	0.55
Std. Dev. (s)	0.11	0.11
Mid. Meter:		
Mean (v)	0.55	0.56
Std. Dev. (s)	0.14	0.14
Bottom Meter:		
Mean (v)	0.39	0.34
Std. Dev. (s)	0.15	0.15

Unclassified

Security Classification

DOCUMENT CONTROL DATA - R & D

(Security classification of title, body of abstract and indexing annotation must be entered when the overall report is classified)

1. ORIGINATING ACTIVITY *(Corporate author)*

Great Lakes Coastal Research Lab.
Dept. of Geosciences, Purdue Univ.
West Lafayette, IN 47907

2a. REPORT SECURITY CLASSIFICATION: unclassified

2b. GROUP: unclassified

3. REPORT TITLE

A Field Investigation of the Spatial and Temporal Structures of Longshore Currents

4. DESCRIPTIVE NOTES *(Type of report and inclusive dates)*

5. AUTHOR(S) *(First name, middle initial, last name)*

Guy A. Meadows

6. REPORT DATE	7a. TOTAL NO. OF PAGES	7b. NO. OF REFS
December 1978	182	50

8a. CONTRACT OR GRANT NO.	9a. ORIGINATOR'S REPORT NUMBER(S)
N 00014-75-C-0716	Technical Report No. 6
b. PROJECT NO. NR 388-089	9b. OTHER REPORT NO(S) *(Any other numbers that may be assigned this report)*
c.	
d.	

10. DISTRIBUTION STATEMENT

Distribution of this document is unlimited

DISTRIBUTION STATEMENT A
Approved for public release;
Distribution Unlimited

11. SUPPLEMENTARY NOTES	12. SPONSORING MILITARY ACTIVITY
	Geography Programs Office of Naval Research Arlington, VA 22217

13. ABSTRACT

This field investigation was conducted to obtain simultaneous and continuous measurements of the horizontal, vertical and temporal variability of the longshore current flow field. The present study has resulted in a two-dimensional mapping, across the surf zone and with depth, of the longshore current flow field. The vertical structure of the mean longshore current flow field is nearly uniform with depth, with a narrow bottom boundary layer and sharp velocity gradients at the water-sediment interface. This investigation has also shown that the total longshore current velocity vector, at any point across the surf zone, is composed of three distinct velocity components. These components are: i) a steady longshore current velocity component; ii) a long-period fluctuating velocity component which tends to be out-of-phase with the incident wave field and; iii) a short-period fluctuating longshore current velocity component which tends to be in-phase with the incident wave field.

The results of this study have further indicated that neither the deterministic radiation stress approach to the prediction of longshore currents, nor a probabilistic formulation, provide adequate prediction of the magnitude or distribution of the longshpre current velocity across the surf zone. In addition, the existence of a low velocity zone in the longshore current flow field has been isolated over the submarine bar. It appears that existing analytical formulations for longshore current flow prediction must be re-evaluated in light of the findings of this study.

DD FORM 1 NOV 65 1473 (PAGE 1)

S/N 0101-807-6801

Security Classification

14. KEY WORDS	LINK A		LINK B		LINK C	
	ROLE	WT	ROLE	WT	ROLE	WT
Longshore currents						
Temporal variability						
Spatial variability						
Field study						

DISTRIBUTION LIST

Office of Naval Research (2)
Geography Programs
Code 462
Arlington, Virginia 22217

Denfense Documentation Center (12)
Cameron Station
Alexandria, Virginia 22314

Director, Naval Research Lab (6)
Attention Technical Information Officer
Washington, D. C. 20375

Director
Office of Naval Research Branch Office
1030 East Green Street
Pasadena, California 91101

Director
Office of Naval Research Branch Office
536 South Clark Street
Chicago, Illinois 60605

Director
Office of Naval Research Branch Office
495 Summer Street
Boston, Massachusetts 02210

Commanding Officer
Office of Naval Research Branch Office
Box 39
FPO New York 09510

Chief of Naval Research
Asst. for Marine Corps Matters
Code 100M
Office of Naval Research
Arlington, Virginia 22217

Office of Naval Research
Code 480
National Space Technology Laboratories
Bay St. Louis, Mississippi 39520

Office of Naval Research
Operational Applications Division
Code 200
Arlington, Virginia 22217

Office of Naval Research
Scientific Liaison Officer
Scripps Institution of Oceanography
La Jolla, California 92093

Director, Naval Research Laboratory
Attn. Library, Code 2628
Washington, D. C. 20375

ONR Scientific Liaison Group
American Embassy - Room A-407
Apo San Francisco 96503

Commander
Naval Oceanographic Office
Attn. Library Code 1600
Washington, D. C. 20374

Naval Oceanographic Office
Code 3001
Washington, D. C. 20374

Chief of Naval Operations
Op 987P1
Department of the Navy
Washington, D. C. 20350

Oceanographer of the Navy
Hoffman II Building
200 Stovall Street
Alexandria, Virginia 22322

Naval Academy Library
U. S. Naval Academy
Annapolis, Maryland 21402

Commanding Officer
Naval Coastal Systems Laboratory
Panama City, Florida 32401

Librarian
Naval Intelligence
Support Center
4301 Suitland Road
Washington, D. C. 20390

Commanding Officer
Naval Civil Engineering Laboratory
Port Hueneme, California 93041

Officer in Charge
Environmental Research Prdctn Fclty
Navy Postgraduate School
Monterey, California 93940

Dr. Warren C. Thompson
Dept. of Meteorology + Oceanography
Navy Postgraduate School
Monterey, California 93940

Director
Amphibious Warfare Board
U. S. Atlantic Fleet
Naval Amphibious Base
Norfolk, Little Creek, Virginia 23520

Commander, Amphibious Force
U. S. Pacific Fleet
Force Meteorologist
Comphibpac Code 25 5
San Diego, California 92155

Commanding General
Marine Corps Development and
Educational Command
Quantico, Virginia 22134

Dr. A. L. Slafkosky
Scientific Advisor
Commandant of the Marine Corps
Code MC-RD-1
Washington, D. C. 20380

Denfense Intelligence Agency
Central Reference Division
Code RDS-3
Washington, D. C. 20301

Director
Coastal Engineering Research Center
U. S. Army Corps of Engineers
Kingman Building
Fort Belvoir, Virginia 22060

Chief, Wave Dynamics Division
USAE-WES
P. O. Box 631
Vicksburg, Mississippi 39180

Commandant
U. S. Coast Guard
Attn=Gecv/61
Washington, D. C. 20591

Office of Research and Development
(DS/62
U. S. Coast Guard
Washington, D. C. 20591

National Oceanographic Data
Center (D764
Environmental Data Services
NOAA
Washington, D. C. 20235

Central Intelligence Agency
Attention OCR/DD-Publications
Washington, D. C. 20505

Dr. Donald Shift
Marine Geology + Geophysics Laboratory
15 Rickenbacker Causeway
AOML-NOAA
Miami, Florida 33149

Ministerialdirektor Dr. F. Wever
RUE/FO
Bundesministerium Der Verteidigung
Hardthoehe
D-5300 Bonn, West Germany

Oberregierungsrat Dr. Ullrich
RUE/FO
Bundesministerium Der Verteidigung
Hardthoehe
D-5300 Bonn, West Germany

Mr. Tage Strarup
Denfence Research Establishment
Osterbrogades Kaserne
DK-2100 Kobenhavn 0, Denmark

Dr. Yoshimi Goda
Director, Wave Research Division
Port and Harbor Research Institute
Ministry of Transporation
1-1 Nagase, 3 Chome
Yokosuka, 329 Japan

Prof. Dr. Rer. Nat. H. G. Gierloff-Emden
Institut F. Geographie
Universitaet Muenchen
Luisenstrasse 37/III
D-800 Muenchen 2, West Germany

Prof. Dr. Eugen Seibold
Geol-Palaeontolog. Institut
Universitaet Kiel
Olshausenstrasse 40-60
D-2300 Kiel, West Germany

Dr. R. Koester
Geol-Palaeontolog, Institut
Universitaet Kiel
Olshausenstrasse 40-60
D-2300 Kiel, West Germany

Prof. Dr. Fuehrboeter
Lehrstuhl F. Hydromechanik U. Kuestenm
Technische Hochschule Braunschweig
Beethovenstrasse 51A
D-3300 Braunschweig, West Germany

Prof. Dr. Walter Hansen
Direktor D. Instituts F. Meereskunde
Universitaet Hamburg
Heimhuderstrasse 71
D-200 Hamburg 13, West Germany

Prof. Dr. Klaus Hasselmann
Institut F. Geophysik
Universitaet Hamburg
Schlueterstrasse 22
D-200 Hamburg 13, West Germany

Prof. Dr. Nils Jerlov
Institute for Physical Oceanography
Kobenhavns Universitet
Haraldsgade 6
DK-2200 Kobenhavn, Denmark

Prof. Kiyoshi Horikawa
Dept. of Civil Engineering
University of Tokyo
7-3-1, Hongo, Bunkyo-Ku
Kokyo 113, Japan

Prof. Yuji Iwagaki
Civil Engineering Department
Kyoto University
9 Shimogamo Zenbucho, Sakyo-Ku
Kyoto, Japan

Dr. H. J. Schoemaker
Waterloopkundig Laboratorium Te Delft
61 Raam, Delft
Netherlands

Dr. M. W. Van Batenberg
Physisch Laboratorium Tno
Oude Waalsdorper Weg 63, Den Haag
Netherlands

Prof. Toshiyuki Shigemura
Civil Engineering Department
National Defense Academy
1-10-20 Hashirimizu
Yokosuka 239, Japan

Mr. William T. Whelan
Telecommunication Enterprises, Inc.
Box 88
Burtonsville, Maryland 20730

Dr. Benno M. Brenninkmeyer, SJ
Dept. of Geology and Geophysics
Boston College
Chestnut Hill, Massachusetts 02167

Coastal Studies Institute
Louisiana State University
Baton Rouge, Louisiana 70803

Dr. Choule J. Sonu
Tetra Tech, Inc.
630 North Rosemead Boulevard
Pasadena, California 91107

Dr. Richard A. Davis, Jr.
Department of Geology
University of South Florida
Tampa, Florida 33620

Dr. William T. Fox
Department of Geology
Williams College
Williamstown, Massachusetts 01267

Dr. Hsiang Wang
Department of Civil Engineering
Dupont Hall
University of Delaware
Newark, Delaware 19711

Dr. John T. Kuo
Henry Krumb School of Mines
Seely W. Mudd Building
Columbia University
New York, New York 100727

Dr. Edward B. Thornton
Department of Oceanography
Naval Postgraduate School
Monterey, California 93940

Prof. C. A. M. King
Department of Geography
University of Nottingham
Nottingham, England NG7 2RD

Dr. Douglas L. Inman
University of California A-009
Shore Processes Laboratory
La Jolla, California 92093

Dr. Omar Shemdin
Jet Propulsion Laboratory 183-501
4800 Oak Grove Drive
Pasadena, California 91103

Dr. William L. Wood
Department of Geosciences
Purdue University
Lafayette, Indiana 47907

Dr. Alan W. Niedoroda
Director, Coastal Research Center
University of Massachusetts
Amherst, Massachusetts 01002

Dr. John B. Southard
Dept. of Earth and Planetary Sciences
Massachusetts Institute of Technology
Cambridge, Massachusetts 02139

Dr. J. Ernest Breeding, Jr.
Department of Oceanography
Florida State University
Tallahassee, Florida 32306

Dr. John C. Kraft
Department of Geology
University of Delaware
Newark, Delaware 19711

Dr. Dag Nummedal
Department of Geology
University of South Carolina
Columbia, South Carolina 29208

Dr. Lester A. Gerhardt
Rennsselaer Polytechnic Institute
Troy, New York 12181

Mr. Fred Thomson
Environmental Research Institute
P. O. Box 618
Ann Arbor, Michigan 48107

Dr. Thomas K. Peucker
Simon Fraser University
Department of Geography
Burnaby 2, B. C., Canada

Dr. Robert Dolan
Department of Environmental Sciences
University of Virginia
Charlottesville, Virginia 22903